Aus der Klinik für Innere Medizin III

im Universitätsklinikum Schleswig-Holstein, Campus Kiel

an der Christian-Albrechts-Universität zu Kiel

Direktor: Prof. Dr. Norbert Frey

Sumoylation-independent activation of calcineurin-NFAT-signaling via SUMO2 causes cardiomyocyte hypertrophy

Dissertation

zur Erlangung des Doktorgrades

der Mathematisch-Naturwissenschaftlichen Fakultät

der Christian-Albrechts-Universität zu Kiel

Vorgelegt von

Alexander Bernt

Kiel, 2015

Erster Gutachter: PD Dr. Derk Frank

Zweiter Gutachter: Prof Dr. Eric Beitz

Tag der mündlichen Prüfung: 29.05.2015

Zum Druck genehmigt: 29.05.2015

gez.: Prof. Dr. Matthias Leippe

(Vorsitzender der Prüfungskommission)

Erklärung

Hiermit erkläre ich an Eides statt, dass diese Abhandlung – abgesehen von der Beratung durch den Betreuer – nach Inhalt und Form meine eigene Arbeit ist, soweit dies nicht explizit vermerkt ist. Ich erkläre weiterhin, dass Teile dieser Arbeit zur Publikation eingereicht wurden und dass die Arbeit unter Einhaltung der Regeln guter wissenschaftlicher Praxis der Deutschen Forschungsgemeinschaft entstanden ist.

_____

Alexander Bernt. Kiel, den

1 Index

List of Figures:

List of Tables:

2 Summary

The calcineurin-NFAT signaling axis is of major importance for the pathological remodeling of the heart as well as for the signal transduction in cardiomyocytes in general. The aim of this study was to systematically identify yet unknown activators of the calcineurin-NFAT signaling pathway. Therefore a human cardiac cDNA library with approximately 10^7 primary clones was utilized and investigated with the help of an NFAT-driven firefly reporter cell line (C2C12 mouse myoblasts). Several steps of dilutions and sub-dilutions of the clones, followed by verifications and validations of the preliminary findings from this screen led to the identification of SUMO2 as a robust activator of calcineurin-NFAT signaling. Moreover, data from the present study revealed that SUMO2 activates NFAT signaling via direct interaction with calcineurin A (CnA), endogenously. Further experiments showed that SUMO2 activates NFAT signaling directly via calcineurin A (CnA). This is supported by the finding that the presence of constitutively active calcineurin A (ΔCnA) in addition to SUMO2 further exaggerates the activation of NFAT signaling. Additionally, wildtype calcineurin A enhanced the SUMO2 mediated NFAT activation further upon activation by Ionomycin/PMA-treatment of the cells. A siRNA mediated knockdown of SUMO2 reduced the NFAT activation. The results obtained from overexpression and knockdown experiments in mouse myoblasts could be reproduced in neonatal rat ventricular cardiomyocytes (NRVCM). Subsequently, the molecular and phenotypical effects of SUMO2 were characterized in NRVCM. SUMO2 induced hypertrophy in NRVCM that could be further enhanced in the presence of ΔCnA. The SUMO2 induced hypertrophy could be abrogated by pharmacological inhibition of calcineurin A by Ciclosporin or Tacrolimus. Surprisingly, a *sumoylation*-deficient mutant of SUMO2 (SUMO2ΔGG) resembled the effects of the sumoylation-capable SUMO2 in almost all parameters investigated, suggesting a mechanism that is independent of a covalent attachment of SUMO2. Mechanistically, it could be shown that in experiments with overexpression of ΔCnA together with SUMO2 or SUMO2ΔGG, calcineurin displayed an enhanced nuclear localization, whereas this effect could not be observed with only ΔCnA overexpression.

Concluding from these findings, SUMO2 was identified as a new, positive modulator of the calcineurin-NFAT signaling pathway. Interestingly, these effects seem to be sumoylation-independent and suggest a nuclear retention of activated calcineurin.

3 Zusammenfassung

Der Calcineurin-NFAT Signalweg ist von entscheidender Bedeutung für die Entwicklung pathologischer Veränderungen am Herzen, sowie auch allgemein für die Signaltransduktion in Kardiomyozyten. Ziel dieser Studie war es, systematisch unbekannte Modulatoren des Calcineurin-NFAT Signalwegs zu identifizieren. Dafür wurde eine humane, kardiale cDNA-Bibliothek (10^7 Primärklone) mithilfe von NFAT-Luziferase-Reporter Zellen (C2C12, murine Muskelzellen) untersucht. Nach mehreren Runden der Verifizierung konnten wir SUMO2 als neuen und starken Aktivator des Calcineurin-NFAT Signalwegs identifizieren. Darüber hinaus fanden wir heraus, dass SUMO2 ein direkter Interaktionspartner mit einem nukleären Calcineurin A-Pool ist. Weitergehende Experimente in C2C12-Zellen zeigten, dass SUMO2 die NFAT-Signaltransduktion mittels Calcineurin A induziert. Dafür spricht, dass selbst in Anwesenheit von konstitutiv aktivem CnA (ΔCnA), die NFAT-Aktivierung durch SUMO2 steigerbar ist. Ebenfalls wurde Wildtyp-Calcineurin, zusätzlich zur Aktivierung durch Ionomycin/PMA-behandlung, verstärkt in Anwesenheit von SUMO2 aktiviert. Eine siRNA-vermittelte Herunterregulierung von SUMO2 reduziert die NFAT-Aktivierung. In neonatalen ventrikulären Rattenkardiomyozyten (NRVCM) lassen sich die durch Überexpression und Herunterregulierung gewonnenen Ergebnisse reproduzieren. Anschließend untersuchten wir die phänotypischen und molekularen Effekte von SUMO2 in NRVCM. SUMO2 induziert eine Hypertrophie in NRVCM, welche sich auch in Anwesenheit von ΔCnA weiter steigern lässt. Die SUMO2-induzierte Hypertrophie ließ sich durch CnA-Inhibitoren (Ciclosporin, Tacrolimus) aufheben. Eine *Sumoylierungs*-defiziente Mutante von SUMO2 (SUMO2ΔGG) hat überraschender Weise einen nahezu identischen Effekt wie das sumoylierungs-fähige SUMO2 in allen untersuchten Parametern, was auf einen Mechanismus hindeutet, der unabhängig von einer kovalenten Modifikation mit SUMO2 ist. Ebenfalls konnten wir zeigen, dass nach Überexpression von ΔCnA zusammen mit SUMO2 oder SUMO2ΔGG, Calcineurin stärker im Zellkern lokalisiert ist, während dies bei einer reinen ΔCnA Überexpression nicht zu beobachten ist.

Schlussfolgernd wurde SUMO2 als neuer und positiver Modulator des Calcineurin-NFAT Signalwegs identifiziert. Interessanter Weise sind diese Effekte Sumoylierungs-unabhängig und könnten auf eine nukleäre Retention von aktiviertem Calcineurin hindeuten.

4 Introduction

4.1 Overview

For each disease a variety of signaling pathways, either alone or in concert, influence the fate of single cells and tissue on multiple levels leading to the disease-specific phenotype. External and internal stimuli direct the cell towards one or the other direction and are yet oftentimes poorly characterized. The deciphering of the crosstalk between different signaling pathways and stimuli causing a certain disease is of great importance to get a chance at delaying, stopping or ideally reversing a certain pathologic development. In this thesis, the calcineurin-NFAT (nuclear factor of activated T-cells) signaling in the context of cardiomyocyte hypertrophy is the focus of investigation. Not only the individual transcription factors and therein directly involved proteins like phosphatases and kinases play a role in development of a disease. Important for the understanding of a certain mechanism or mechanistic feature is the investigation of posttranslational modifiers and protein-protein interactions that can cause a modulation of the signaling pathways. More so, this regulation can vary between different conditions within the cell and modulate according to an external or internal stimulus. Here, the mechanistic link between the calcineurin-NFAT axis and the system of small ubiquitin like modifier 2 is investigated on several levels of regulation.

4.2 Cardiac hypertrophy

The heart's reaction to elevated and enduring biomechanical stress is the development of cardiac hypertrophy. The term hypertrophy describes a distinct set of pathological events that can be observed in the cells involved. In terms of a hypertrophic heart, it firstly refers to an increased mass. This however is prone to bias due to the assumption that the increased mass results from increased cardiomyocyte size. Hearts that retained fluid or perfused hearts will have a different wet mass than otherwise harvested organs so the desiccated mass is a more reliable parameter apart from single-cell size comparison. A broad overview of cardiac hypertrophy and its cellular and organ consequences was given by Gerald W. Dorn in 2003 (Dorn et al., 2003).

Initially, this stress-response is physiologic, similar to the changes the heart undergoes when constantly challenged with exercise. This can be well observed in athletes for example. In this adaptive hypertrophy, the cardiac muscle cells grow to increase the function, meaning increased pressure and blood volume ejection overall and especially of the left ventricle. This compensation for the need of a stronger and more capable heart is beneficial. On the contrary, enduring pressure overload and thus biomechanical stress switches this adaptively compensating state to a maladaptive stage, where the mechanical capacity of the heart decreases. This is a harmful state for the heart and has to be treated accordingly. Often times this maladaptive state is a result of heart tissue remodeling followed by myocardial infarction, chronic hypertension or valvular heart disease, among others (Ertl and Frantz, 2005; Frantz et al., 2009; Pfeffer and Braunwald, 1990; Zwadlo and Borlak, 2005). Adaptive and maladaptive hypertrophy need to be well differentiated to be able to successfully modulate the disease outcome. To study the mechanistic features of cardiac hypertrophy, cell culture systems are needed to observe the adverse effects that various proteins and signaling molecules have on the disease outcome prior to the investigation in animal models and ultimately in humans.

In cell culture the term hypertrophy also mainly refers to an increase in cell size, measured by the cell surface area but there are distinct genetic parameters adding to hypertrophy that can be precisely assessed. This increase in cell surface area is typically accompanied by the elevated expression of hypertrophy associated fetal genes, encoding for natriuretic peptides: *nppa* (protein: atrial natriuretic peptide) and *nppb* (protein: brain natriuretic peptide). Several

other genetic factors and protein expression patterns can be investigated but seem to vary according to the type of induction of hypertrophy such as pharmacologic stimulation or the generation of biomechanic stress through dynamic stretch of the individual cells. An involvement of calcineurin A in the hypertrophic response is often times accompanied by the increased expression of the regulator of calcineurin 1.4 (Rcan1-4) on both, RNA and protein levels as will be discussed in detail.

All these factors taken together provide valuable information about the type of hypertrophy observed and can already provide hints on the involved proteins and signaling pathways. As an investigative means for the assessment of hypertrophic effects, hypertrophy can be pharmacologically induced within defined parameters in cell culture systems through the addition of the pharmacologic agent phenylephrine (PE). PE leads to an increased cell size and upregulation of the above described hypertrophy-associated fetal genes. This induction of cardiomyocyte hypertrophy typically occurs within 48 hours after stimulation. PE is a selective α_1-adrenergic receptor agonist of the phenethylamine class and thus a sympathomimetic.

4.3 Calcineurin

The protein calcineurin or PPP3CA (also known as PP2B) is a serine/threonine protein phosphatase that belongs to the PPP family of protein phosphatases. This family alone is responsible the main phosphatase activity of serine/threonine phosphatases *in vivo.* The family shows a conserved catalytic domain stretch of about 280 residues alongside non-conserved N- and C-termini. Their assembly varies and includes many different accessory proteins and distinct regulatory subunits (Barford et al., 1998). Originally isolated in 1976, calcineurin has been extensively studied over the last decades and throughout the different fields of research (Wang and Desai, 1976). Calcineurin is a heterodimer built up of two different subunits. The regulatory subunit calcineurin B (CnB) has a molecular weight of ~17 kDa and is smaller than the catalytic subunit calcineurin A (CnA). CnA has a molecular weight of approximately 59 kDa (Guerini et al., 1992). In mammals, there are three genes that encode for calcineurin A (α, β, μ), of which CnAα and CnAβ are expressed in the heart (Bueno et al., 2002b; Taigen et al., 2000). The smaller regulatory subunit CnB is encoded by two genes, CnB1 and CnB2 of which only CnB1 is expressed in the mammalian heart (Ueki et al., 1992). The catalytic subunit of CnA is localized at the N-terminus, whereas the autoinhibitory domain (AID) is localized at the C-terminus as can be seen in Figure 1. The AID inhibits the catalytic domain, maintaining an inactive status of the protein. Upon binding of calcium/calmodulin on the one hand, or a cleavage of the AID by calpain, a calcium dependent protease on the other hand, the protein shifts to its active state (Bueno et al., 2002a; Burkard et al., 2005). The calcium/calmodulin binding domains are located c-terminal of the catalytic domain (**Figure 1**). Of note, elevated levels of activated calcineurin have been observed in the human hypertrophied and failing heart (Haq et al., 2001; Lim and Molkentin, 1999; Ritter et al., 2002).

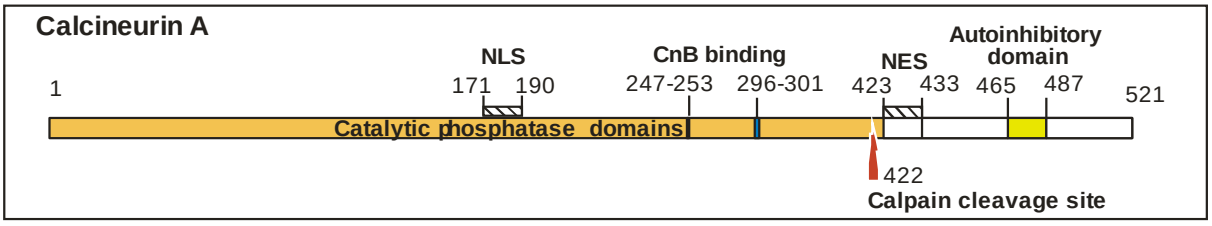

Figure 1: Schematic drawing of calcineurin A with depicted domains, nuclear import and export sites as well as calpain cleavage site and autoinhibitory domain.

Many efforts have been taken to identify the role of calcineurin within the cell. A rise of intracellular Ca^{2+} levels activates calcineurin by conformational change and a displacement of its AID. Upon activation, calcineurin can dephosphorylate conserved N-terminal serine residues on cytoplasmic localized transcription factors such as members of the NFAT family, shifting their localization towards the nuclear compartment. In the nucleus, the NFAT transcription factors bind to the DNA as homodimer, heterodimer or monomer (Hogan et al., 2003). Together with accessory proteins and other transcription factors like MEF2 or GATA1, and GATA4, NFATs can activate a set of pro-hypertrophic genes (Hogan et al., 2003; Wilkins et al., 2004; Wilkins and Molkentin, 2004).

Calcineurin also has reported functions throughout the cell including contraction, metabolism, synaptic transmission, RNA splicing and cell cycle control (Beullens et al., 1992; Cohen, 1989; Shenolikar and Nairn, 1991; Wera and Hemmings, 1995). On the level of cell cycle regulation, it interacts with and inhibits the cyclin-dependent kinase CDC25, playing an inhibitory role in mitosis. CDC25 removes phosphates from various cyclin dependent kinases and subsequently activates them for cell-cycle progression (Wera and Hemmings, 1995). There are a variety of other examples where calcineurin has influence on cell cycle progression and other signaling pathways, reviewed in a variety of articles from different fields of research.

4.3.1 Animal models for calcineurin-NFAT signaling

The importance of calcineurin regarding signal-transduction in the heart and specifically the involvement in the pro-hypertrophic signaling pathways gave rise to a variety of different animal models in which the protein phosphatase was further characterized and validated for physiologic and pathophysiologic relevance.

Activation of the Calcineurin-NFAT pathway in transgenic mice overexpressing a constitutively active mutant of Calcineurin causes a strong cardiac hypertrophy with severe fibrosis and activation of the molecular hypertrophic program (Molkentin et al., 1998). Moreover, cardiomyocytes from these mouse hearts are disorganized and hypertrophic, accompanied by a doubling of the cross-sectional area compared to wild type cardiomyocytes. The opposite effect can be achieved by inhibition of Calcineurin-NFAT signaling that can be observed in *calcineurin Aβ*−/− and *Nfatc3*−/− and *Nfatc2*−/− mice, leading to the inhibition of pathological cardiac hypertrophy in response to pressure overload or stimulation with neuroendocrine

agonist infusion (Bueno et al., 2002b; Molkentin et al., 1998; Wilkins et al., 2002). Both findings demonstrate a critical and indispensable role Calcineurin-NFAT signaling plays in the pathological remodeling of the heart and their sufficient and necessary role in the development of cardiac hypertrophy following biomechanical stress.

4.3.2 Subcellular localization

It has been reported, that depending on the availability of calmodulin, different concentrations are needed for an activation of calcineurin (Stemmer and Klee, 1994). With higher concentrations of calmodulin within the cell, less Ca^{2+} is needed for a full activation of calcineurin. For a complete activation however, Ca^{2+} levels similar to those present in the cell during the systole are needed. Calcineurin might therefore integrate the contractile Ca^{2+} signal and decode alterations of its frequency into subcellular signaling and even that of rapid Ca^{2+}-oscillations (Colella et al., 2008). Concluding from this, a separation between “contractile” and “signaling” Ca^{2+}has been proposed (Molkentin, 2006). The signaling-calcium is thought to be active in specific micro domains within the cell that are insulated from the fluctuating contractile calcium. In those micro domains, proteins are exposed to high local amounts of Ca^{2+} alongside their target molecules, which could also explain why the high concentrations of calcineurin present in the cytosol (Heineke et al., 2010) are not undergoing constant activation, due to the high levels of Ca^{2+} during the muscle contraction. The cytoplasmic calcineurin might thus be located in micro domains for example together with the different NFAT target proteins and becomes activated only upon calcium/calmodulin binding or calpain cleavage (Heineke and Ritter, 2012). A complete inhibition of calcineurin in failing or hypertrophied hearts seems to be a possible therapeutic means, however this leads to severe heart failure and accelerated death in mice (Maillet et al., 2010). There, the ablation of the regulatory calcineurin subunit CnB1 completely abrogates CnA protein in the heart. For this reason, instead of an unspecific complete inhibition, Heineke and Ritter propose a micro domain-specific inhibition for a possible therapeutic approach (Heineke and Ritter, 2012). The classical role for calcineurin as a cytoplasmically localized protein phosphatase that mediates signaling effects by mere activation of NFAT through dephosphorylation of the transcription factor has been challenged early on by various research groups. Interestingly, it has been shown that a subpool of calcineurin itself also translocates to the nucleus (Burkard et al., 2005), implying the existence

of additional targets for dephosphorylation or even a distinct interacting role for calcineurin with the transcription factor apart from a dephosphorylation.

In failing human hearts, a significant increase in nuclear calcineurin levels has been reported (Burkard et al., 2005), hinting at an important role for calcineurin in the development or maintenance of cardiac disease, mediated by this nuclear subpool. When calcineurin's AID is targeted and cleaved by the protease calpain, it becomes constantly active and independent of calmodulin but not Calcium as well as it translocates to the nuclear compartment (Stemmer and Klee, 1994; Yang and Klee, 2000). The cleavage exposes the phosphatase domain and thus enhances the enzyme activity. Interestingly, the nuclear localization sequence (NLS) is also exposed upon cleavage and at the same time, the nuclear export sequence (NES) is removed alongside the AID (Heineke and Ritter, 2012). Calcineurin can be exported from the nucleus by the export-protein Crm1 or exportin. Once devoid of its NES, Crm1-mediated shuttling cannot occur and constitutively active calcineurin is retained in the nuclear compartment (Hallhuber et al., 2006). This is particularly interesting since the constitutively active calcineurin is now shuttled into the nucleus and because of the lack of the NES, will be retained there, even after the loss of a pro-hypertrophic stimulus (Hallhuber et al., 2006). The method of calcineurin import through the nuclear pore complex (NPS) is Ran-GTP mediated and energy dependent (Gorlich et al., 2003; Hallhuber et al., 2006; Jans et al., 2000; Rout and Aitchison, 2001). The precise role of active CnA in the nucleus remains elusive. For one, the classical phosphatase role for the activation of NFAT in the nucleus can be executed similar to the originally identified NFAT-dephosphorylation occurring in the cytoplasm. A nuclear subpool of calcineurin could also counteract the role of different kinases present in the nucleus to shift the reaction-equilibrium towards the side of dephosphorylated and consequently active DNA-bound NFAT. Examples of nuclear localized kinases are glycogen synthase kinase 3 beta (GSK3β) and c-Jun N-terminal kinase (JNK) as well as the dual-specificity tyrosine phosphorylation-regulated kinase 1A (DYRK1A) (Antos et al., 2002; Chow et al., 1997; Kuhn et al., 2009). However, experiments showed that phosphatase-deficient, mutated calcineurin constructs can also block the NFAT-export, suggesting that counteraction of kinase activity is not a major mechanism of action mediated by nuclear calcineurin (Zhu and McKeon, 1999). Lastly, NFAT-bound calcineurin seems to inhibit the Crm1-mediated export of NFAT from the nucleus to the cytoplasm by masking NFAT's NES (Zhu and McKeon, 1999). Nuclear calcineurin could therefore displace Crm1 from NFAT nuclear export sequence to retain

calcineurin-NFAT complexes in the nucleus with successive enhanced transcription factor activity (Hogan et al., 2003; Hogan and Rao, 1999; Zhu and McKeon, 1999). Heineke and Ritter conclude in their review, that truncated and constitutively active nuclear calcineurin mainly exhibits its functions by an interference with Crm1-mediated export of NFAT (Heineke and Ritter, 2012).

4.3.3 Calcineurin inhibitors

The research efforts taken for the identification of endogenous modulators of calcineurin activity have been large, their majority yielding the identification of proteins that have an inhibitory effect on the phosphatase activity. A variety of CnA inhibitors have been published so far. For example the protein Cain is an inhibitor for calcineurin in neurons that acts in a non-competitive way (Lai et al., 1998). The protein AKAP79 however directly interacts and blocks calcineurin activity in cardiomyocytes and acts as a competitive inhibitor (Taigen et al., 2000). Another example for inhibition of CnA by other proteins is a protein family called calsarcins. These proteins are necessary for the induction of a hypertrophic calcineurin-NFAT response by a negative regulation of CnA phosphatase activity and consequently NFAT activation (Frey et al., 2000). Along the same lines, the animal model of calsarcin-1 knockout mice show exaggerated hypertrophy following pressure overload (Frey et al., 2008). Apart from interacting and thereby inhibiting proteins, there are two pharmacologic agents known to inhibit CnA, ciclosporin A (CsA) and FK506/tacrolimus. These two substances have been widely used in immunosuppressant therapy following organ transplant action. Interestingly the mechanism of action has been unclear as they were only later found to inhibit calcineurin not directly, but by binding to endogenous immunophilin proteins, cyclophilin A and FKBP12, respectively (Liu et al., 1991). Liu and colleagues utilize purified CnA from bovine brain tissue and described a retention effect of calcineurin, when FK506-FKBP12 or CsA-cyclophilin A complexes bind to calcineurin and also calcineurin-calmodulin complexes subsequently rendering the phosphatase inactive (Liu et al., 1991). This is another example of how calcineurin influences signal transduction in other cell-types apart from muscle-tissue. Another important modulator of the Calcineurin-NFAT signaling pathway is Rcan1-4. Changes in the Rcan1-4 protein levels can be assessed to endogenously indicate the activation of calcineurin-NFAT signaling (Yang et al., 2000). The expression of Rcan1-4 is regulated by NFAT transcription factors, yet its

precise function is still under debate. This is due to both inhibitory and activator roles that have been observed by different groups and under various experimental conditions (Fox and Heitman, 2005; Sanna et al., 2006; Vega et al., 2003a; Vega et al., 2003b). A more recent study however suggests a diverse role for Rcan1-4, using a systems biology approach and single-cell experimentation in combination with *in silico* simulations. In this study, Shin and colleagues suggested a dose dependent effect of Rcan1-4 as an inhibitor at lower levels but as a facilitator at higher expression levels, which highlights the complexity of calcineurin regulation (Shin et al., 2011). On the activator-side of calcineurin interacting proteins, a protein termed Dyxin/LMCD1 has been reported that may act as a strong activator of calcineurin-mediated cardiac hypertrophy (Frank et al., 2010).

4.4 Small ubiquitin-related modifiers – SUMO proteins

4.4.1 Overview

SUMO (small ubiquitin-related modifier) proteins were originally identified as post-translational modifiers. Two initial studies link SUMO1 to binding with RAD51 and RAD52 (Chen et al., 1998; Shen et al., 1996) and finally SUMO1 was found to covalently bind to RanGAP1 (Matunis et al., 1996). This initial finding of a covalently attached SUMO already hinted at the influence that SUMO1 has on subcellular-localization because it was found that unsumoylated RanGAP1 remained cytoplasmically localized, whereas sumoylated RanGAP1 translocated to the nucleus that implies a fundamental regulating role for SUMO1 in the nuclear-cytoplasmic trafficking of various proteins. The reversibility of this process was yet another groundbreaking finding from the original study and opened the door for a variety of characterization approaches as well as the generation of hypothesis for SUMO's mechanisms of action. Apart from the already discovered ubiquitin protein, with SUMO1 these studies laid the foundation for the investigation of yet another family of posttranslational modifiers and their role in cell-signaling and disease development. The discovery of the reversibility of sumoylation rapidly led to the characterization of the responsible proteases and ever since an increasing amount of SUMO-interacting proteins were discovered, their majority being localized in the nucleus. With the characterization of SUMO, a consensus-sequence for sumoylation evolved that proved a useful tool for the studies of sumoylation-dependent processes. As a method for the observation of SUMO-mediated effects, potential SUMO-binding sites could now be artificially mutated and sumoylation competent- and incompetent proteins were compared. Apart from sumoylation, SUMO-proteins can modify proteins by non-covalent interaction through so-called SUMO-interaction/binding-motifs (SIM/ SBM), adding another layer of complexity to this type of post-translational modification.

The family of SUMOs comprises four distinct and structurally similar proteins (SUMO-1, -2, -3 and -4) whose functions were reviewed in great detail by Melchior and Geiss-Friedlander (Geiss-Friedlander and Melchior, 2007). All of the SUMOs are 10-15 kDa in size, sharing many secondary-structural elements with the name-giving protein ubiquitin B (Figure 2). All shown proteins share a common set of tertiary structure elements with two alpha-helices and four to

five beta-sheets. Amino-acid similarity between SUMO proteins and ubiquitin however does not exceed 20%. The overall surface charge of SUMOs and ubiquitin differs as well. SUMO proteins are expressed as precursor molecules containing a C-Terminal diglycine-motif (X-Gly-Gly-X) followed by a varying amount of different amino-acids. The diglycine motif has to be exposed by C-terminal cleavage in order for SUMOs ability to be covalently attached to target proteins as further described in 4.4.3. The expression of SUMO1-3 is ubiquitous throughout the organ system and various cell types of many species whereas SUMO4 seems to be majorly expressed in the kidney, spleen and lymph node (Guo et al., 2004). The primary structures of processed SUMO2 and SUMO3 are 97% identical and the proteins are commonly referred to as SUMO2/3 due to a lack of knowledge about individually delimiting functions. Both share only about 50% sequence similarity with SUMO1 which results in distinct conjugation to different target proteins *in vivo (Saitoh and Hinchey, 2000)*.

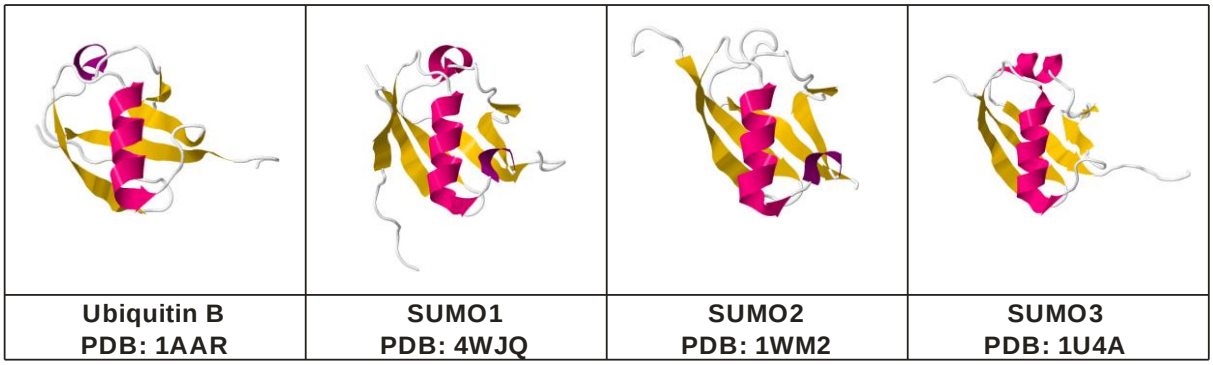

Figure 2: Side-by-side comparison of human ubiquitin B, SUMO-1, -2 and -3 with alpha-helices shown in pink and beta-strands shown in yellow. All structures were extracted from the RSCB Protein database (Cappadocia et al., 2015; Cook et al., 1992; Ding et al., 2005; Huang et al., 2004).

4.4.2 The SUMO family

Human SUMO1 was originally discovered in yeast as SMT3 and was cloned to identify suppressors of the temperature-sensitive *MIF2* allele. SUMO1 contains the characteristic ubiquitin-fold ββαββαβ that is preserved among ubiquitin-like proteins as reviewed by Mayer and colleagues (Mayer et al., 1998). Ubiquitin and SUMO1 share 50% of their amino acid sequence and the secondary and tertiary structure are closely related as can be seen in Figure 2. Even though both proteins are structurally close, the proteins involved in the processing and

subsequent ligation are related, but not identical. While ubiquitin is typically attached to target proteins in poly-ubiquitin chains and therefor often attached to itself (Pickart, 1997), SUMO1 does not seem to be able to self-conjugate when covalently attached, supposedly because the lysine residues used for poly-ubiquitination are not conserved within SUMO1.

The investigation of the effect that a SUMO1-knockout had on mice, lead to somewhat contradicting studies. Alkuraya and colleagues studied a patient with cleft lip and palate caused by a chromosomal translocation with disrupted SUMO1 gene. In the SUMO1-knockout mouse model they could recreate the cleft lip phenotype and also observed embryonic demise between E13.5 and E18.5 and immediate postnatal death (Alkuraya et al., 2006). Contradicting with this finding is a study of SUMO1-knockout mice in which the last three SUMO1-exons were targeted for disruption (Zhang et al., 2008). SUMO-1 mRNA abundance was halved in heterozygotes and undetectable in Sumo-1(-/-) mice. Further, SUMO-1-conjugated RanGAP1 was undetectable in SUMO1-knockout mice. The authors neither observed embryonic or early postnatal lethality nor a defect in lip and palate development in knockout mice. They concluded that that most, if not all, SUMO-1 functions are compensated for, *in vivo,* by SUMO-2 and SUMO-3.

The SUMO conjugation plays a critical role in embryogenesis. Mouse embryos that are deficient in the SUMO-E2 enzyme UBC9 die at the post implantation stage (Nacerddine et al., 2005). Yuan and colleagues show an indispensable but functionally redundant role for SUMO-paralogues for the early zebrafish development (Yuan et al., 2010). Driven by these studies, Wang and colleagues studied the effect of SUMO2 and SUMO3 in mouse with knockdown approaches for both proteins (Wang et al., 2014). They show viable SUMO3-knockout mice whereas SUMO2-knockout mouse embryos exhibited severe developmental delay and died at embryonic day 10.5. Including additional evidence for SUMO2 being the predominantly expressed isoform. Furthermore they could show that SUMO2 and SUMO2/3 heterozygous mice lacked any overt phenotype, concluding that the expression levels but not functional differences between SUMO2 and SUMO3 are critical for normal embryogenesis.

Apart from the finding that SUMO4 seems to be majorly expressed in the kidney, spleen and lymph node, not much is known about its functions to date (Guo et al., 2004). SUMO4 shares 90% nucleotide identity and 87% amino acid homology with SUMO2. Patients with a single nucleotide substitution and subsequently altered amino-acid Methionin^{55} to Valine show a strong association to type 1 diabetes, however no mechanistic link is provided yet apart from

a suggested interaction with IκB and subsequently enhanced NFκB activation (Guo et al., 2004; Hwang et al., 2011). SUMO4 has so far not been investigated in animal-models.

4.4.3 Posttranslational modification: sumoylation

The majority of the discovered SUMO-involved mechanism is mediated by its ability to be covalently attached to target proteins. As can be seen in Figure 3, many proteins are involved in the sumoylation process. Firstly, the expressed precursor SUMO-protein with a variable stretch of amino acids following the diglycine motif has to be cleaved off by so called sentrin-specific proteases (SENP). The cleaved SUMO has to be activated in an ATP-dependent reaction involving a protein complex called the E1-activating enzyme heterodimer comprised of UBA2 and AOS1 (Lin et al., 2003; Xu and Au, 2005) which attaches the adenylate-SUMO conjugate intermediate to UBA2. In the next step, SUMO is transferred from the E1-complex to the E2-conjugating enzyme UBC9, linking the catalytic cysteine residue to the C-terminal carboxy-group of SUMO (Saitoh et al., 1998; Ueki et al., 1992). Of note, the E2-conjugating enzyme UBC9 is only an E2-enzyme for SUMO-proteins but not for ubiquitin (Stemmer and Klee, 1994). In a last step, SUMO is transferred to its target protein, forming an isopeptide bond between the target lysine and the C-terminal carboxy-group of SUMO's glycine residue. This process is typically catalyzed by E3-ligase enzymes, which contain a SP-RING motif, similar to the ubiquitin RING E3-ligases (RE) which are essential for the enzyme's function (Hochstrasser, 2001). SP-RING ligases bind their targets directly and bind to SUMO in a non-covalent way through SUMO-interacting motifs, thus possibly functioning as scaffolding proteins to bring the relevant residues in close proximity and consequently catalyzing the isopeptide-bond formation.

Even though the majority of sumoylation processes result in a single SUMO attachment to a target lysine, mammals possess the ability to form poly SUMO chains, very similar to poly ubiquitin chains which could be shown for SUMO2/3 in mammals (Mukhopadhyay et al., 2006; Tatham et al., 2001). In addition to their initial cleavage of the SUMO precursor proteins, the sentrin specific proteases can also reverse the process of sumoylation by their isopeptide cleavage activity (Di Bacco and Gill, 2006; Di Bacco et al., 2006; Gong and Yeh, 2006). The challenging and fascinating circumstance is, that there is no easy way to determine, which result a SUMO-conjugation or interaction will have on a given target protein yet.

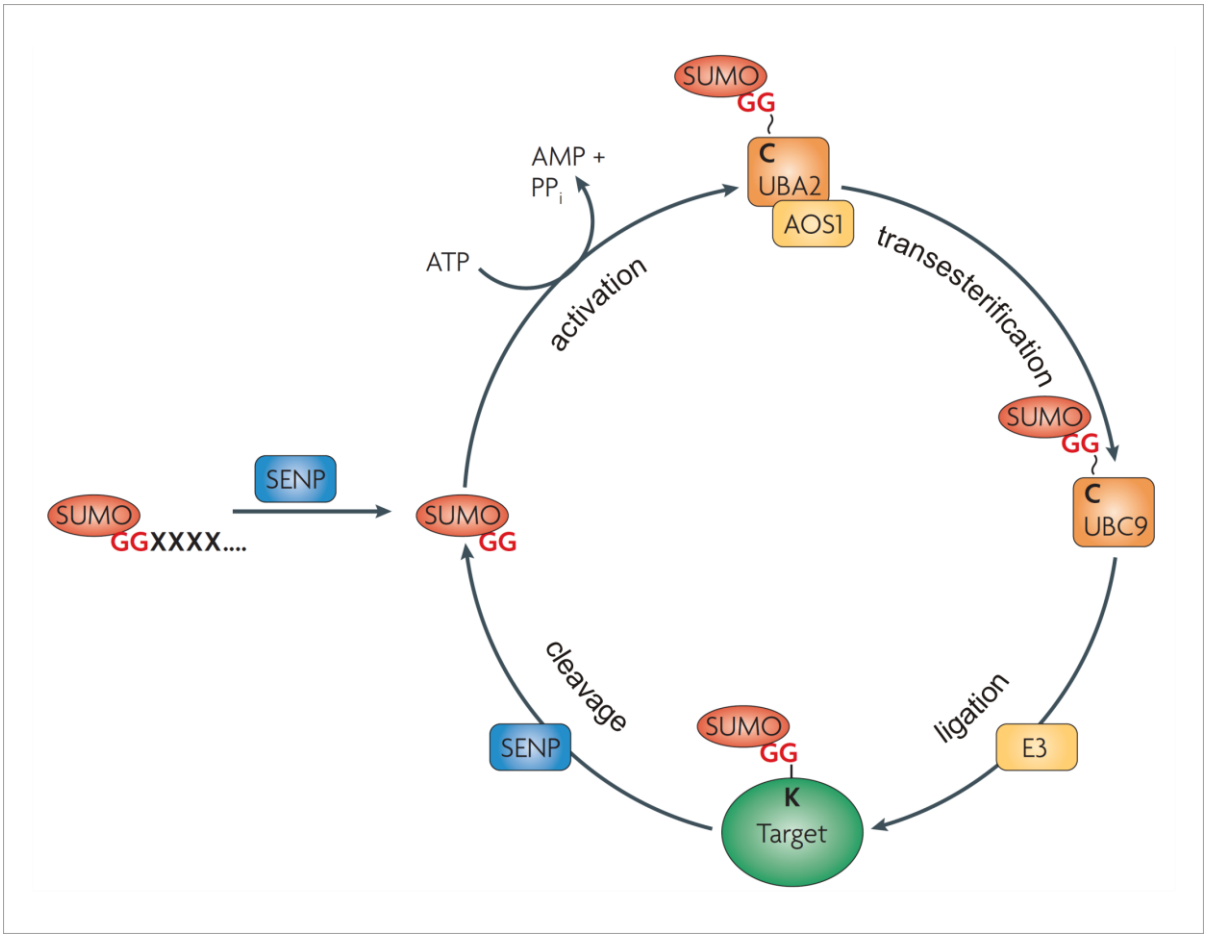

Figure 3: Schematic overview of the sumoylation enzyme-cascade. Figure, modified from (Geiss-Friedlander and Melchior, 2007), page 498.

4.4.4 Consequences of sumoylation and SUMO-interaction

The molecular consequences of sumoylation of a given target protein or the SUMO-interaction are difficult to assess and very diverse. Sumoylation can enable or enhance protein-protein interactions on the one hand, but on the other hand can also disturb those interactions. For example RanGAP1 interacts with RanBP2 upon sumoylation (Brattstrom et al., 2010; Matunis et al., 1996) whereas sumoylated E2-25K loses its interaction capability with the ubiquitin E1-enzyme (Pichler et al., 2005). Another example is a study, where the mutation of the SUMO acceptor site in CtBP1, K428R, shuttles CtBP1 from the nuclear compartment to the cytoplasm (Lin et al., 2003).

One possible molecular consequence of sumoylation is the modulation of DNA binding-abilities of transcription factors. An example is the hepatoma-derived growth factor (HDGF) that loses its DNA binding affinity in comparison to the non-sumoylated protein (Goodson et al., 2001). In contrast to this, the sumoylation of the heat shock transcription factor 2 (HSF2), that plays a critical role in the modulation of heat shock protein expression upon external stimulation, enhances its DNA-binding affinity (Thakar et al., 2008). This is a good example for the diversity of SUMO-interaction consequences and that the same modification can have on two different transcription factors.

The alteration of protein-protein interaction can also be a result of sumoylation. Sumoylated aryl hydrocarbon receptor repressor (AhRR) will partially enhance its inhibitory effect on the receptor activity as a result of a potentiated interaction of sumoylated AhRR with its corepressors (Oshima et al., 2009).

The increase of protein turnover and degradation has for a long time only been linked to ubiquitination and not sumoylation. This has been challenged in 2007, when Prudden and colleagues could show in yeast, that SUMO specific ubiquitination E3-ligases targeted sumoylated proteins for degradation (Prudden et al., 2007). Since then, many other proteins have been implicated with enhanced degradation upon sumoylation, broadening the range of molecular consequences of sumoylation and SUMO-interaction.

SUMO interaction and sumoylation can thus be regarded, as extenders of possible protein-protein interactions and their modulation capabilities are promising targets to link basic molecular interaction studies to possible disease development and/or progression.

4.4.5 SUMO interaction / binding motif (SIM/SBM)

Apart from the well-studied sumoylation modifications, there has been a rather recent discovery of non-covalent sumo-interaction or –binding motifs (SIM/SBM) (Hecker et al., 2006; Song et al., 2004) which influence their targets, all of which are themselves sumoylated proteins (Lin et al., 2006; Minty et al., 2000; Shen et al., 2006; Song et al., 2004). The understanding of SUMO protein function and mechanistic biology has been majorly advanced with the knowledge about SUMO interaction. Unlike the motifs that mediate ubiquitin binding, SUMO binding motif diversity seems more limited and is not fully understood and characterized

(Kerscher, 2007). First in 2000, Minty and colleagues identified a specific SUMO interacting protein with conserved SIM/SBM sites (Minty et al., 2000). In a yeast-two-hybrid system they could show an interaction with the sumoylated version of the protein p73. By sequence comparison, they revealed a common Serine-X-Serine (S= serine, X=hydrophobic amino acid) motif. They proposed that the two serine residues flanking the hydrophobic (-X-) core are required for SUMO interaction. This motif however was challenged four years later by Song and colleagues who proposed a different consensus sequence, also from yeast-two-hybrid experiments (Song et al., 2004). They suggested a motif with a hydrophobic core and a consensus sequence of V/I-X-V/I-V/I (V= valine, I= isoleucine) that can be found in many proteins, including those already identified as sumoylation targets. The structure of the SUMO1-PIASX complex reveals the interaction to lie between individual hydrophobic and aromatic residues between SUMO and the interacting peptide (Song et al., 2005). For SUMO1 and SUMO2 it could be shown, that this interaction assumedly lies within the groove between the α-helix one and the β-strand two. From NMR and crystal structures, crucial hydrophobic residues of SUMO1, e.g. valines, phenylalanines and Leucines have been found to interact with SIM on target proteins (Baba et al., 2005; Hecker et al., 2006). One example is that SUMO1 can inhibit RAD51-mediated homologous recombination by interaction with RAD51 (Li et al., 2000). Along the same lines and also through SUMO interaction, SUMO1 can protect against cell decay by interacting with Fas and tumor necrosis factor receptor 1 (TNFR1) (Okura et al., 1996). The inhibition of dynamin-dependent endocytosis was also shown to be mediated through sumoylation-independent SUMO1 binding (Mishra et al., 2004). As an example for another SUMO-protein, SUMO3 was found to co-activate EBNA2 (Epstein-Barr virus nuclear antigen 2) in the absence of direct conjugation to EBNA2 (Rosendorff et al., 2004). These are just a few of the many examples of already known SUMO interactions with various proteins and the investigation of the interactions as well as the characterization of new tentative SIM/SBM will provide valuable information about the SUMO-family mediated modulation of proteins and signaling pathways.

4.4.6 Implications in cardiac disease

SUMO can modulate a variety of proteins that are important for gene regulation, including various transcription factors involved in fetal gene expression and heart development as well

as pro-hypertrophic signaling pathways, cell cycle regulation, transcription and subcellular transport (Kim and Baek, 2009) via alterations in molecular interaction patterns of the modified target (reviewed in (Geiss-Friedlander and Melchior, 2007)). Examples for SUMO-modified transcription factors that are involved in normal cardiac development are Nkx2.5 (Wang et al., 2008), GATA binding protein 4 (GATA4) (Komatsu et al., 2004; Wang et al., 2004), the serum response factor (SRF) (Matsuzaki et al., 2003) and myocardin (Wang et al., 2007). The involvement of SUMO in such a variety of transcription factors involved in cardiac development supports an important role for SUMO-modification in the heart. SUMO2 among other SUMO family members has recently been implicated in cardiac disease as extensively reviewed by Wang and Schwartz (Maejima and Sadoshima, 2014; Wang, 2011; Wang and Schwartz, 2010). Therefore, studying the effect of SUMO2 in this context is potentially very valuable. A particularly promising example of SUMO implication in cardiac disease in human was investigated by Kho and others, who discover a link between SUMO1 and the regulation of SERCA2a in the context of heart failure, stabilizing the protein and its ATPase activity (Kho et al., 2011). In failing hearts, sumoylation of SERCA2a and overall levels of SUMO1 were reduced (Kho et al., 2011). Also they could rescue the contractile function mice with induced hypertrophy by SUMO1 gene transfer. Last year, Gupta and others showed that the SUMO-conjugating enzyme UBC9, which is the only known SUMO2-E2 enzyme yet, is of importance for protein maintenance in cardiomyocytes (Gupta et al., 2014). They used loss- and gain of function approaches to study the importance of the SUMO E2-enzyme UBC9. They found out that an overexpression of UBC9 elevated the function of the ubiquitin proteasome system (UPS) in cardiomyocytes, whereas knockdown of UBC9 by small interfering RNA (siRNA) caused significant accumulations of aggregated protein (Gupta et al., 2014). A particularly interesting finding for this study is the implication of SUMO2 in human cardiomyopathy in a way where reduced sumoylation of the protein Lamin A resulted in enhanced cell death. Lamin A is a direct SUMO2 target with two known naturally occurring mutants that are directly associated to familial cardiomyopathy. Those natural mutations are localized in a sumoylation consensus-motif around Lysine^{201} (Zhang and Sarge, 2008).

Another interesting implication for SUMO-proteins in cardiac disease is an overexpression approach of the sentrin-specific protease 5 (SENP5) that is responsible for the reversible sumoylation by cleaving SUMO-proteins off their targets. Kim and colleagues show that the levels of SENP5 are significantly increased in human idiopathic failing hearts (Kim et al., 2015).

Cardiomyocyte-specific overexpression of SENP5 led to cardiac dysfunction, accompanied by decreased cardiomyocyte proliferation and elevated apoptosis. SUMO attachment to dynamin related protein (Drp1), a factor critical for mitochondrial fission was decreased. The authors suggest the SUMO conjugation pathway as a potential target in the prevention/treatment of cardiomyopathy.

4.5 Rationale

The role for the calcineurin-NFAT signaling axis has been under investigation for a long time, yet mainly inhibiting molecules were discovered for this significant pathway that plays a pivotal role in the development of cardiac hypertrophy and other cardiac diseases. For a possible therapeutic use, activators of this pathway needed to be identified in order to a) understand the mechanism of action that activates calcineurin for pathologic signaling and b) study the chances for a successful indirect inhibition of this pathway by regulation of calcineurin activators. The purpose of this study was to identify yet unknown activating modulators of calcineurin-NFAT signaling in the heart. Therefor a screening approach was utilized where an NFAT-reporter driven luciferase construct was stably transfected into mouse myoblasts. These cells were then exploited by co-transfection with calcineurin and an unknown pool of cDNAs to reveal those coding sequences that activate calcineurin signaling by observing the subsequent NFAT activation in the different conditions. This approach revealed the small ubiquitin related modifier 2 (SUMO2) to be a strong activator of calcineurin-NFAT signaling. From the screening, a series of tasks for this thesis evolved that include I) the thorough characterization of the structural and functional interaction between SUMO2 and calcineurin II) the investigation of the effect of gain- and loss of function approaches III) the observation of SUMO2's influence on cardiomyocyte hypertrophy and ultimately IV) to encode the underlying mechanism of action by which SUMO2 mediates its effects on the cell.

5 Material and methods

5.1 Materials

5.1.1 Hardware and consumables

Amersham Hybond-P PVDF membrane	GE Healthcare
Axiovert 40 C Microscope	Zeiss
Cell Scraper 16cm 2-position blade	Sarstedt
Cellstar cell culture dishes 6-, 12-, 24-well, 6cm-, 10cm dishes	Greiner Bio one
Centrifuge 5810	Eppendorf
CFX96 Real-Time PCR Detection Sys	BioRad
Coverslips 18 mm diameter	Karl Hecht KG
Duomax 1030 horizontal rotator	Heidolph
DynaMag-2 Magnetic Particle Conc.	Invitrogen
ECX-F26.M UV-trans illuminator	Peqlab
Electroporation cuvette	Peqlab
Filter, paper 110 mm diameter	Schleicher & Schuell
FluorChem Q Camera (Western Blot)	Alpha Innotech
Galaxy Ministar Microcentrifuge	VWR
Heraeus Fresco 21 Centrifuge	Thermo Scientific
Heraeus Pico 21 Centrifuge	Thermo Scientific

Horizon 11-14 Gel-electrophoresis	Life Technologies
Infinite M200Pro microplate reader	Tecan
Mini PROTEAN Tetra System	Bio Rad
Mr. Frosty™ Freezing Container	Thermo Scientific
MyCycler Thermal Cycler	Bio Rad
NanoDrop 2000 spectrophotometer	Thermo Scientific
Neubauer- cell counter	Assistent
Slide 76x26x1 mm	MARIENFELD
Olympus BX53 microscope	Olympus
Olympus DP72 camera	Olympus
Parafilm	BEMIS
Pasteur pipettes, glass	ROTH
Pipettes Eppendorf-Reference	Eppendorf Research
Pipette tips Biosphere Filter Tip	Sarstedt
Pipette tips, with filter	Sarstedt
Pipetus	Hirschmann Laborgeräte
Power Pac HC	Bio Rad
PP-Microplate 96-well	Greiner-Bio One
RCT Basic magnetic stirrer	IKA
Tubes 0.5 mL, 1.5 mL, 2 mL, 5 mL	Sarstedt
Tubes 15 ml, 50 ml	Sarstedt
Pipettes 2 mL, 5 mL, 10 mL, 25 mL	Sarstedt
Precellys 24 homogenizer	Peqlab
qRT-PCR plates, 96-well, semi skirted	Bio-Rad

Seven Easy pH-meter	Mettler-Toledo
Stemi 2000-C microscope	Zeiss
Steril-Cult 200 incubator	Labotect
Sterile filter 0.2µm pores	Nalgene Labware
SterilGARD Hood	The Baker Company
TE1502S precision scale	Sartorius
Thermomixer Comfort	Eppendorf
Titan PCR-working station	Scanlaf
Vacusafe ventilation	Integra Biosciences
Variomag Poly magnetic stirrer	Thermo Scientific
Vortex-Genie 2	Scientific Industries
Cell culture flasks 75cm^2, 175cm^2	Sarstedt

5.1.2 Chemicals

Agarose	Biozym Scientific GmbH
Albumin fraction V, bovine	Merck KG
Carbenicillin	Sigma-Aldrich
DAPI	Sigma-Aldrich
DEPC	Sigma-Aldrich
DMEM	PAA Laboratories
DMSO	Sigma-Aldrich
DNA Loading Dye 6x	Fermentas
Collagen I – solution, bovine skin	BD Biosciences

DreamTaq 10x green buffer	Thermo Scientific
DynaBeads Protein G sepharose	Novex by Life Technologies
EDTA	Serva Electrophoresis
Ethanol	Carl Roth
Ethidiumbromide	Invitrogen
FCS Gold	PAA Laboratories
Fluor Preserve Reagent	Calbiochem
Formamide	Sigma-Aldrich
GeneRuler 1kb Plus DNA Ladder	Fermentas
HEPES	Carl Roth
Hygromycin B	Invitrogen
Ionomycin	Sigma-Aldrich
iQ PowerMix Reagent, multiplex qRT	Bio-Rad
Kanamycine	Sigma-Aldrich
Lipofectamine 2000 Reagent	Invitrogen
Methanol	Carl Roth
NCS (Newborn Calf Serum)	PAA Laboratories
PageRuler Plus prestained Protein Ladder	Thermo Scientific
Penicillin/Streptomycin	Invitrogen/GIBCO
Phenol/Chloroform/Isoamylalcohol	Carl Roth
Phenylephrine	Sigma-Aldrich
PMA (Phorbol-12-myristat-13-acetat)	Sigma-Aldrich
Protein-Assay dye-concentrate (Bradford)	Bio-Rad
QIAzol Lysis Reagent	Qiagen

Sodium chloride	AppliChem
Sodium hydroxide	AppliChem
SDS	Serva Electrophoresis
Spectinomycin	Sigma-Aldrich
TEMED 99% p.a. Electrophoresis	ROTH
Tris-Base	Carl Roth
Tris-HCl	Carl Roth
Triton X 100	Serva Electrophoresis
Trypane blue	Sigma-Aldrich
Tween 20	Sigma-Aldrich
Vectashield HardSet Mounting Medium	Vecta-Labs

5.1.3 Enzymes

Collagenase type 2	Worthington/Cellsystems
Complete-Proteinase Inhibitor Cocktail	Roche Diagnostics
Desoxyribonuclease I (DNase I)	Sigma-Aldrich
DreamTaq DNA-Polymerase (GreenTaq)	Thermo Scientific
LR-Clonase ™ II	Invitrogen
Pac I	BD Biosciences Clontech
BP-Clonase ™ II	Invitrogen
Platinum® Pfx DNA Polymerase	Invitrogen
Phosphatase-Inhibitor 2 und 3	Sigma-Aldrich
Proteinase K	Invitrogen

Trypsin-EDTA-solution Invitrogen/GIBCO

5.1.4 Antibodies

5.1.4.1 Primary Antibodies

Table 1: List of primary antibodies, IF=Immunofluorescence, WB=Western Blot, IP= Immunoprecipitation.

Antibody anti-	**species**	**clonality**	**Company**	**Description**
Alpha-Actinin	mouse	Mono	Sigma-Aldrich	IF
Calcineurin A	mouse	Mono	Transd. Lab (BD)	IF / WB
Calcineurin A	mouse	Mono	Sigma-Aldrich	IP
SUMO2/3 ab	mouse	mono	Abcam	IF / IP
SUMO2/3 CS	rabbit	mono	CellSignaling	IF / WB
α-Tubulin	mouse	mono	Sigma	WB
Gapdh	mouse	mono	Sigma	WB
β-Actin	mouse	mono	Sigma	WB
SUMO1	rabbit	poly	CellSignaling	WB
Ubiquitinated Proteins	mouse	mono	Millipore	WB
Rcan1-1&1-4	rabbit	poly	in-house	WB
Hexon-FITC coupled	mouse	mono	Sigma-Aldrich	WB

5.1.4.2 Secondary Antibodies

Table 2: List of secondary antibodies, IF=Immunofluorescence, WB=Western Blot, HRP= Horseradish peroxidase, AF=AlexaFluor®.

Antibody anti-	species	conjugate	Company	Description
mouse	goat	HRP	SantaCruz	WB
rabbit	goat	HRP	SantaCruz	WB
mouse	donkey	AF546	Life Technologies	IF
mouse	sheep	FITC	Life Technologies	IF
mouse	goat	AF488	Life Technologies	IF
mouse	donkey	AF546	Life Technologies	IF
rabbit	donkey	FITC	Life Technologies	IF
rabbit	goat	AF488	Life Technologies	IF

5.1.5 Oligonucleotides and Primers

Table 3: Oligonucleotide primers for the generation of open reading frame (ORF) fragments of the target gene. Primers are flanked by partial attB1 (forward) and attB2 (reverse) adapters to amplify with the attB1/2 adapter primers in a second PCR and to yield gateway® compatible fragments.

Primer name	Sequence 5' -> 3'	Description
attB_SUMO2-F	TTCCAACAGCAGACGGTCTACTGAGGCGAC	SUMO2 ORF primer
attB_SUMO2-OSR	TGGGTCGCCGTAGACCGTCTGCTGTTGGAA	
attB_SUMO2ΔGG_R	GCTGGGTCGCCTCAGTAGACCGTCTGCTGTTGGAA	SUMO2ΔGG mutation reverse primer
attB_ΔCnA-F	GCTGGCACCATGTCCGAGCCCAAGGC	ΔCnA ORF primer
attB_ΔCnA-OSR	GCTGGGTCGCCGTTTCTGATGACTTCCTTCCGG	
attB_CnA-F	GCTGGCACCATGTCCGAGCCCAAGGC	wt-CnA ORF primer
attB_CnA-MSR	GCTGGGTCGCCTCACTGGATATTGCTGC	
attB1 adapter	GGGGACAAGTTTGTACAAAAAAGCTGGCACC	adapter for full length attB-Fragments
attB2 adapter	GGGGACCACTTTGTACAAGAAAGCTGGGTCGCC	

Table 4: Oligonucleotide primers for annealing and ligation into pCDNA.6.2/GW-miR Vector for expression of micro RNA's in mammalian cells or shuttling into Destination vectors via gateway shuttling.

Primer Name	**Sequence 5' -> 3'**	**Description**
Block-iT_miR-S2_Top	TGCTGATTGGTTGCCCGTCAAATCGGGTTTTGG CCACTGACTGACCCGATTTGGGGCAACCAAT	Micro RNA sequence against SUMO2 within the Block-iT® system by Invitrogen
Block-iT_miR-S2_Bot	CCTGATTGGTTGCCCCAAATCGGGTCAGTCAGT GGCCAAAACCCGATTTGACGGGCAACCAATC	
Block-iT_miR-Neg_Top	GAAATGTACTGCGCGTGGAGACGTTTTGCCACT GACTGACGTCTCCACGCAGTACATTT	Scrambled micro RNA sequence with no specificity for mammalian genes
Block-iT_miR-Neg_Bot	AAATGTACTGCGTGGAGACGTCAGTCAGTGGCC AAAACGTCTCCACGCGCAGTACATTTC	

Table 5: Primers for gene quantification via quantitative real-time PCR (qRT-PCR)

Primer name	**Sequence 5' -> 3'**	**Description**
qRT-SUMO2_F	CCGATTTGACGGGCAACCAATCA	qRT-Primers for *Sumo2*
qRT-SUMO2_R	ACACCTCCCGTCTGCTGTTGGA	
qRT-CnA_F	CCCAGTCACAGTTTGCGGG	qRT-Primers for *ppp3ca* (Calcineurin A)
qRT-CnA_R	GAGGTAGCGAGTGTTGGCAG	
Rpl32_F	CTGCTGATGTGCAACAAATCT	qRT-Primers for *Rpl32* housekeeping / control)
Rpl32_R	GCTGTGCTGCTCTTTCTACAAT	

Table 6: Oligonucleotide primers for gene quantification via Multiplex quantitative real-time PCR (qRT-PCR).

Primer name	**Sequence 5' -> 3'**	**Description**
Nppa_F	GGAGCAAATCCTGTGTACAGTG	Multiplex Primer and probe labeled with dye and quencher for *Nppa*
Nppa_R	ACCTCATCTTCTACCGGCAT	
Nppa_probe	FAM-TGATGGATTTCAAGAACCTGCTAGACCA-BHQ1	
Nppb_F	ACAAGATAGACCGGATCGGA	Multiplex Primer and probe labeled with dye and quencher for *Nppb*
Nppb_R	AGCCAGGAGGTCTTCCTACA	
Nppb_probe	HEX-TCAGTGCGTTACAGCCCAAACGA-BHQ1	
Rpl32_F	CTGCTGATGTGCAACAAATCT	Multiplex Primer and probe labeled with dye and quencher for *rpl32* (housekeeping/control)
Rpl32_R	GCTGTGCTGCTCTTTCTACAAT	
Rpl32_probe	Texas Red-ACTGTGCTGAGATTGCTCACAATGTGT-BHQ2	
Rcan1_fw	TAGCTCCCTGATTGCTTGTG	Multiplex Primer and probe labeled with dye and quencher for *rcan1-4*
Rcan1_rev	GGATTCAAATTTGGCCCTGG	
Rcan1_probe	Cy5.5-ACGATGATGTCTTCAGCGAAAGTGAGAC-Eclipse	

5.1.6 Plasmids

pDonR 221	Invitrogen
pcDNA-DEST40	Invitrogen
pAd/CMV/V5-DEST	Invitrogen
pcDNA3.1	Invitrogen

5.1.7 Viruses

Table 7: Adenoviral constructs used for the overexpression of the depicted constructs in neonatal rat ventricular cardiomyocytes.

Virus Name	**Description**
AdSUMO2	Overexpression construct, wild type
AdSUMO2GG	Overexpression construct, sumoylation-deficient
AdRenilla-Luc	Overexpression construct, housekeeping control
AdNFAT-RE Luc	NFAT-activation response expression construct
AdCnA	Overexpression construct, wild type
AdΔCnA	Overexpression construct, constitutively active
AdmiR-SUMO2	micro-RNA expression

5.1.8 Kits

Block-iT™ Pol II miR RNAi - Expression Vector Kit	Invitrogen
ECL-Select detection system	GE Healthcare
Nucleo Spin Plasmid Kit	Macherey-Nagel
Platinum SYBR Green qPCR SuperMix	Invitrogen
Qiagen PLUS Plasmid Midi Kit	Qiagen

QIAquick Gel Extraction Kit	Qiagen
Quikchange II-XL Mutagenesis Kit	Agilent Technologies
Superscript III First Strand Kit	Invitrogen

5.1.9 Buffers and solutions

ADS-Buffer 10x

1.16 M	NaCl
197 mM	HEPES
94 mM	$NaH_2PO_4 \cdot H_2O$
55.5 mM	Glucose
53.6 mM	KCl
8.3 mM	$MgSO_4$, pH 7.4, sterile filtration

RIPA lysis buffer

50 mM	Tris-HCL
pH 7.5	titrate with 1 M NaOH
150 mM	NaCl
0.5 % (w/v)	Sodium Deoxycholate
1 % (v/v)	NP-40
0.2 %	SDS

NLB (Native Lysis Buffer)

50 mM	Tris-HCL
pH 7.5	titrate with 1 M NaOH
150 mM	NaCl

1 mM	EDTA
5 % (v/v)	Glycerol

Addition of Inhibitors prior to harvest (For NLB and RIPA):

Add to 1 mL of lysis buffer:

40 µl	25x Proteinase-Inhibitor-Cocktail
10 µl	Phosphatase-Inhibitor 2
10 µl	Phosphatase-Inhibitor 3
1 µl	1 M DTT

Running buffer, SDS-PAGE (10x)

250 mM	Tris
1.9 M	Glycine
1 % (w/v)	SDS

PBS

137 mM	NaCl
2.7 mM	KCl
4.3 mM	Na_2HPO_4
1.47 mM	KH_2PO_4, pH 7.4, autoclaved

Laemmli buffer (4x)

250 mM	Tris pH 6.8
5 % (w/v)	SDS
40 % (v/v)	Glycerin
0.005 % (w/v)	Bromophenole blue
10 % (v/v)	2-Mercaptoethanol

Collecting gel buffer

0.5 M	Tris-HCl, pH 6.8

TBS

100 mM	Tris-Cl, pH 7.5
0.9 % (w/v)	NaCl

Transfer buffer

20 % (v/v)	Methanol
25 mM	Tris
192 mM	Glycine
0.037 % (w/v)	SDS

Separating gel buffer

1.5 M	Tris, pH 8.8

Trypsin-EDTA solution

0.25 % (w/v)	Trypsin
0.53 mM	EDTA

In PBS.

5.1.10 Media

LB-Medium (Luria-Bertani)

1 % (w/v) Tryptone

0.5 % (w/v) Yeast-extract

1 % NaCl

Titration to pH 7.0 with NaOH

Growth medium (NRVCM)

DMEM with 4.5 g/L Glucose and 110 mg/l Sodium pyruvate

10% (v/v) FCS Gold

(No FCS in media starting from 24 h of culture)

100 U/L Penicillin G

100 µg/ml Streptomycin

2 mM L-Glutamine

Growth medium (C2C12-NFAT)

DMEM with 4.5 g/L Glucose and 110 mg/l Sodium pyruvate

10 % (v/v) FCS Gold

100 U/L Penicillin G

100 µg/ml Streptomycin

200 µg/mL Hygromycin B

2 mM L-Glutamine

Growth medium (HEK293-A)

DMEM with 4.5 g/L Glucose and 110 mg/l sodium pyruvate

4 % (v/v) FCS Gold

100 U/L Penicillin G

100 µg/ml Streptomycin

2 mM L-Glutamine

5.1.1 Bacteria

DH10B, electro-competent	Life-Technologies
OneShot TOP10, electro-competent	Life-Technologies

5.1.2 Cell lines

HEK293-A

Human embryonic kidney cells, adenovirally transformed, stably expressing Adenovirus Type 5 Genes E1 and E3 among others and the SV40 large T-antigen for episomal replication of SV40 promoter-containing plasmids.

C2C12-NFAT

C2C12 myoblasts were stably transfected using the “pHTS-NFAT” (Biomyx Technology) reporter vector carrying a luciferase expression cassette under control of four NFAT enhancer sites and an additional Hygromycin selection marker (Frey et al., 2008).

5.1.3 NRVCM

Neonatal rat ventricular cardiomyocytes, a primary cell line from 1-3 day old neonatal rat ventricles. Cultivation of these cells is explained in detail in the methods section.

5.1.4 Animals

New born rats for obtaining hearts for primary cell culture of NRVCM.

Adult Wistar rats were ordered from the company Charles-River and bred in the central animal facility of the University Hospital of Kiel, UKSH.

5.2 Methods

5.2.1 Microbiological methods

5.2.1.1 Generation of electro-competent bacteria

For transformation via electroporation, bacteria are needed that are able to uptake plasmids from the culture media after application of high voltages. Therefore 50 mL of LB-medium with E. *coli*DH10B bacteria are pre-incubated overnight at 37°C at 200 rpm in an incubator. The next day, 1 L of pre-warmed LB-Medium was inoculated with the overnight culture to gain an OD_{600} of 0.1. This culture was then incubated at 37°C and 200rpm until an OD between 0.4 and 0.8 was measured (~2 h). Rapid cool down of the culture in an ice and water bath was carried out and after that, bacteria were pelleted in a centrifuge at 4 °C for 15 minutes at 11000 g. The pellet was then washed in ice-cold, autoclaved ddH_2O and centrifuged. Two of those washing-steps were carried out. After the second washing, the pellet was re-suspended in 250 mL 10 % (v/v) glycerol in ddH_2O and centrifuged as before. The pellet was then re-suspended in 1.5 mL 10 % (v/v) glycerol in ddH_2O and aliquoted in autoclaved tubes in a 50 µL scale and frozen to -80 °C on dry ice immediately. Transformation efficiency was determined by separately transforming three of the stocks with a control plasmid as described below and spreading 1/100 of the reaction onto a 100 µg/mL ampicillin containing LB-Agar plate. Overnight cultivation at 37 °C and counting of yielded clones determined the efficiency.

5.2.1.2 Electroporation

Electro-competent E. *coli* bacteria were thawed on ice for five minutes. About 5 ng of Plasmid-DNA was added directly to the bacteria and the suspension was carefully mixed by pipetting up and down. The mix was transferred into a pre-chilled (-20 °C) electroporation-cuvette and transformed at 2.5 kV, 200 Ω und 25 µF. After the electric pulse, 1 mL of LB-Medium was added to the bacteria and transferred into a new, autoclaved reaction tube. The transformed bacteria were incubated at 37 °C for 1 h in a thermomixer at 700 rpm. A portion of the incubated

bacteria was then plated onto LB-Agar containing the appropriate antibiotic for selection of successfully transformed containing E. *coli*.

5.2.1.3 Agar plate preparation

LB-Medium was prepared with the addition of 1.5 % (w/v) agar. After autoclaving the solution it was cooled down in a water bath to 55 °C. The respective antibiotic was added at that temperature to prevent structural breakdown. Instead of ampicillin the substitutable antibiotic carbenicillin was used at a concentration of 100 µg/mL. Kanamycin and spectinomycin were used at concentrations of 50 µg/mL. The warm, antibiotic containing solution was then casted into 10 cm petri dishes under a sterile hood. Cooled-down agar plates were stored at 4 °C until use.

5.2.1.4 Spreading of bacteria cultures

Transformed bacteria were spread onto agar plates employing 4-6 sterile glass beads and vigorous shaking. The volume of electroporation mix depended on the respective plasmid, typically 100 µL. Plates with bacteria were then incubated at 37 °C overnight or for 14-16 h. Individual colonies were then picked with a pipette tip for further experiments.

5.2.1.5 Growth of the bacteria in liquid-culture

To the desired amount of LB-medium the appropriate antibiotic was added at the above mentioned concentrations. Single colonies picked with a pipette tip or low µL amounts of liquid bacteria in culture were inoculated to the LB-medium and incubated at 37 °C and 200 rpm horizontal shaking over night or for 14-16 h.

5.2.2 Cell culture methods

5.2.2.1 Culture of mammalian Cells

All cell culture operations were performed under a sterile hood, separately for each cell line to avoid cross-contamination of the cells. Cells were incubated in a 37 °C incubator with 5 % CO_2.

5.2.2.2 Coating of cell culture dishes with bovine collagen I

All culture dishes and flasks to be used for the culturing of NRVCM had to be coated with collagen I prior to seeding the cells. Therefore a collagen I stem-solution (3.1 mg/mL) was diluted to a concentration of 50 µg/mL. Dished were coated with 5-10 µg/cm² collagen I solution for at least 1 h at RT or overnight. After two washing steps with sterile ddH_2O the plates were air-dried and stored at 4 °C until usage. Plates were stored for no longer than 7 days.

5.2.2.3 Primary culture of neonatal rat ventricular cardiomyocytes

This protocol describes the procedure for the purification and culturing of 40 hearts. For the generation of primary cultures from neonatal rat left ventricles, about 40 neonatal rats were sacrificed per preparation. After short immerse in 75 % ethanol solution, the rats were rapidly decapitated with scissors. An incision of about 2cm into the thorax was made left of the sternum. Under application of mild pressure on the abdomen, the heart was taken out and immediately placed in ice-cold ADS-buffer. The atria were removed and ventricles moved into fresh ice-cold ADS buffer. After removal of the buffer, the ventricles were dissociated with scissors until only small pieces of connected tissue were visible. The tissue was transferred into digestion-solution. This solution contains 0.5 mg/µL collagenase type 2 and 0.6 mg/mL pancreatin in ADS buffer and was sterile-filtered and heated to 37°C prior to use. Digestion took place at 37°C in a water bath at 40 rpm horizontal shaking. After 20 minutes, the supernatant was removed and discarded. Fresh digestion-solution (1 mL per heart) was added and incubated for 20 minutes. The supernatant containing single cells was further processed and to the remaining tissue, fresh digestion-solution was added and further incubated until the

tissue was dissociated completely. The supernatants were pipetted through a cell-strainer into a 50 mL reaction tube and 8 mL of new born calf serum (NCS) was added to inactivate collagenase and pancreatin. The solution was then centrifuged at 1000 g, the supernatant discarded and the cells resuspended in 5 mL NCS and stored at 37°C in an incubator until further use. After four to five of these digestion steps, the pooled and in NSC resuspended cells were centrifuged, pelleted and resuspended in 50 mL ADS buffer.

This solution contains cardiomyocytes along with fibroblasts, blood-cells and other types of cells found in the heart an needs to be purified. Therefore cells were separated by their density over a percoll-gradient column (Iwaki et al., 1990). A percoll stem-solution was made from 27 mL percoll and 3 mL 10x ADS. From this stem-solution, two solutions with high and low density were generated. Low-density percoll solution contains 9 mL of stem solution and 11 mL ADS buffer. 4 mL of the low density-solution was pipetted into a 15 mL reaction tube. High-density percoll solution contains 13 mL stem-solution and 7 mL ADS buffer and was added to the 15 mL tube by carefully pushing the pipette through the low-density percoll solution and pipetting the high-density percoll solution to the bottom of the tube. For column-integrity it is crucial to pipette the solution very slowly and avoid pipetting air-bubbles into the mixture. Addition of phenol-red dye to the low-density solution allows for visualization of gradient-phase separation. 500µL of the cell-solution was carefully pipetted onto one gradient and centrifuged at 3000 g and 4 °C for 30 minutes with slow acceleration and deceleration without breaks. Cells are separated by their density and three phases of the column are visible. Cardiomyocytes travel through the column till the phase-border between low and mid phase and can be isolated/removed with a transfer pipette. Fibroblasts are less dense and do not travel as far, whereas erythrocytes pellet at the bottom of the tube. The myocytes were resuspended and washed twice in 50 mL ADS and centrifuged at 1000 g for 5 min. After two washing steps, NRVCM were resuspended in 1 mL cardiomyocytes growth medium and counted in a Neubauer Chamber with Trypane-blue staining. Cells were seeded onto different plates at various densities for the respective dishes and experiments as depicted in table 7.

Table 8: Individual seeding density of neonatal rat ventricular cardiomyocytes in different cell-culture plates and dishes.

Plate-type	Experiment type	Cells / well	mL Medium / well
10 cm dish	Protein isolation	10*10^6	10
6-Well plate	Protein isolation	1*10^6	2
12-Well Plate	RNA isolation	3.5*10^5	1
12-Well Plate	Luciferase experiment	4*10^5	1
12-Well Plate with coverslips	Immunofluorescence	1.8*10^5	1

NRVCM are seeded and incubated in growth medium containing 10 % FCS for the first 18h of culture. For all experiments with NRVCM mentioned in this thesis, the cells were washed with warm PBS on the next day and supplemented with FCS-free growth medium for the remaining time of culture.

5.2.2.4 Culture of immortalized cell lines

5.2.2.5 Culture of cells from liquid nitrogen cell stocks

Cry conserved cells are stored in liquid nitrogen. Cells are thawed rapidly in a 37°C water bath and 1 mL of pre-warmed growth medium is added to the cells. The cell solution is then transferred into a T75 cell culture flask containing 8 mL of warm growth medium.

5.2.2.6 Culture of HEK293-A cells

HEK293-A cells grow in a monolayer on non-coated plastic surfaces.

The doubling time of HEK293-A is 36h under optimal conditions. Cells were passaged at 70-80 % of confluence. Culture medium was removed and cells washed with warm PBS that was removed afterwards. Cells were dissociated by addition of 2 mL Trypsin-EDTA solution and incubation for 1-2 min at 37 °C until single cells were visible under the microscope. 10 mL of growth medium were added to the cell-solution to stop the trypsin activity completely. The cells were then centrifuged at 1000 g at RT for 5 min. The supernatant was discarded and the

cells were resuspended in warm growth medium. Afterwards the cells were either counted in a Neubauer chamber and seeded in the respective plate or - without counting - seeded at a ratio of 1:10 into new T175 flasks for maintenance of the cell line.

5.2.2.7 Culture of C2C12-NFAT cells

The C2C12 cell line grows in monolayer on non-coated plastic surfaces. It differentiates rapidly, forming contractile myotubes and producing characteristic muscle proteins when grown confluent and/or supplemented with differentiation medium. All experiments were carried out in undifferentiated C2C12 cells, therefor they were not allowed to grow confluent and were passaged in the same way as the HEK293-A in a different growth medium containing hygromycin for plasmid-carrier selection.

5.2.2.8 Cryo-conservation of the cell lines

To generate cryo-stocks of the cells, one T175 flask was passaged as described but finally resuspended in media containing 20 % FBS and 10 % glycerol. Cell density should be $1\text{-}2*10^{12}$ cells/mL. 1 mL of the cell-solution was pipetted into a cryo-vial and cooled down at 1 °C per minute in a freezing-container to -80 °C over night. On the next day, cells were transferred into liquid nitrogen for storage.

5.2.3 Molecular biology methods

5.2.3.1 Plasmid DNA extraction – Mini preparation

For extraction of small amounts of Plasmid DNA from 5 mL E. *coli* DH10B overnight cultures, the NucleoSpin® Mini-Preparation-Kit was used. Single clone from agar plates or 5 µL of a liquid culture were inoculated into 5 mL of LB-medium containing the appropriate antibiotic. Bacteria were cultured overnight as described above. 5 mL of the bacterial culture were pelleted at 4 °C and 10.000 g for 15 min. All centrifugation steps in this protocol were carried out at RT and 11.000 g in a benchtop centrifuge. The pellet was resuspended in 250 µL of

buffer A1 (resuspension buffer). 250 µL of buffer A2 (lysis buffer) was added, mixed and incubated at RT for 5 minutes. 300 µL of buffer A3 (neutralization buffer) was added to stop the lysis reaction. The solution was then centrifuged for 5 min, the supernatant loaded onto the provided silica-membrane column and centrifuged. In this step the plasmid DNA binds to the column. The flow-through was discarded and after addition of ethanol-containing washing buffer A4 the columns were then centrifuged, flow-through was discarded and the columns were centrifuged 'dry' for 2 minutes. 22 µL of EB-buffer was pipetted onto the column-membrane and incubated at 55°C for 3 minutes to support the solving of the Plasmid DNA into the EB-buffer. Centrifugation for 1 minute elutes the DNA from the membrane. The final flow-through contains the plasmid DNA extracted from the bacteria culture.

5.2.3.2 Plasmid DNA extraction – Midi preparation

For extraction of small amounts of Plasmid DNA from 5 mL E. *coli* DH10B overnight cultures, the Quiagen Plasmid Plus Purification Midi-Kit was used. Single clones or 5 µL of liquid culture were incubated overnight in a 50 mL or 100 mL scale. Bacteria were pelleted in 50 mL reaction tubes at 4 °C and 6.000 xg for 20 minutes. 2 mL of buffer P1 is added followed by 2 mL of P2 (lysis buffer) and then incubated at RT for 3 minutes. For neutralization of the alkaline lysis conditions 2 mL of buffer P2 was added and placed into a filter cartridge. After 10 min of incubation, a plunger was inserted into the cartridge and the cell lysate filtered through the membrane to remove cell debris. To the flow through, 2 mL of buffer BB was added, mixed and transferred to the spin column, attached to the vacuum-generator. The solution was then sucked through the spin column by applying -300 mbar. Endotoxins were removed by addition of 700 µL of ETR buffer to the column and application of vacuum, followed by a washing step with 700 µL of ethanol-containing washing buffer PE. For complete removal of buffer residues, the column was centrifuged at 11.000 g for 2 min. 200 µL of 55 °C warm EB-buffer was added to the column and incubated at 55 °C for 3 min. The column was then centrifuged at 11.000 g for 1 min and the plasmid DNA was eluted.

5.2.3.3 Agarose gel electrophoresis

Agarose gel electrophoresis was utilized to separate DNA based on the size of the fragment. Therefore a 1 % agarose (w/v) was solved in TAE buffer by cooking the solution for one minute in a microwave. The solution was then cooled down to approximately 60°C and supplemented with 0.5 µg/mL ethidiumbromide. The solution was casted into the gel-chamber and allowed to polymerize at RT for 20 min. A comb was inserted into the liquid solution to create pockets in the gel for the samples. After polymerization, the comb was removed and the gel was then placed into the electrophoresis chamber, filled with TAE buffer to cover the gel. DNA-containing samples were pipetted into the pockets and an electric field at 100 V was applied. The negatively charged DNA travels through towards the anode and is separated according to the size of the fragment, were large fragments travel slower than small fragments.

5.2.3.4 Open reading frame (ORF) PCR

For the amplification of the gene of interest, polymerase chain reaction was used. Different DNA polymerases can be used, depending on the length of the construct, the annealing temperature of the primers and also the GC-content. For the experiments shown in this thesis, the Platinum® *Pfx* DNA Polymerase was used, a DNA-dependent DNA-polymerase with 3'-5' exonuclease activity ("proof reading") to avoid mutations in the amplified construct. The standard-reaction mix was modified according to the manufacturer's manual if needed, varying either the salt concentration ($MgSO_4$) or addition of DMSO for an increase of the primer-annealing temperature range. Typically the PCR was carried out in a 50 µL scale to yield enough amplified DNA fragments for extraction from an agarose gel.

5.2.3.5 Cloning of full length and ΔGG-deletion of SUMO2

Full-length and ΔGG mutant of mouse *Sumo2* were cloned from mouse heart cDNA by using the below explained Gateway® system of molecular cloning with the primers listed in Table 3 for a first PCR, and attBFor and attBRev for a second step PCR. The PCR product was recombined into the pDonR221 plasmid using the Gateway technology and then subsequently recombined into expression plasmids pcDNA-DEST40 (SUMO2ΔGG-construct) and

pcDNA3.1 (full length construct), for expression in C2C12 cells or into pAd/CMV/V5-DEST for adenoviral expression in NRVCM.

5.2.3.6 DNA extraction from agarose gels

DNA that was separated via agarose gel electrophoresis can be isolated and purified from the gel. The QuiaQuick® Gel-extraction system was used. Therefore the ethidiumbromide-stained DNA in the gel was visualized under UV-light, cut out with a new scalpel and transferred into a 2 mL reaction tube. The sample was then weighed and three times the volume of the gel-slice QG-buffer was added to the tube (e.g. 100 µL for every 0.1 g of gel). The gel-slice was then incubated at 55 °C for ten minutes or until the gel had dissolved completely. The solution was transferred into a spin-column containing a silica-membrane for DNA binding 500µL portions at a time and subsequently centrifuged at 11.000 g for 1 min each. Finally another 500 µL of fresh QG-buffer was added to the column and centrifuged. The flow-through was discarded for each of the steps. The columns were then washed with 600 µL of ethanol containing PE buffer by centrifugation. Residual buffer was removed by centrifuging at 11.000 g for 2 min. Addition of 22 µL EB-buffer allows for elution of the membrane-bound DNA in another centrifugation step.

5.2.3.7 DNA and RNA concentration measurement

DNA and RNA concentration was determined with the NanoDrop™ photometer. Optical density was measured at 260 nm and 280 nm and concentrations automatically calculated for DNA or RNA respective to the used diluent. Measurements were carried out in duplicates an the mean concentration determined

5.2.3.8 Molecular cloning using Gateway®-technology

For the cloning of open reading frames or micro-RNAs, I utilized the Gateway®-System that uses a recombination-system from the bacteriophage λ, which can enzymatically integrate genomic regions into the genome of E. *coli*. The reaction is site specific and reversible. As a first step, the gene of interest is amplified via ORF-PCR from a cDNA pool of the desired

species (e.g. cDNA isolated from mouse, human or rat tissue), using primers that contain partial attB1 and attB2 flanking sequences. This yields cDNA copies of the open reading frame of interest flanked by the specific parts of the attB-sequences. In a second PCR, the first product was used as a template and amplification was carried out with primers containing the full attB1 and attB2 sequences using the same conditions as for the ORF PCR. This generates copies of the ORF of interest flanked by the full-length attB sites.

These flanked constructs were then recombined into the specific donor (DONR) vector with the BP Clonase ® II by incubating 150 ng of PCR-product along with 150 ng of pDonR221 vector, 1 µL of BP Clonase II in a reaction volume of 10 µL overnight at RT. This enzyme is able to cut out regions flanked by specific regions called attP and replace them with attB flanked sequences. This step allows the integration of the generated ORF sequences into the pDonR221 vector. The generated flanking sites are called attL-sites (attB-insert + attP-vector → attL vector). Similar to this step, the shuttling of the sequence of interest from pDonR to a destination (DEST) vector is carried out with another enzyme, the LR Clonase ® II. This enzyme catalyzes the recombination between attL and attR sites. The insert-carrying pDonR and the destination vector are recombined by the Clonase in the same way than the BP Clonase reaction was prepared to yield the destination vector constructs containing the sequence of interest.

The empty vectors contain a resistance for specific antibodies for selection of plasmid-carrying bacteria after transformation as well as a ccdb-gene (“suicide cassette”) that is only removed when the gene of interest or micro RNA is recombined into the plasmid. All generated plasmid-constructs were amplified in E. *coli*, DNA isolated and sequenced to assure insertion of correct and unmutated sequences.

5.2.3.9 Generation of artificial micro-RNA constructs using the Gateway®-compatible Block-iT system

For the cloning of micro RNAs, the Block-iT RNAi-designer by Invitrogen was used to generate target-specific miRNAs flanked by specific sequences that allow formation of hairpin-structures and subsequently correct processing of the miRNA in the mammalian cell.

Therefore the generated oligonucleotides with 3' and 5' overhangs were annealed in 10x oligo-annealing buffer and ligated into the linear pcDNA6.2-GW/miR vector via T4 DNA ligase (1 U/µL). The insertion into the vector is next to a polymerase II promotor sequence that is flanked by the attB1 site, generating an attB site flanked, Pol II promoter and miRNA sequence. The so generated plasmid is then transformed into E. *coli* OneShot® TOP10 bacteria, since DH10B have a natural spectinomycin resistance which is the selection marker of the pcDNA6.2 vector. Thus, only TOP10 bacteria carrying the plasmid will survive the spreading on spectinomycin (50 µg/mL) containing agar plates. Plasmids were amplified in bacteria as described before. The shuttling into a donor and subsequent destination vector is carried out by BP Clonase® II and LR Clonase® II as described.

5.2.3.10 RNA extraction from cells grown in vitro

Total RNA was isolated from cultured cells using QIAzol lysis reagent. 1 mL of QIAzol was added to each well of twice washed cells after removing the PBS. Cells were further lysed by pipetting up and down and the solution then pipetted into a fresh 1.5 mL reaction tube. 200 µL of chloroform was added and the solutions mixed by inversion of the tubes. The reaction was then centrifuged at 15.000 g for 15 min at 4 °C to separate the phenolic and the aqueous phase. The RNA-containing aqueous phase was carefully removed with a pipette without disturbing the interphase and placed in a fresh, RNAse and DNase free reaction tube. 500 µL of Isopropanol was added and the DNA precipitated for 30 min at RT. The precipitated DNA was centrifuged down at 17.500 g for 20 min and the supernatant carefully decanted. The pellet was washed with 1 mL of 75 % ethanol and centrifuged down for 5 min at 15.000 g. The supernatant was decanted and the pellet was air-dried for 5-10 min. The DNA was then solved in DEPC-treated, RNAse and DNase free water and concentration determined via NanoDrop photometer. 5 µg of RNA were DNase I digested in a reaction mix of 50µL containing 5 µL of DNase I and 5 µL of DNase 1 buffer for 15 min at RT to disintegrate any DNA that contaminated the RNA preparation. The DNase I was then precipitated by addition of 50µL of a 25:24:1 phenol-chloroform-isoamylacohol solution and centrifuged at 17.500 g for 10 min. The supernatant was pipette into a fresh RNAse-free reaction tube and 300 µL of 99.99 % ethanol was added together with 10 µL of 3 M sodium acetate. Precipitation of the RNA occurred at -20 °C for 30 min and afterwards the samples were centrifuged at 17.500 g for 40 min at 4 °C.

The supernatant was discarded and the pellet washed with 500 µL of 75 % ethanol. After another centrifugation at 17.500 g for 5 min at 4 °C the pellet was air-dried for 5-10 min and solved in an appropriate amount of RNAse-free H_2O (approximately 25 µL H2O for RNA from 1 Well of a 12-well-plate).

5.2.3.11 Generation of cDNA from RNA samples

One µg of DNA-free total RNA was transcribed into cDNA using the Superscript III first strand cDNA synthesis kit. Therefore the DNA was diluted in a total volume of 13 µL RNAse and DNase free water containing 250 ng of random-hexamer primers and 0.5 µL of 10 mM dNTPs (2.5 µM of each: desoxy adenosine, desoxy thymine, desoxy guanine and desoxy cytosine) and denatured for 5 min at 65 °C in a PCR-cycler. The master mix for the RNA-dependent DNA-polymerase was prepared for a volume of 7 µL for each reaction containing 4 µL of 5x FS (First strand) buffer, 1µL of 0.1 mM DTT, 1 µL RNAseOUT RNase inhibitor and 1 µL of SuperScript III DNA Polymerase. To the denatured RNA, 8 µL of master mix was pipetted and placed into a Thermocycler for the synthesis of cDNA. Cycling conditions were 10 min at 25°C, 1 h at 50 °C, 15 min at 70 °C and then cooled down to 4 °C on hold. The approximate synthesis of 1 µg of cDNA was then diluted 5-fold to a final approximate concentration of 2 ng/µL cDNA which was then further analyzed by qRT-PCR.

5.2.3.12 RNA extraction from tissue samples

To harvest RNA from whole mouse hearts, the tissue had to be broken down using the Precellys® 24 homogenizer. The hearts were placed in reaction tubes and 1 mL QIAzol lysis solution was added along with plastic beads and placed in the homogenizer. The homogenization program used, depended on the size of the hearts and was either 2 x 20 s at speed 5000 or 2 x 15 s at speed 6500 until complete dissociation of the tissue. The dissolved tissue was then centrifuged at 12.000 g for 20 min and the supernatant placed into a fresh 1.5 mL reaction tube. The RNA-extraction with subsequent cDNA synthesis was carried out as described for cell-culture based RNA extraction.

5.2.3.13 Quantitative real-time PCR

For the quantification of genes, the Platinum® SYBR® Green qPCR Supermix-UDG was used. SYBR Green binds to the newly amplified DNA and raises a signal proportional to the amount of cDNA in the reaction. The dye is then excited with a laser and its emission is measured and automatically detected by the PCR-cycler. Therefore 18 µL of a master mix for each sample were prepared, containing 10 µL Platinum® SYBR® Green qPCR Supermix, 0.4 µL of Forward+Reverse Primer (10 µM each) and 7.6 µL of DNase-free H_2O. The master mix was pipetted into the wells of the real-time PCR plate and 2 µL of cDNA (4 ng) was added. After sealing the plate with adhesive foil, the samples were spun down and measured in the qRT-PCR cycler. Cycling conditions are: 3 minutes at 95°C, followed by 40 cycles of (15 seconds at 95°C and 45 seconds at 60°C, a common step for annealing and extension at which step the fluorophor was excited and the emission was collected). Rpl32 was used as an internal normalization control (Frank et al., 2008). Samples were prepared in hexaplicates and qRT-measurement was carried out in duplicates for each sample. For the quantification, the principle of threshold-cycling was utilized were the threshold is the first value that is significantly higher than the background.

5.2.3.14 Protein extraction from tissue samples

To harvest Protein from whole mouse hearts, the tissue was broken down using the Precellys® 24 homogenizer. The hearts were placed in reaction tubes and 1 mL of lysis buffer was added along with plastic beads and placed in the Precellys. The homogenization program used depended on the size of the hearts and was either 2 x 20 s at speed 5000 or 2 x 15 s at speed 6500. The dissolved tissue was then centrifuged at 12.000 g for 20 min and the supernatant placed into a fresh 1.5 mL reaction tube. The protein concentration was measured by DC™-Protein concentration measurement assay.

5.2.3.15 Protein extraction from cell culture

The cell culture media is removed and cells are washed with ice-cold PBS twice prior to addition of the lysis buffer containing protease and phosphatase inhibitor cocktails. Plates are

then directly placed on ice and incubated for 15 min. From this step on, the protein is constantly kept at 4 °C or on ice. The cells were scraped off with a cell-scraper and transferred into a reaction tube. NRVCM were further lysed by 3 freeze-thaw cycles from -80 °C to 4 °C. The solution was then centrifuged at 12.000 g for 20 min and the supernatant carefully transferred to a fresh tube without disturbing the pelleted cell-debris.

5.2.3.16 Protein concentration measurement using DC protein-assay kit

For determination of the protein concentration from the above mentioned, harvested protein-solutions from tissue or cells, the DC™-Protein assay kit was used. Therefor a standard-curve with a known protein concentration had to be generated. The stock-solution of 4 mg/mL BSA (w/v) solved in the respective lysis buffer was diluted in a way were 6 tubes were filled with 20 µL of lysis-buffer and to the first tube, 20 µL of the stock was added to obtain a concentration of 2 mg/mL. From this tube, 20 µL were pipetted to the next tube until all 6 tubes were serially diluted. The stock and protein were pipetted into an appropriate 96 well plate that allowed for measurement of the OD at 750 nm. 5 µL of the standard and sample were pipetted into each well, 25 µL of provided solution A' was added, followed by 200 µL of solution "B". After an incubation of 15 min, the samples were measured photometrically and by linear regression of the standards, the protein concentration in the samples was measured respectively if in range between first and last standard concentration.

5.2.3.17 Reporter gene assays

All the reporter gene assays shown in this work were performed either in NRVCM or C2C12-myoblasts. Cells were infected with combinations of different viruses listed in *Table 7* along with adenoviruses carrying NFAT-responsive element firefly luciferase and Renilla luciferase for normalization of the measurements. Studies were performed in a 12-well-plate format using a dual luciferase reporter assay. Therefore the media was removed and cells washed twice with ice-cold PBS. 100 µL of passive lysis buffer provided with the kit was added and the plates were freeze-thawed twice to -80 °C and then shaken at maximum speed on a horizontal plate shaker for 15 min at RT. 20 µL of the cell-lysate was pipetted into one well of a chemiluminescence compatible 96-well-plate and placed in the infinite m200 PRO system.

Chemiluminescent solutions were automatically injected into the well, where first solution A was injected and firefly luciferase derived chemiluminescence was measured. After that, solution B was injected that quenched the luminescence of the firefly luciferase, followed by the measurement of the Renilla luciferase chemiluminescence measurement.

5.2.3.18 Co-Immunoprecipitation

Mouse left ventricles were homogenized as described in 5.2.3.14 in native lysis buffer (NLB). Protein concentration was measured with the DC assay (5.2.3.16) and 1 mg of protein diluted in a total volume of 1 mL in a fresh reaction tube. Approximately 4 µg of anti-SUMO2+3 antibody (mouse monoclonal, Abcam) or anti-HA antibody (mouse monoclonal, Sigma, control) was allowed to interact with 1 mg of protein for 6 h at 4 °C on a rotating wheel (speed 12), to which 50 µl of equilibrated Dynabeads were pipetted. The beads were equilibrated prior to usage by adding 1 mL of NLB to 50 µL of beads in a reaction tube and rotating the solution on a wheel for 5 min at 4 °C, then placed on a magnetic rack and discarded off the buffer. This equilibration step was carried out three times. The IgG-bound proteins were incubated with the beads for IgG-to-beads binding overnight at 4 °C. The supernatant was removed after placing briefly centrifuged tubes on a magnetic stand. Beads were then washed for 6 times with native lysis buffer in the same way as equilibration was carried out. Precipitated proteins were eluted by incubating the buffer-free beads with 50 µl of 2x Laemmli buffer for 5 min at 95 °C. Samples were spun down in a micro centrifuge and placed on a magnetic rack. The eluted samples were pipetted into a fresh reaction tube and the beads discarded. 10-20 µl of the eluted IP-sample was subjected to SDS-polyacrylamide gel electrophoresis (SDS-PAGE), followed by western-blot transfer to polyvinylidenefluoride membranes and western blotting.

5.2.3.19 SDS polyaclylamide gel electrophoresis (SDS-PAGE)

To separate proteins according to their molecular weight, we used a sodium-dodecyl-sulfate polyacrylamide gel electrophoresis. SDS is a molecule that stoichiometrically binds to and denatures protein chains as well as masking the protein's charges, creating an overall negative charge and therefor allowing the protein to travel along a discontinuous electrical field. The SDS-containing samples are separated with the help of a polyacrylamide gel. Therefor the

appropriate gel-casting-cassette is set up and filled to ¾ with separating gel containing 8 to 12 % polyacrylamide. Therefore, separating gel buffer, water and a 37.5:1 acrylamide: bisacrylamide-solution were mixed and TEMED and APS were added to aid the polymerization and provide free radicals. The cassette is then immediately filled up with isopropanol on top of the separating gel to remove any air bubbles and create an even horizon. After 20 min, the isopropanol was discarded and the collecting gel containing 4 % polyacrylamide is poured on top of the separating gel and a comb, creating 10 or 15 pockets is inserted into the collecting gel. After polymerization, the gel-chamber was set up and the combs removed. The pockets were then flushed with running buffer and samples could be loaded into the pockets. Alongside the samples, a pre-stained marker had to be loaded to determine the range of travel of the different size proteins. An electrical field was applied at constant voltage of 120 and the proteins separated until the bromphenole-blue from the samples reached the bottom of the gel-cassette.

5.2.3.20 Western blotting

To transfer the proteins from the polyacrylamide-gel to a polyvinylidenefluoride (PVDF) membrane, we used a tank-transfer blotting chamber. The SDS gel is therefore carefully taken out of the cassette and set up in the so called “blotting sandwich”. The setup is from bottom to top: a sponge, two cellulose filter papers, the SDS gel, the PVDF membrane, two cellulose filter papers and a sponge. The PVDF-membrane has to be incubated in methanol for 10 s prior to usage. The sandwich has to be set up in the transfer buffer and completely free of air-bubbles to ensure quantitative transfer of the proteins along the membrane surface. The sandwich-containing cassettes are then placed in the blotting-tanks that are filled up with transfer-buffer and cooled via -20 °C cold ice-packs inside the tank. An electrical field is then applied at constant 380 mA for 90 min. The transfer can be visualized after blotting by assessing the transfer of the pre-stained protein ladder that ran alongside the samples and is visible on the white PVDF-membrane. The membrane containing the size-separated proteins is the placed in 5 % (w/v) dry-milk powder solved in TBS-T buffer and “blocked” for 1-2 h. In this step the unspecific protein-binding sites of the membrane are saturated with the protein in the milk-powder.

5.2.3.21 Detection of specific proteins on a PVDF membrane

After blocking of unspecific protein binding sites on the membrane, it was incubated in primary antibody. Therefore the appropriate antibody that binds to the protein-of-interest's epitope is diluted in 5 % (w/v) dry-milk in TBS-T according to *Table 1*. The membrane is then rolled up in a 50 mL reaction-tube, with the protein-side facing the inside of the tube. A minimum of 3.5 mL of the diluted antibody is pipetted into the tube. The membrane was incubated in primary antibody overnight at 4 °C on a rotating mixer with integral roles. Afterwards, the membrane was washed three times for 10 min in TBS-T buffer and incubated with the secondary antibody, coupled to a horseradish-peroxidase (HRP) according to *Table 2* for 1 h at RT. After washing the membrane trice for 10 min in TBS-T at RT, the membrane was developed using the Enhanced-chemiluminescence (ECL) system. This is a method that uses solutions of diacylhydrazine luminol and peroxide to obtain chemiluminescence specifically at those sites on the membrane, where the HRP-coupled secondary antibody is bound to the protein of interest through the primary antibody. The HRP catalyzes the oxidation of the luminol in the presence of hydrogen-peroxide resulting in a chemiluminescence at 425 nm that was detected with a camera. Therefore the Luminol-peroxide solutions are mixed 1:1, pipetted onto the membrane and incubated for 4-5 min in the dark. The residual solution is removed from the membrane that is then placed into the detection chamber FluorChem Q. The emitted chemiluminescence was detected and densitometrically quantified using the AlphaView Q software, provided by the manufacturer.

5.2.3.22 Generation of recombinant adenoviruses for recombinant protein or miRNA expression

The adenoviruses that were used, were generated using the ViraPower™ Adenoviral Kit. Therefore a cDNA that had been previously cloned into the pDonR 221 vector was shuttled into the pAd/CMV/V5-DEST Gateway vector and then Pac I digested in a way where 10 µg of vector-DNA were incubated with 1x CutSmart buffer and 1 µL of Pac I-enzyme (10 U/µL) in a total volume of 50 µL overnight at 37 °C to receive linear DNA. Pac I restriction enzyme digested pAd/CMV/V5-DEST constructs were transfected into HEK293-A cells to produce protein expressing adenoviruses. The HEK293-A cells provide the genes encoding for the

packaging of the viruses and allow for lytic virus-production. Therefore HEK293-A were seeded into 6-well-plates on the day prior to the transfection at a density that after 24 h approximately 70 % of confluence was reached. The cells were then transfected with 1 µg and 2 µg of the linear pAd/CMV/V5-DEST vector containing the cDNA of interest. One well was transfected with each concentration of vector. The HEK-cells were then incubated for 48 h and the media was changed 24 h after transfection. The cells were then trypsinized as described and transferred into a T75 flask containing 12 mL of growth media. Every 72h, 50 % of the growth media was replaced with fresh, warm growth media to provide sufficient nutrients and buffering of the solution. The cells were microscopically checked for virus production twice a day, typically after 12 days the cells show a round-up shape and wholes appear in the cell-layer with detached cells at the edges. This showed that the virus started to lyse the cells and is present in the supernatant. The cells were incubated further until lysis was almost complete. The remaining cells were detached from the surface by pipetting up and down and the media containing viruses and cells in centrifuged down for 5 min at 1000 g. The supernatant is transferred into a 15 mL tube, the pellet resuspended in 1 mL of PBS and further lysed by three freeze-thaw cycles as described before. After centrifugation for 5 min at 1000 g, the supernatant was pipetted into the 15 mL tube containing the first supernatant. This “lysate 1” is then stored at -80 °C until further usage. For the generation of greater amounts of virus particles, HEK293-A cells were seeded into T175 flasks and incubated until they reached 100 % of confluence. 1-3 mL of the lysate 1 is then added to the flasks and incubated to 24-48 h until the cells show first signs of lytic virus production. Based on the assumption, that every cell has been infected by the adenoviruses from lysate 1, the cells were not incubated until lysis is complete but detached from the flask and centrifuged down when most of the cells still remain their membrane integrity. The supernatant was discarded and the cell-pellet containing intact, virus filled cells is resuspended in 2 mL of PBS and lysed by three freeze-thaw-cycles. After centrifuging for 10 min at 12.000 g and 4 °C, the supernatant was aliquoted into fresh reaction tubes in 20-30 µL portions. One of these aliquots was then used for the determination of the amount of infectious viruses per µl (ifu/µL).

5.2.3.23 Virus particle titration

Titration of the viruses was carried out by staining infected HEK293-A cells with FITC-labeled anti-Hexon antibody. Therefore HEK293-A cells were seeded in a 12-well-format at $3*10^5$ cells per well in 1 mL of growth media. Cells were then infected with the adenoviruses produced at different concentrations. Therefore a serial dilution of 50 µL of the virus aliquots was prepared in 1.5 mL reaction tubes. Dilutions ranged from 10^{-2} to 10^{-7} with ten-fold dilution in every step, resulting in in 6 different dilutions. One well was not infected, serving as a negative control, whereas the first dilution of 10^{-2} served as a positive control and was only pipetted into one well. The remaining dilutions were pipetted into two wells each, each dilution at 50 µL per well. The infected cells were incubated at 37 °C for 48 h. The media was removed and the cells were fixed with 1 mL -20 °C cold methanol for 10 min at -20 °C. After three washing steps PBS containing 1 % BSA, the cells were incubated with 100 µL of the FITC-coupled anti-Hexon antibody for each well for 1 h at 37 °C in the dark. After three washing steps with PBS containing 1 % BSA the number of infected cells was counted. Therefore the FITC was excited under UV-light and the emitted green fluorescence was microscopically observed. Infected and thus green cells were counted in ten randomly chosen fields of view with the 20 x objective. The mean cells per field of view was calculated. For the 20 x objective, 313 field-of-view can be chosen to cover the whole well. The mean number of infected cells was then multiplied by 313 to approximate the total number of infected cells per well. Division of this number by the manifold of dilution multiplied with the amount of virus pipetted into each well yields the infectious units per mL (ifu/mL) and is used to maintain a constant amount of infectious virus particles between individual virus-stocks and control viruses.

5.2.3.24 Immunofluorescence

For immunofluorescence staining, NRVCM were seeded on collagen-coated glass-coverslips and grown in DMEM-Medium as described. NRVCM were washed three times with ice-cold PBS and fixed with 1 mL 4% paraformaldehyde for 10 min at room temperature and washed three times with cold PBS. The cells were then permeabilized and further fixed in 1 mL of -20 °C cold methanol at -20 °C and washed three times in cold PBS. The cells were blocked with 1 mL of 2.5% BSA in PBS for one hour at room temperature. The coverslips with the attached and

fixed cells were then incubated for 90 minutes with primary antibody as listed in *Table 1* and washed three times for 10 min with PBS at RT. Respective secondary antibodies conjugated with fluorescent dyes was added to the cells and incubated for 1 h with the dilutions listed in *Table 2*. The cells were finally washed three times for 10 min in PBS and then mounted on a glass slide on 14 µL of mounting-media with the cell-side facing towards the slide.

Fluorescence images were taken with a Keyence BZ-9000 fluorescence microscope with a 20x CFI Plan Apo λ lens with an NA of 0.75 at RT. Images taken with the in-built CCD-camera were processed and analyzed by BZ-II Analyzer.

5.2.3.25 Cell surface area measurements

Cell size measurements were carried out by taking 5x5x5 (x y z) side-by-side 20 % overlapping pictures in a 20x magnification. The individual pictures were then merged with the BZ-II Analyzer software and a full-focus was generated from the z-stack to create a single, two dimensional picture from the multiple pictures taken. The cell size was measured using Keyence's HybridCellCount software module in fluorescence intensity single-extraction mode. First, fluorescence-intensity thresholds were set for a reference picture. Therefore α-actinin whole-cell staining was set as the target area and the DAPI-stained nuclei were then computationally extracted from each target area in order to determine the number of nuclei per target area (per cell). Only those cells were taken into the measurement that contained one nucleus within one target area. This ensured that only singe cells with one nucleus and no cell-cell contacts were counted.

5.2.3.26 Animal housing and experiments

Animals were housed in the central animal housing at the University Hospital of Schleswig-Holstein (UKSH) in Kiel. The animals had access to standardized dry-pellet food and water at all times and had a cycle of 12 h day and 12 h night. Room temperature was at constant 24 °C ± 1 °C. Protein samples for the analysis of the SUMO2-expression in animal models of pressure overload and hypertrophy, (TAC and Calcineurin-transgene) were provided by Prof. Dr. Frey. TAC animals undergo minimal-invasive surgery to constrict their transverse aorta to a defined

diameter to increase the afterload of the heart and create constant pressure overload to generate a phenotype of cardiac hypertrophy followed by heart failure.

All applications for animal experiments mentioned in this thesis were approved by the government and the animal protection commissary. Individual experiments were carried out in strict accordance to the university ethics guidelines to prevent unnecessary harm and suffering to the animals.

6 Results

6.1 A screening for calcineurin-NFAT activators

In order to identify unknown activators of calcineurin-NFAT signaling a cDNA screening strategy was devised, utilizing a commercially available human heart cDNA-library with approximately 10^7 primary clones. These clones were diluted to yield individual pools of approximately 200 clones each. Each pools was transformed into bacteria and amplified. The plasmids were then isolated and transfected into C2C12 myoblast cells, stably carrying an NFAT-responsive element driven firefly-luciferase gene in a 24-well format (Figure 4). Individual pools were co-transfected with CnA and analyzed for firefly-luciferase activity. A cutoff for further investigation of cDNA-pools that showed increased luciferase activity was selected and experiments were carried on with those pools of cDNAs that showed comparable or more luciferase activity than the positive controls. Transfected cDNA pools that resulted in elevated luciferase activity and thus possibly containing calcineurin-NFAT-activating cDNAs were further diluted, amplified and transfected in multiple steps to finally reach a dilution of approximately 12 cDNA constructs per dilution. After another round of transformation, amplification and plasmid preparation, these pools were re-transfected into C2C12 cells in a 24-well format and analyzed for NFAT-signaling activation. After one additional round of dilutions, single clones were transfected and positives were sequenced to identify two possible calcineurin-NFAT activating Proteins, SUMO2, a posttranslational modifier and PRP31, a protein involved in the assembly of the spliceosome. Further verification was achieved by co-overexpression of CnA together with a vector carrying SUMO2 or PRP31. Despite the promising calcineurin-NFAT-activation of both candidates within the screening conditions, only SUMO2 turned out to be a strong activator of the calcineurin-NFAT signaling pathway and was thus subjected to thorough characterization to identify a possible mechanism of action. These screening experiments were carried out in the University Hospital of Heidelberg in the research group of Prof. Dr. Frey. Data sets were provided upon the start of the experiments for this thesis and are therefore to be regarded as previous achievements.

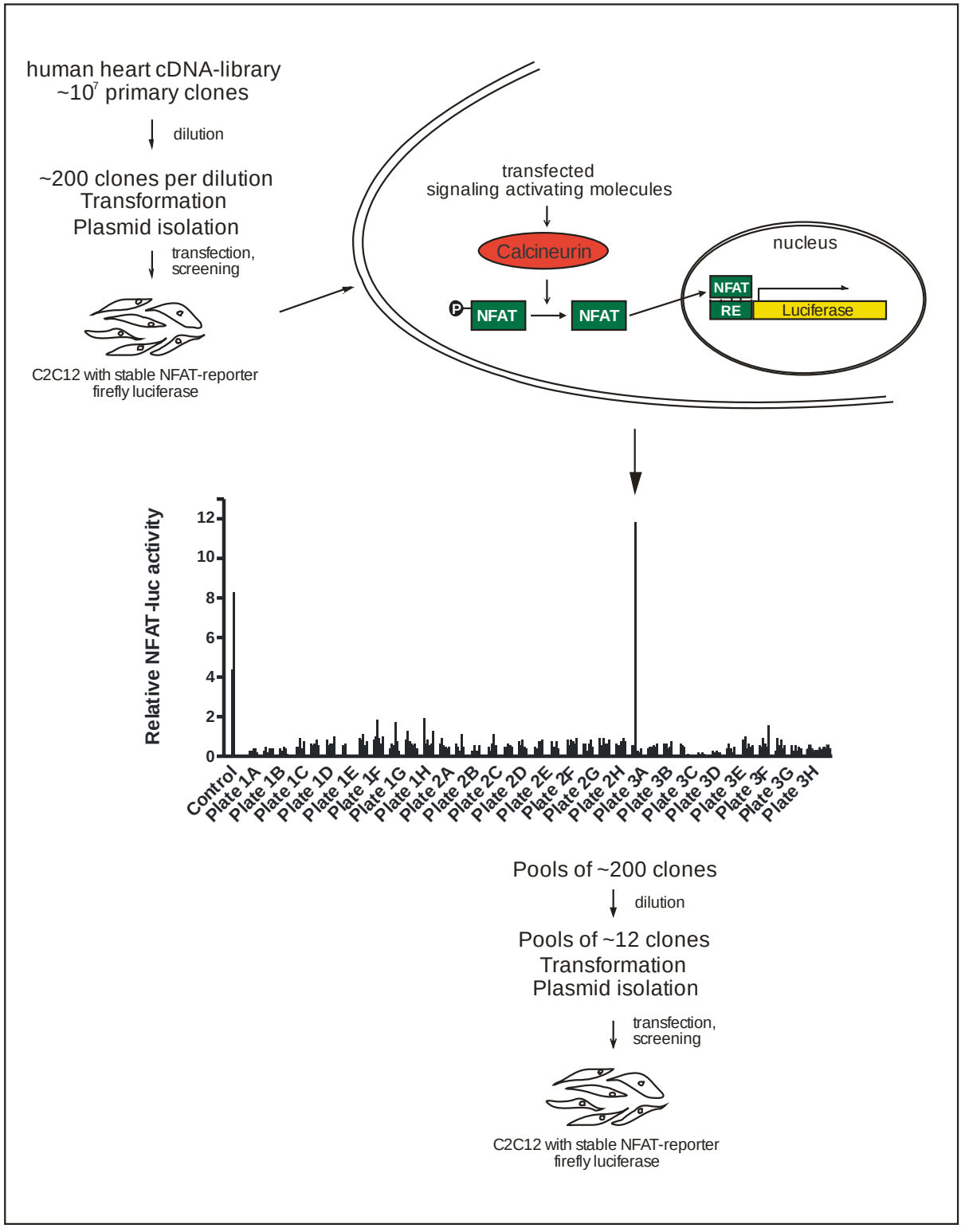

Figure 4: A screening strategy for calcineurin-NFAT activators. Starting from 10^7 cDNA-clones from fetal human heart serial dilutions were performed and plasmid preparations for transfection of C2C12 cells, stably carrying NFAT-reporter firefly luciferase. Diluted pools of cDNAs were transfected and tested for Calcineurin-NFAT signaling activation through luciferase activity screening. Further dilutions

and plasmid preparations were carried out, first giving rise to pools of 200 cDNAs, then 12 cDNAs, until single clones could be transfected, screened, and subsequently sequenced for individual Calcineurin-NFAT activating clones. Shown is an exemplary result of a transfection in a 12 well plate scale with transfected pools of 12 cDNAs, where one well of plate 2H showed a significantly increased NFAT-luciferase activity, compared to the positive control and all other plates and wells.

6.2 Generation and verification of mammalian expression constructs for SUMO2 and calcineurin

To further validate the data from the screening experiment, a SUMO2 wild-type construct for the expression in C2C12 myoblasts was generated, using a mammalian expression vector (see materials section for details). SUMO2 was successfully overexpressed on both, protein (14-fold, Figure 5A &Figure 5B) and RNA-level (67-fold, Figure 5C). Also a wild type CnA-construct was generated as well as a truncated mutation lacking the calmodulin-binding and autoinhibitory domains, making this mutant constitutively active (ΔCnA, Figure 5D). The expression of the truncated protein was confirmed by western blot analysis (Figure 5E) with the same antibody that detects endogenous or overexpressed wild type CnA.

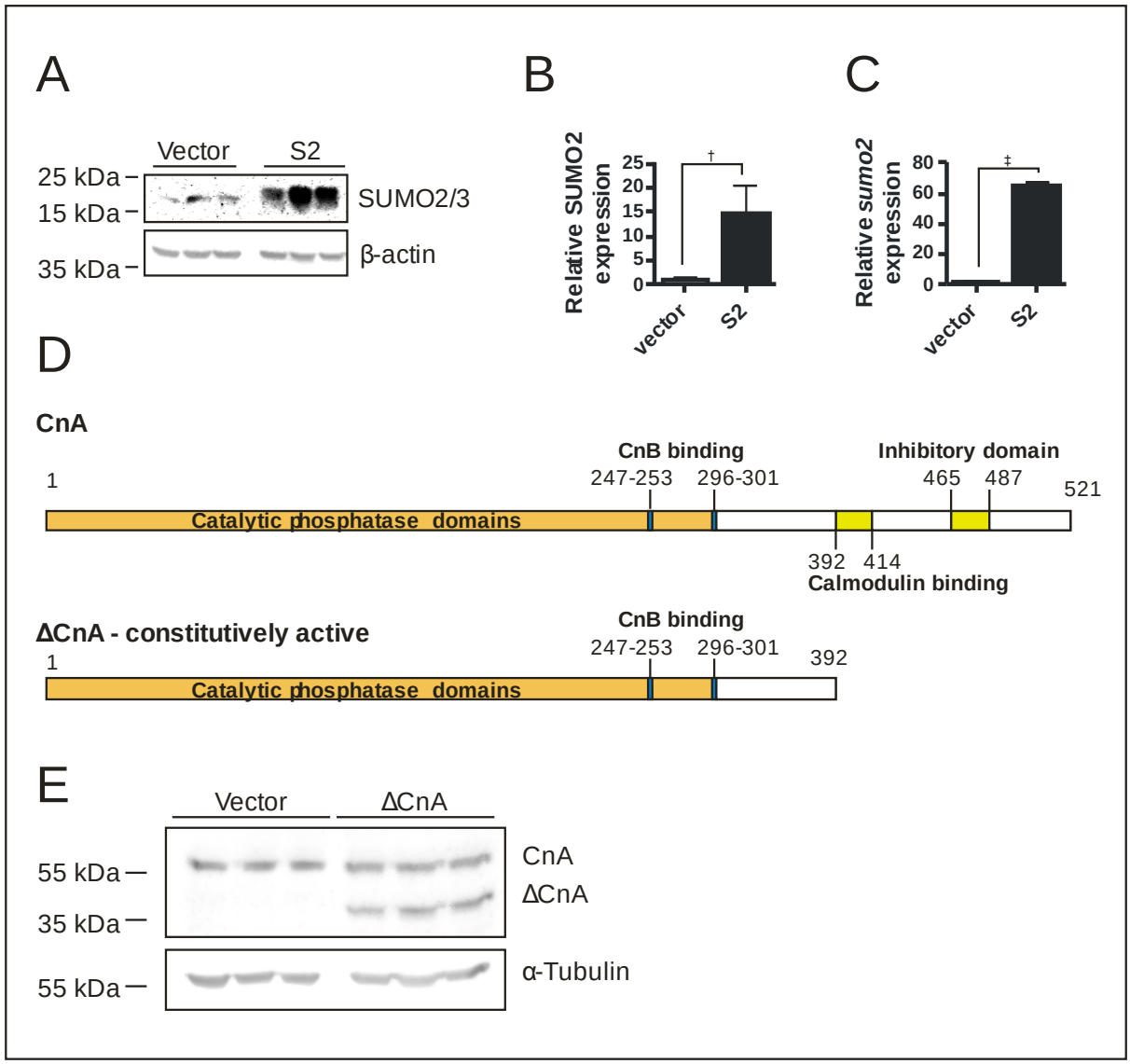

Figure 5: Generation and verification of mammalian expression constructs for SUMO2 and Calcineurin. A, B, western blot analysis showing SUMO2 overexpression, relative densitometry was calculated through β-actin equal loading control. C, qRT-PCR analysis of *sumo2* mRNA expression with overexpressed SUMO2 compared to the empty vector control. D, schematic overview of the wild type and truncated CnA expression constructs that were generated. E, western blot analysis showing endogenous CnA and ΔCnA overexpression. †: $p<0.01$, ‡: $p<0.001$.

6.3 SUMO2 activates calcineurin-NFAT-signaling in C2C12 cells

The activation of NFAT-signaling was reconfirmed by transfecting the cells with NFATc4 or SUMO2 in the presence or absence of constitutively ΔCnA and observed a strong activation of NFAT-signaling through ΔCnA at baseline conditions as well as a significantly additive effect of SUMO2 on NFAT-signaling in the presence of ΔCnA (Figure 6A). To prove a physiological relevant interaction, the effect on overexpressed wild type CnA that can be pharmacologically activated was also studied. Therefore C2C12 cells were transfected with wild type CnA and activated it through addition of Ionomycin and PMA, leading to a robust Calcium influx (Frey et al., 2008) and thus to the activation of Ca^{2+} dependent proteins like CnA (Figure 6B). A strong activation of NFAT-signaling through SUMO2 or CnA overexpression was observed at baseline conditions (Ctrl) as well as an increased activation of NFAT-signaling in the presence of CnA and SUMO when CnA was pharmacologically activated (IONO/PMA).

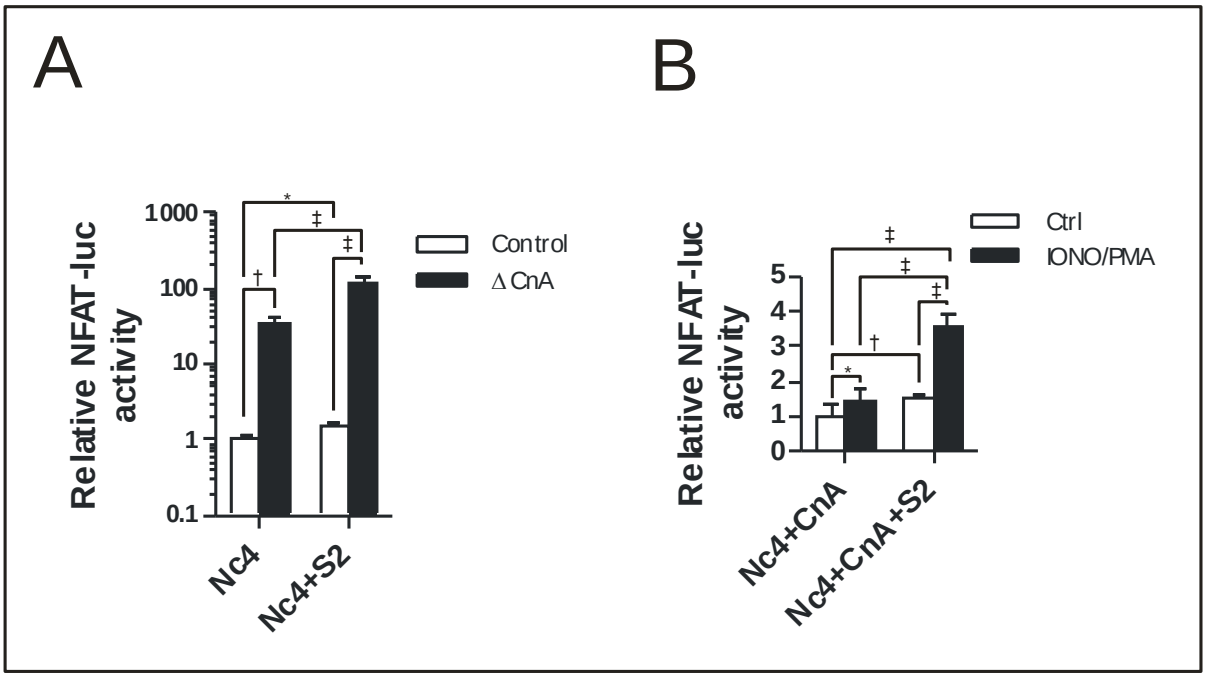

Figure 6: SUMO2 activates calcineurin-NFAT-signaling in C2C12 cells. A, cells carry functional NFAT-responsive element (RE) driven firefly luciferase. ΔCnA is either or not transfected in the presence or absence of SUMO2. Shown is the mean of three independent experiments in quadruplicates, logarithmic scale for improved differentiation. B, NFAT-responsive element driven firefly luciferase activity in the presence of wild-type CnA and NFATc4 and in the presence or absence of SUMO2. CnA is either or not activated by Ionomycin (2 µM) + PMA (1 µM) addition. Shown is the mean of two

independent experiments in quadruplicates. Statistical calculations were carried out with two-way ANOVA *: $p<0.05$, †: $p<0.01$, ‡: $p<0.001$.

6.4 SUMO2-knockdown reduces calcineurin-NFAT-signaling in C2C12 cells

Next, a potentially essential role of SUMO2 on CnA and hence NFAT-signaling via siRNA mediated knockdown of SUMO2 in C2C12 cells was investigated. Transfection of these cells with a SUMO2 siRNA led to 85% knockdown on protein- and 78% knockdown on RNA level, respectively (Figure 7A, 4B & 4C). Although ΔCnA increased NFAT-signaling compared within the control siRNA conditions, upon knockdown of SUMO2 there was significantly less NFAT-activation compared to control-siRNA (Figure 7D), strengthening the screening-experiment derived hypothesis of an important regulatory role for SUMO2 on calcineurin- and consequently NFAT-signaling.

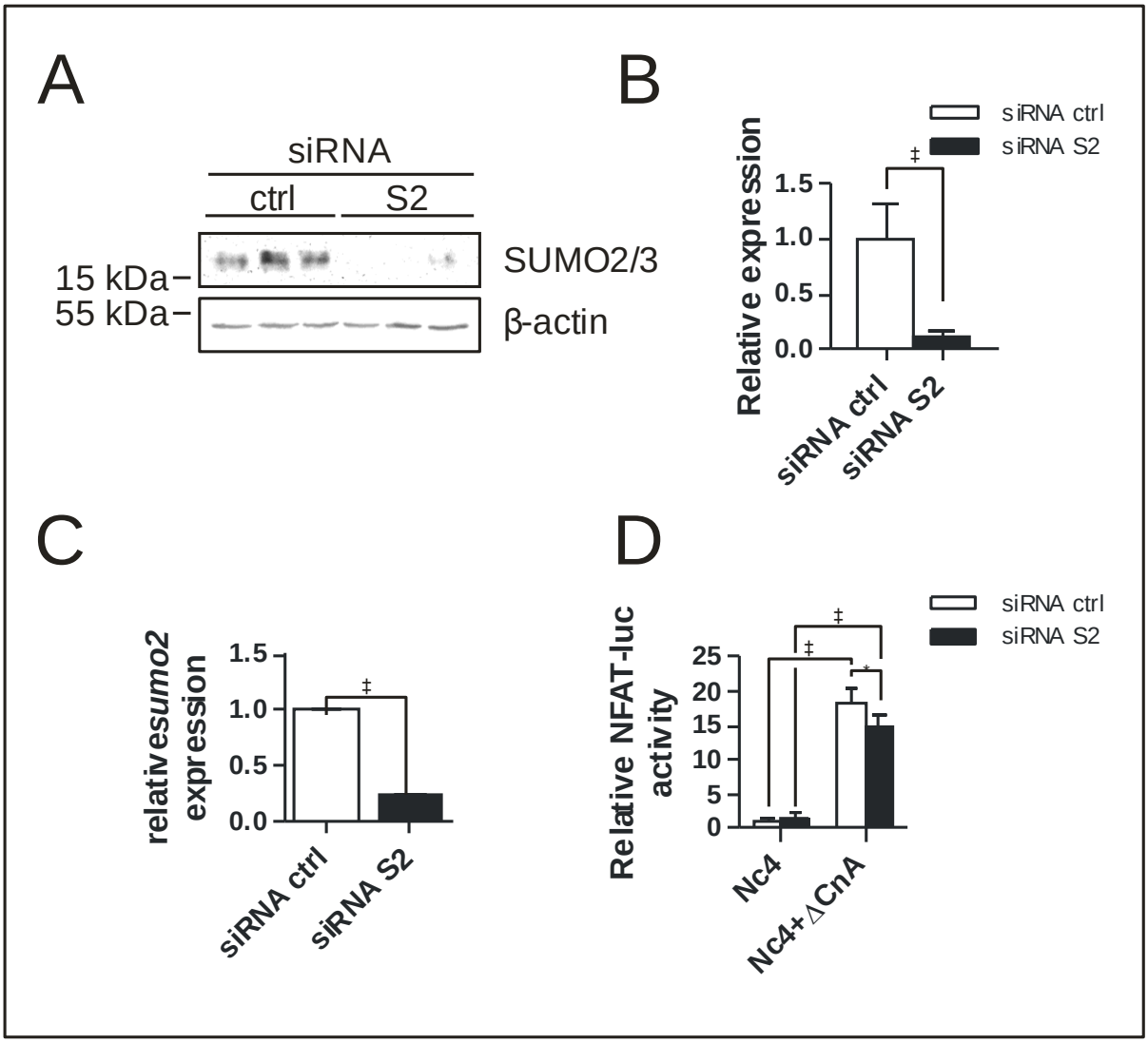

Figure 7: SUMO2-knockdown reduces Calcineurin-NFAT-signaling in C2C12 cells. A, B, western blot analysis showing knockdown of SUMO2 and relative densitometry was calculated through β-actin equal loading control. C, expression of *sumo2* in the presence of siRNA against *sumo2* compared to non-targeting control siRNA. D, NFAT-RE firefly luciferase activity in the presence of NFATc4 and in the presence or absence of ΔCnA and / or siRNA against *sumo2* or control siRNA. Shown is the mean of two independent experiments in hexaplicates. All experiments were performed in C2C12 cells stably expressing NFAT-RE driven firefly luciferase. Statistical calculations were carried out by two-tailed Student's t-test (B, C) or two-way ANOVA (D). *: $p<0.05$, †: $p<0.01$, ‡: $p<0.001$.

6.5 SUMO2 dependent sumoylation is increased in disease animal models of pressure overload and hypertrophy

In order to assess a pathophysiological relevance of SUMO2, the SUMO2-dependent sumoylation status in two different mouse models of cardiac disease, calcineurin transgenic and TAC operated mice was studied (Molkentin et al., 1998). Calcineurin transgenic mice show pronounced hypertrophy followed by heart failure. TAC operated mice suffer from pressure overload, resulting in hypertrophy and heart failure. Both animal models display a significant increase in monomeric 'free' SUMO2 compared to respective control mice (Figure 8A, 5B, 5D & 5E). While SUMO2 is involved in many pathways and its covalent attachment to other proteins is therefore expected to be differentially regulated, both disease models showed an overall increase in protein sumoylation, displayed by a stronger intensity of the bands and a 'ladder like' appearance of the band throughout the whole membrane. The observed increase was more prominent in calcineurin transgenic mice, adding evidence for a calcineurin-dependent effect of SUMO2 (Figure 8A, 5C, 5D & 5F). I observed ubiquitous expression pattern of *sumo2* in various tissues including lung, liver, kidney, etc. Moreover, *sumo2* expression was relatively higher in the heart compared to the skeletal muscle (Figure 8G)

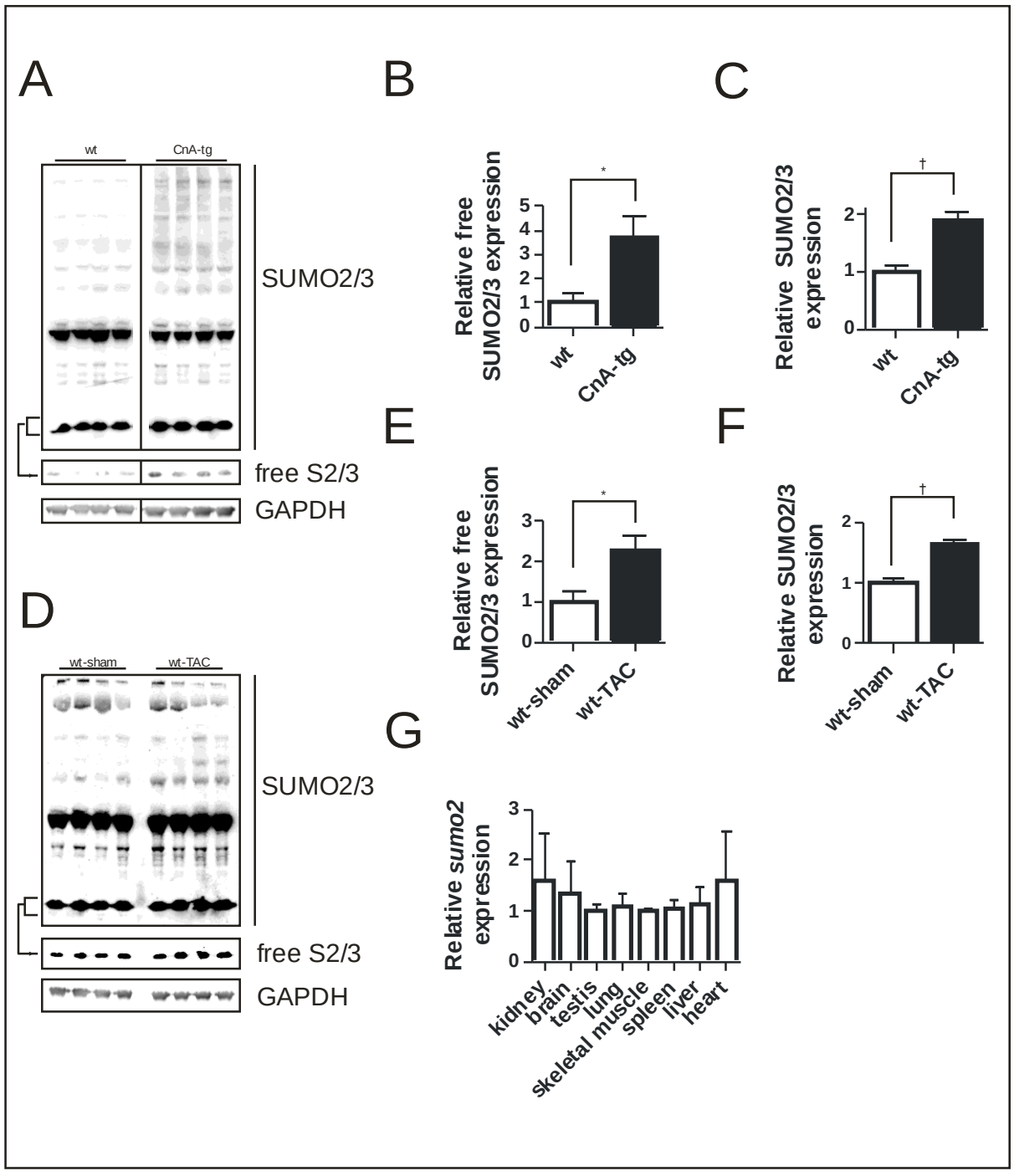

Figure 8: SUMO2 dependent sumoylation is increased in disease models of pressure overload and hypertrophy. A, western blot showing SUMO2 expression in wild type (wt) and Cn transgenic mice (age: 18 weeks); “free SUMO2/3” shows a shorter exposure band of the above shown monomeric, unsumoylated protein-band, upper panel shows the whole membrane. Relative expression of free SUMO2/3 (B), and total SUMO2/3 (C) was calculated by densitometric analysis using GAPDH as an endogenous control. D, western blot showing SUMO2 expression in sham and TAC operated mice (age: 8 weeks, following 4 weeks under pressure overload (TAC); “free SUMO2/3” shows a shorter exposure

band of the above shown monomeric, unsumoylated protein-band, upper panel shows the whole membrane. E, F, Relative expression of free SUMO2/3 (E), and total SUMO2/3 (F) was calculated by densitometric analysis using GAPDH as an endogenous control. Statistical calculations were carried out by two-tailed Student's t-test (B, C, D, F) *: $p<0.05$, †: $p<0.01$. Dividing lines represent rearrangements of respective lanes within one membrane. MRNA levels of *sumo2* in different tissue samples from wt C57BL/6 mice, normalized to skeletal muscle expression, n=4 mice.

6.6 SUMO2 activates Calcineurin-NFAT signaling in NRVCM

Through our luciferase screen, SUMO2 was identified as a robust activator of NFAT-signaling in C2C12 cells, a mouse skeletal myoblast cell line. Therefore it was investigated, whether SUMO2 overexpression also effects cardiac NFAT-signaling. An adenoviral construct for SUMO2 was generated to be used in NRVCM, which expressed recombinant protein at significant levels (Figure 9A & 6B). The “free” SUMO2, running at approximately 18 kDa is strongly expressed as well as an increase in overall sumoylation, represented by increased streak-pattern throughout the lanes in SUMO2 overexpression conditions compared to LacZ control. To reproduce the findings from C2C12 cells, I also generated an adenoviral expression construct for ΔCnA and were able to overexpress the protein in NRVCM. Alike previously observed in C2C12 cells, overexpression of SUMO2 in NRVCM led to activation of NFAT-signaling at baseline conditions without further challenging the cells (Figure 9D). The ΔCnA mediated increase in NFAT-luciferase activity was further increased when SUMO2 was co-expressed, resembling our findings from C2C12 and justifying cardiac-specific advance of our analyses.

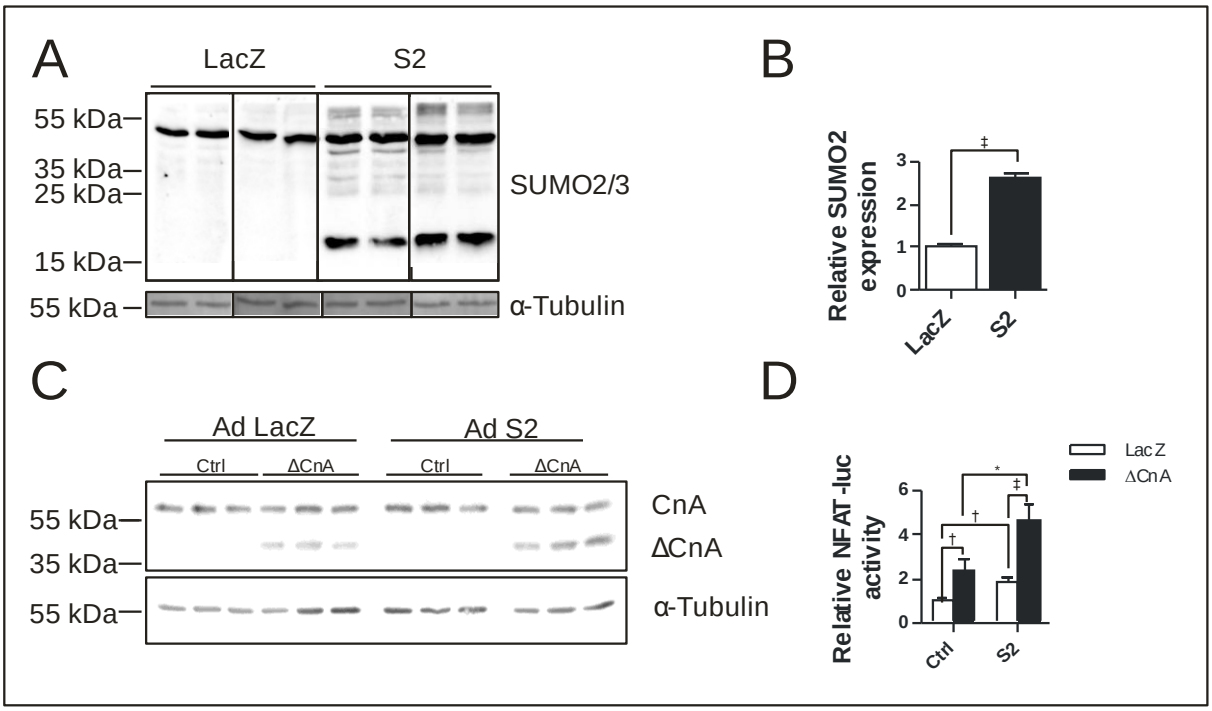

Figure 9: SUMO2 activates Calcineurin-NFAT signaling in NRVCM. A, B, western blot analysis showing SUMO2 overexpression in the presence or absence of adenoviral (Ad) SUMO2

overexpression, relative densitometry was calculated through α-tubulin equal loading control. C, western blot showing overexpression of truncated ΔCnA and wild type CnA in the presence or absence of overexpressed SUMO2 compared to LacZ control. D, NFAT-RE firefly luciferase construct was expressed via adenoviral infection and luciferase activity measured in the presence or absence of ΔCnA and SUMO2. Shown is the mean of three independent experiments in hexaplicates. Statistical calculations were carried out by two-tailed Student's t-test (B) or two-way ANOVA (D). *: $p<0.05$, †: $p<0.01$, ‡: $p<0.001$.

6.7 Knockdown of SUMO2 inhibits calcineurin-NFAT signaling in NRVCM

A synthetic miRNA against *sumo2* and an adenoviral expression construct for this miRNA were generated. I was able to successfully knock down SUMO2 in NRVCM on protein and RNA level (Figure 10A & Figure 10B). Then, the effects of a knockdown of endogenous SUMO2 on NFAT activation via NFAT-luciferase-RE that was expressed by co-infection along with the miRNA constructs was investigated. The effect of a SUMO2 knockdown on NFAT-signaling was then investigated at baseline condition, as well as in challenged cardiomyoctes. Two doses of NFAT-signaling activator PE, at 1 µm and 5 µM were utilized and led to a dose dependent increase of NFAT-luciferase activity at baseline conditions (miR Neg, Figure 10C). Along these lines, an induction of Ca^{2+} dependent signaling, that also activates endogenous CnA and subsequently NFAT-signaling, led to an increase in NFAT-luciferase activity (Figure 10C). In all conditions the knockdown of SUMO2 resulted in a substantial decrease in NFAT-luciferase activity (miR S2, Figure 10C). Moreover, NFAT activation through constitutively active CnA leads to a strong expression of Rcan1-4, an exquisitely NFAT-sensitive gene, the increased expression of which is almost abrogated when SUMO2 is knocked down (Figure 10D & Figure 10E). Rcan1-4 expression is already reduced when SUMO2 is knocked down at baseline conditions (Figure 10D & Figure 10E, control). Both findings further support a necessary role for SUMO2 on calcineurin-mediated NFAT-signaling.

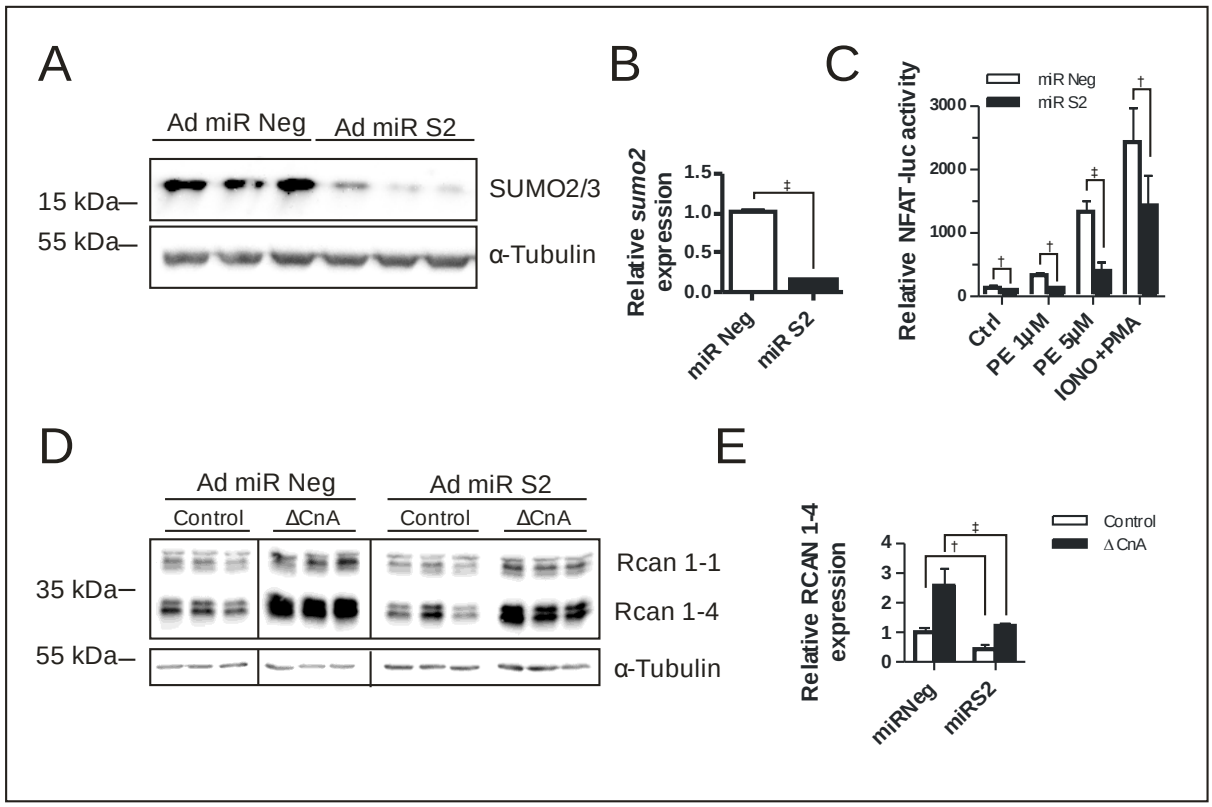

Figure 10: Knockdown of SUMO2 inhibits calcineurin-NFAT signaling in NRVCM. A, western blot showing SUMO2 knockdown with miRNA against *sumo2* (Ad miR S2) compared to negative control miRNA (Ad miR Neg) and relative densitometry was calculated through α-tubulin equal loading control. B, expression of *sumo2* in the presence of miR S2 compared to miR Neg. Shown is the mean of two independent experiments in quadruplicates. C, Ad NFAT-RE firefly luciferase activity in the presence of miR S2 (96h knockdown) compared to miR Neg in the presence of PE (1 µM or 5 µM) and Ionomycin/PMA (2 µM/4.5 nM). Data represented as a mean of two independent experiments performed in hexaplicates. All experiments were performed in NRVCM cells. Statistical calculations were carried out by two-tailed Student's t-test (B) or two-way ANOVA (C & E). †: $p<0.01$, ‡: $p<0.001$. Dividing lines represent rearrangements of respective lanes within one membrane.

6.8 SUMO2 induces hypertrophy in cardiomyocytes

Calcineurin-NFAT signaling is one of the key signaling pathways directly involved in the induction of pathological cardiac hypertrophy. Given the strong activation of NFAT-signaling that was observed in NRVCM and C2C12 cells, the potential phenotypic and molecular effects of SUMO2 in NRVCM was further investigated. Adenoviral overexpression of SUMO2 led to a significant increase in NRVCM surface area compared to LacZ control virus infected cells, visualized by alpha-actinin staining, resembling the actin cytoskeleton (Figure 11A). Cell size was measured in a semi-automated way, whereby pictures of different randomly chosen fields of view were taken manually and the cell size measurement was executed via previously programmed computed script, equal for all pictures taken. Only cardiomyocytes with one nucleus, not in cell-cell contact with others were included, yielding a median cell-size increase of about 200 μm^2 and overall a larger 95^{th} percentile, resembling an increased amount of larger cells (Figure 11B). In line with the SUMO2 induced increase in cell size, a significant upregulation of the fetal genes *nppa* and *nppb*, which are recognized as markers for *in vitro* cardiomyocyte hypertrophy was observed (Figure 11C & Figure 11D). Moreover, the expression of *rcan1-4*, a known NFAT-responsive marker gene, was increased upon SUMO2 overexpression (Figure 11E). Taken together, these data clearly indicate that SUMO2 overexpression induces cardiomyocyte hypertrophy, consistent with the robust activation of calcineurin-NFAT signaling *in vitro*.

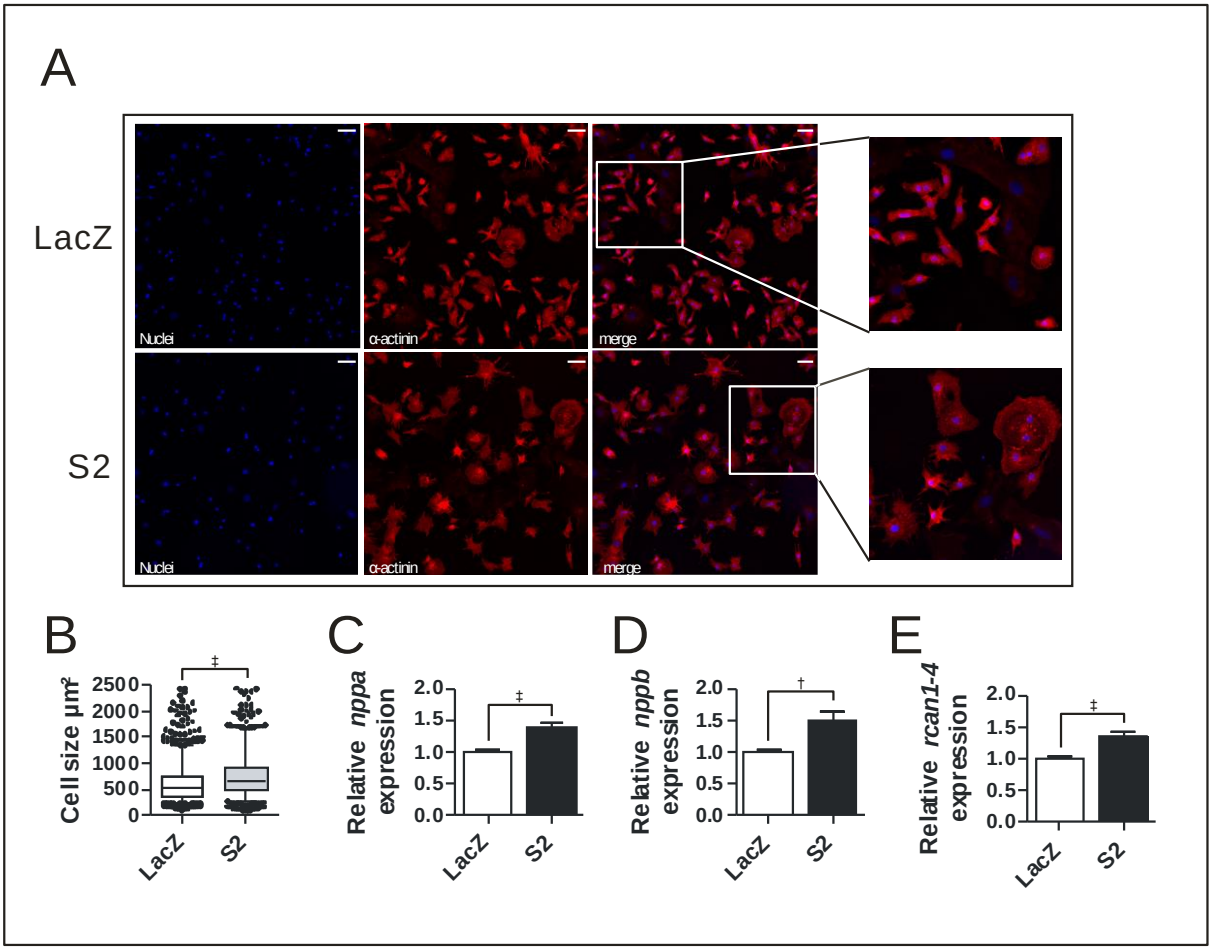

Figure 11: SUMO2 induces hypertrophy in cardiomyocytes. A, representative immunofluorescence analysis of fixed NRVCM, overexpressing LacZ or SUMO2 (scale bar 50 µm). B, cell surface area. Shown is the analysis of two independent experiments in triplicates with n>1000 counted cells per replicate. C, D, E expression levels of *nppa*, *nppb* and *rcan1-4* respectively in the presence or absence of Ad S2. Shown is the mean of two independent experiments in hexaplicates. All experiments were performed in NRVCM cells. Statistical calculations were carried out by two-tailed Student's t-test (C, D, and E) or one-way-ANOVA (B). †: $p<0.01$, ‡: $p<0.001$.

6.9 SUMO2 effects on NFAT-signaling and hypertrophy are sumoylation independent

As sumoylation of proteins is the major mechanism of modification by which SUMO proteins exert their structural and/or functional effects and published data on SUMO- proteins largely involves sumoylation dependent mechanisms, a sumoylation-deficient SUMO2 mutant was investigated. This tentative approach was to determine whether the effects observed for SUMO2 are sumoylation-dependent or independent. I therefore created the *sumo2ΔGG* mutant construct via site directed mutagenesis (Figure 12A). The two glycine-residues C-terminal of the protein are the site of covalent attachment with other proteins, thus our construct missing this diglycine motif is unable to attach to other proteins (sumoylation deficient). It was cloned into an adenoviral expression vector for overexpression in NRVCM and I was able to overexpress SUMO2ΔGG (Figure 12B & Figure 12C). Also the NFAT-reporter mediated luciferase assay with SUMO2ΔGG in the presence or the absence of ΔCnA in our starting model of C2C12 myoblasts was repeated, for which a mammalian expression vector containing the ΔGG construct was created. In presence of overexpressed ΔCnA, the sumoylation deficient SUMO2ΔGG leads to a strong activation of NFAT-signaling in NRVCM, comparable to overexpressed wild type SUMO2 (Figure 12D). Likewise, in the absence of ΔCnA there was no significant difference in the activation of NFAT-signaling between LacZ control and SUMO2 and SUMO2ΔGG (Figure 12D). I also repeated the initial NFAT-luciferase activity assay (Figure 12D, for C2C12 data) in NRVCM and obtained a similar increase in luciferase activity whether SUMO2 or SUMO2ΔGG were overexpressed when compared to the empty vector control. There was no significant difference between the two SUMO-constructs at baseline conditions, as well as in ΔCnA challenged cells. Finally, SUMO2ΔGG overexpression increased NRVCM cell size in the same magnitude as SUMO2 when compared to LacZ control (Figure 12F). These observations rule out a solely sumoylation dependent mechanism for the SUMO2 dependent activation of calcineurin-NFAT-signaling.

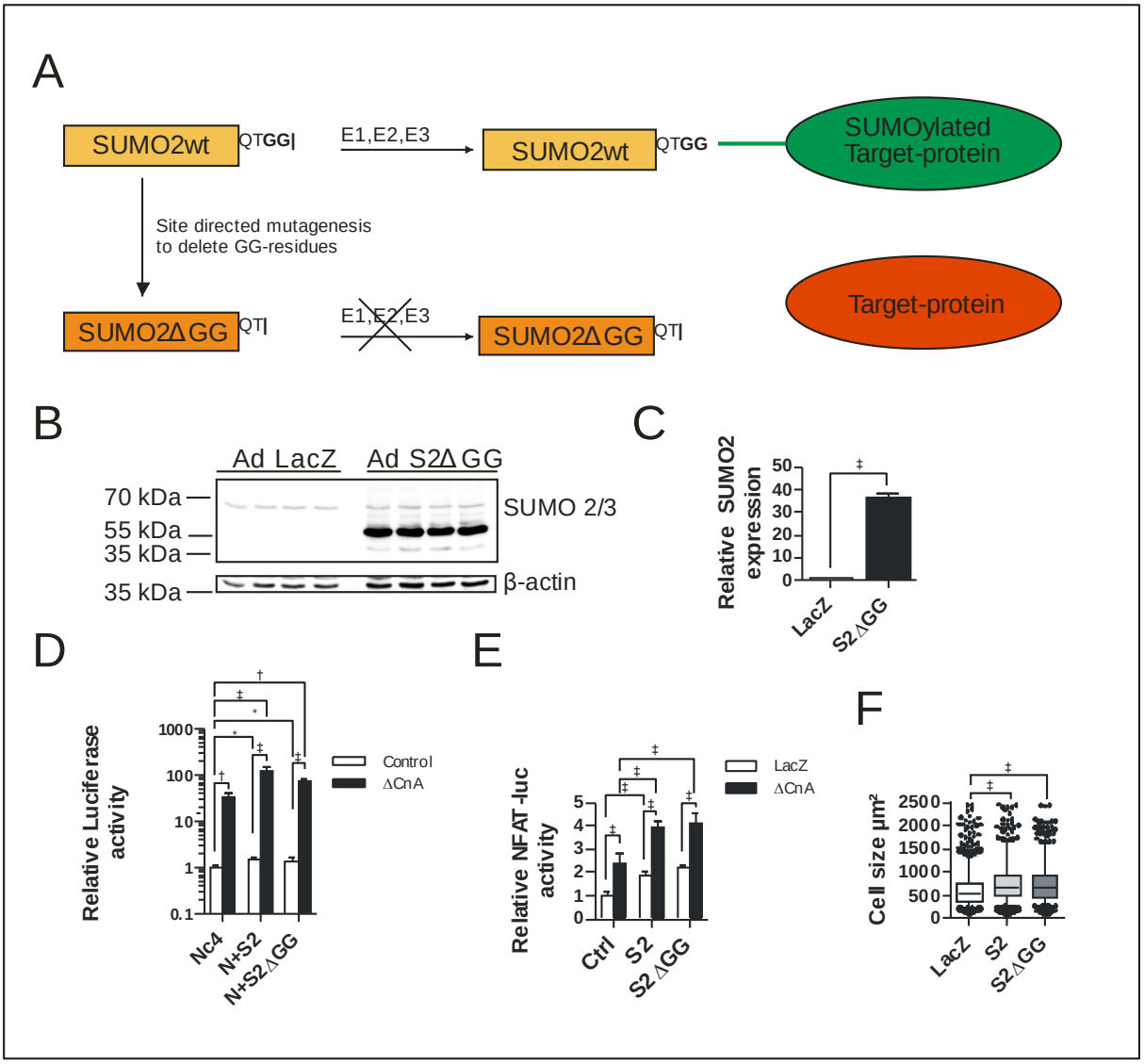

Figure 12: SUMO2 effects on NFAT-signaling and hypertrophy are sumoylation independent. A, site directed mutagenesis strategy to generate sumoylation-deficient SUMO2-mutant protein (SUMO2ΔGG). B, western blot showing overexpression of SUMO2ΔGG compared to LacZ. C, densitometric analysis of SUMO2 overexpression normalized to β-actin housekeeper. D, C2C12 cells carry functional NFAT-RE driven firefly luciferase, ΔCnA is either or not transfected in the presence or absence of SUMO2 or sumoylation deficient SUMO2ΔGG, shown is the mean of three independent experiments in quadruplicates. E, NFAT-RE firefly luciferase activity in the presence of either SUMO2 or SUMO2ΔGG and in the presence or absence of ΔCnA compared to LacZ control. Shown is the mean of two independent experiments in hexaplicates. F, cell surface area measurement in the presence or absence of overexpressed SUMO2 or SUMO2ΔGG compared to LacZ control. Shown is the analysis of two independent experiments in triplicates with n>1000 counted cells per replicate. All experiments except for B were performed in NRVCM. For firefly luciferase activity experiments in NRVCM, Renilla-

luciferase was adenovirally expressed as normalization control. Statistical calculations were carried out by two-tailed Student's t-test (C) or Two-way ANOVA (D, E, and F). *: p<0.05, †: p<0.01, ‡: p<0.001.

6.10 SUMO2 induces cardiomyocyte hypertrophy via CnA

A strong impact of overexpressed SUMO2 and SUMO2ΔGG on NFAT-signaling, cell size, expression of hypertrophy associated markers like *rcan1-4* and fetal genes *nppa and nppb* in the presence of ΔCnA in NRVCM and C2C12 cells was observed. Driven by this evidence, a functional interaction between SUMO2 and CnA that induces cardiomyocyte hypertrophy was hypothesized that is not solely dependent on sumoylation. In line with this hypothesis, an additive increase in cell size when co-overexpressing ΔCnA with SUMO2 or SUMO2ΔGG in NRVCM compared to SUMO2 or SUMO2ΔGG alone can be observed (Figure 13A & Figure 13B). Similarly, the addition of ΔCnA to SUMO2ΔGG overexpression increases expression levels of *nppa*, *nppb* and *rcan1-4* (Figure 13C, Figure 13D & Figure 13E), very similar to the previously observed SUMO2 mediated effects on these parameters. SUMO2 or SUMO2ΔGG again exaggerate the increased expression mediated via CnA, further strengthening the hypotheses of SUMO2 being an activator of cardiomyocyte hypertrophy, as well as the mechanism for this being independent of sumoylation.

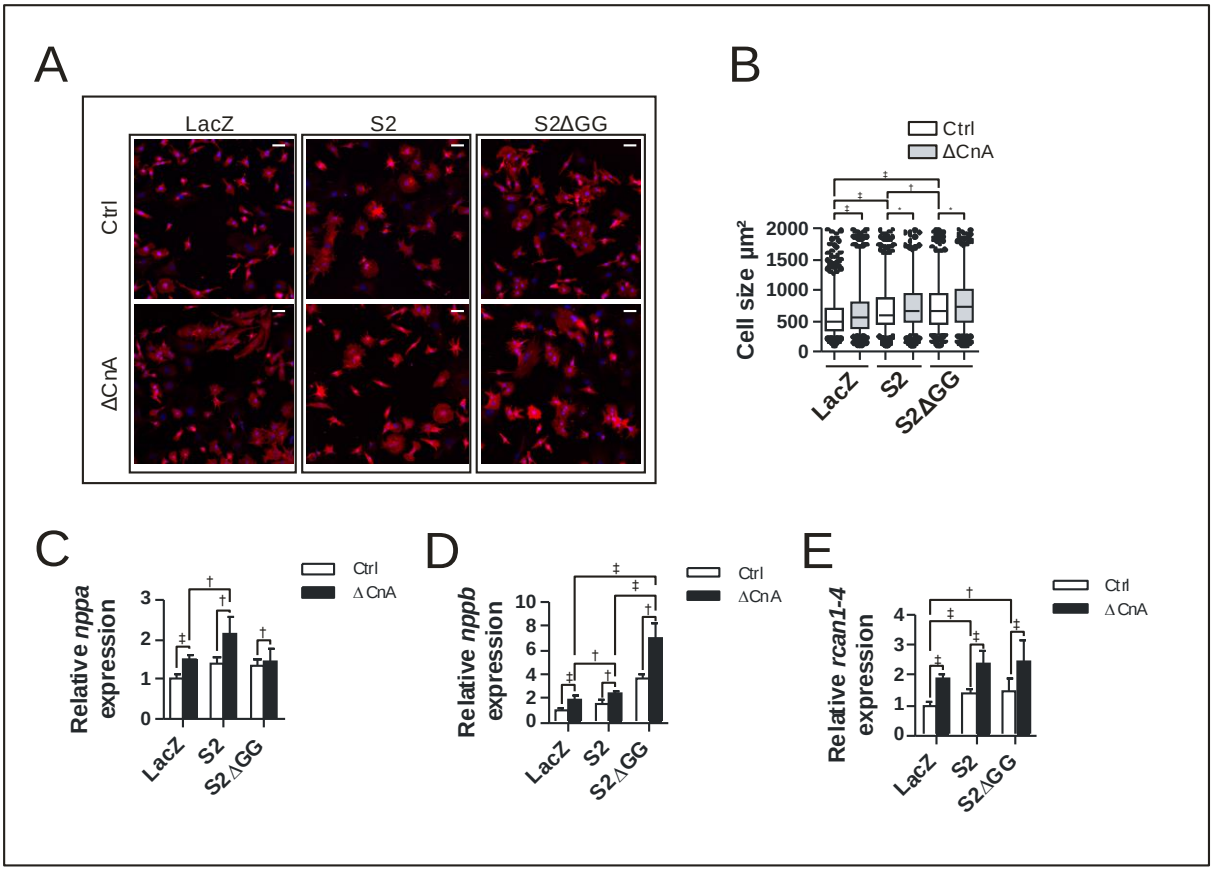

Figure 13: SUMO2 induces cardiomyocyte hypertrophy via CnA. A, representative pictures of the immunofluorescence analysis of fixed NRVCM cells in the presence or absence of overexpressed ΔCnA along with overexpression of LacZ (control) SUMO2 or SUMO2ΔGG (scale bar 50 µm). B, respective cell surface area, shown is the analysis of two independent experiments in triplicates with n>1000 counted cells per replicate. C, D, E, expression levels of *nppa*, *nppb and rcan1-4* respectively in the presence or absence of overexpressed ΔCnA alongside with overexpressed LacZ (control), SUMO2 or SUMO2ΔGG. For C, D, E, shown is the mean of two independent experiments in hexaplicates. All experiments were performed in NRVCM cells. Statistical calculations were carried out by two-way-ANOVA. *: p<0.05, †: p<0.01, ‡: p<0.001.

6.11 Cell-size increase, mediated by SUMO2 and SUMO2ΔGG relies on CnA function

To further strengthen the findings of a direct interaction between SUMO2 and CnA, I investigated, whether or not the inhibition of CnA by two differently acting pharmacological inhibitors would abrogate the observed increase in cell size. Ciclosporin and tacrolimus were utilized, both indirectly inhibiting CnA by forming a complex with immunophilins and then binding to and inhibiting CnA. SUMO2 and SUMO2ΔGG overexpression, as well as phenylephrine stimulation of the cells increased the cell size significantly, similar to the previously observed effect. When endogenous CnA is inhibited by either ciclosporin or tacrolimus, the increase in cell size in the presence of overexpressed SUMO2 or SUMO2ΔGG is abolished or significantly decreased (PE), consistent with the notion that SUMO2 directly exerts its effects via CnA (Figure 14).

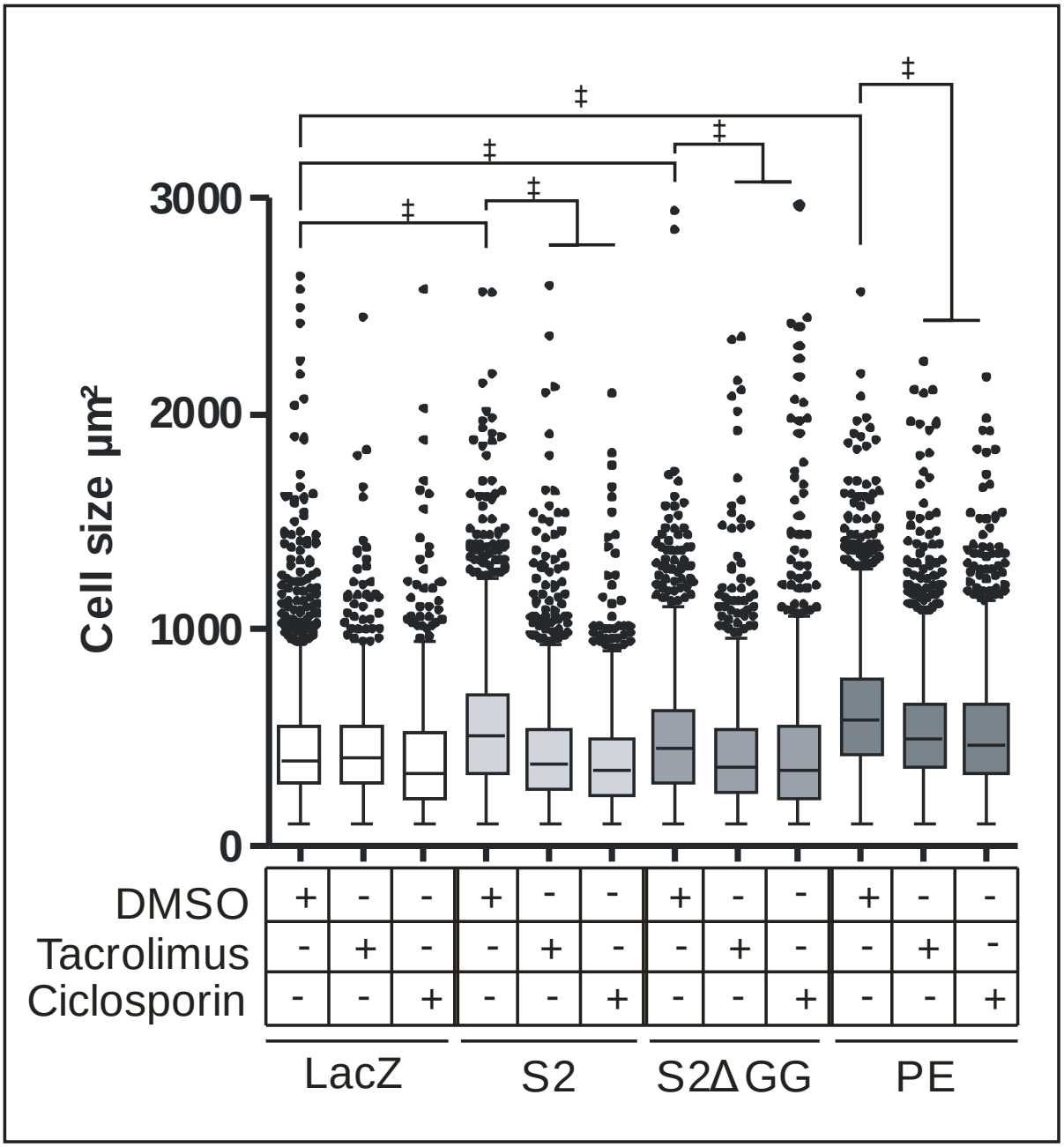

Figure 14: Cell-size increase, mediated by SUMO2 and SUMO2ΔGG relies on CnA function. Respective cell surface area of fixed NRVCM-cells overexpressing LacZ (negative control), SUMO2, SUMO2ΔGG or stimulated with 10µM Phenylephrine (PE, positive control) for 48h. 10µM of ciclosporin or 1 µM of tacrolimus or DMSO as control were added as depicted by "+" below the respective bar. Statistical calculations were carried out by Kruskal-Wallis-test. ‡: $p<0.001$.

6.12 SUMO2 directly interacts with and tethers CnA to the nucleus in cardiomyocytes

The localization of SUMO2 and CnA within the cell were analyzed next. Adenoviral constructs for GFP-ΔCnA, SUMO2 and SUMO2ΔGG, alone or in combination were used. SUMO2 can typically be found throughout the cell with predominant localization to the nucleus, whereas Calcineurin is mainly localized in the cytoplasmic compartment in unchallenged cells. As shown in Figure 15A, CnA was shuttled to the nucleus in NRVCM overexpressing ΔCnA and SUMO2 (I, rows 2 & 3), whereas it remained cytoplasmic in cells overexpressing CnA alone (I, rows 2 & 3; III, row 2) Specially compelling evidence can be found in row I, where two side by side cells are visible with only the upper cell being infected with the SUMO2-containing virus and only this cell showing nuclear calcineurin, whereas the other cells shows a retention of calcineurin to the cytoplasm. In line with the previous findings, this SUMO2 mediated effect on CnA seems to be sumoylation-independent since SUMO2ΔGG also induced activation and subsequent translocation of CnA to the nucleus, without any apparent difference compared to wild type SUMO2 (Figure 15A, column II). To evidence a direct interaction between SUMO2 and CnA, a co-immunoprecipitation of endogenous SUMO2 and CnA was performed in C2C12 cells and in mouse heart tissue using a buffer for native protein isolation. As shown in Figure 15B, SUMO2 endogenously interacts with CnA in C2C12 cells and in mouse heart lysate under native conditions. The data collected for Figure 15A was obtained in cooperation with Prof. Dr. Oliver Müller in the University Hospital of Würzburg, Germany.

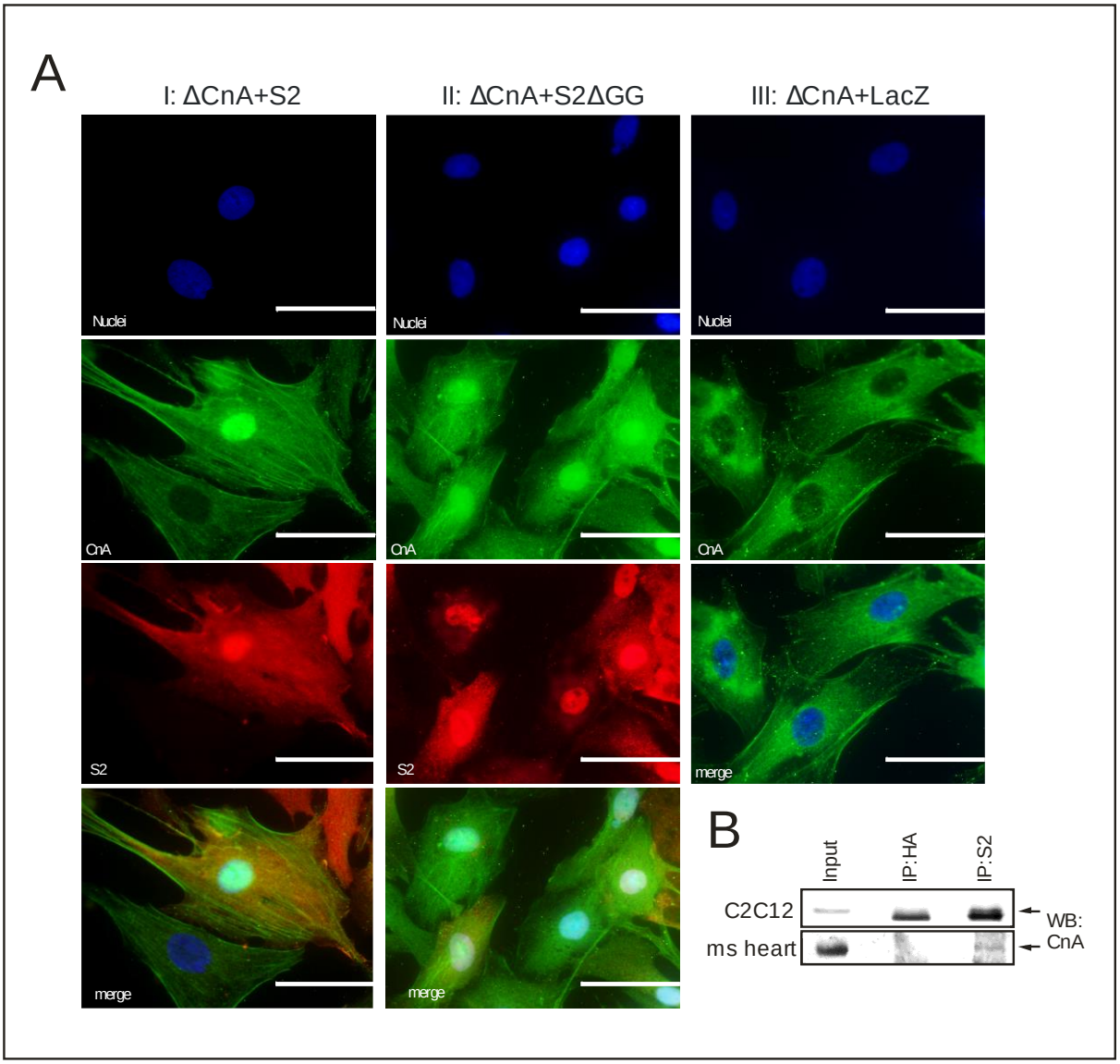

Figure 15: SUMO2 directly interacts with and tethers CnA to the nucleus in cardiomyocytes. A**,** Representative immunofluorescence analysis of fixed NRVCM-cells overexpressing GFP-ΔCnA in combination with SUMO2 (I), SUMO2ΔGG (II), or alone (III) show that CnA is translocated to the nucleus in cells overexpressing both, CnA and the respective SUMO construct, whereas it remains cytoplasmic in cells overexpressing CnA alone; CnA, green; SUMO2 and SUMO2ΔGG, red; Dapi, blue (scale bar 50 µm). B, Immunoprecipitation was performed using Dynabeads and Antibodies against HA (sigma, control) and SUMO2+3 (Abcam) as explained in methods section. 50µg of input lysate was loaded, 1 mg of protein was used for precipitation. For western blotting CnA antibody (BD) was used.

7 Discussion

The heart's reaction to increased and persisting biomechanical stress is the development of cardiac hypertrophy. Initially, this response is physiologic, similar to the changes the heart undergoes when challenged with exceptional exercise. In this adaptive hypertrophy, the cardiac muscle cells grow to enable an accelerated function, that is an increase in pressure build-up and ejected blood volume overall. In cultured cells this increase in cell surface area is typically accompanied by the elevated expression of the genes encoding natriuretic peptides *nppa* (protein: natriuretic peptide A) and *nppb* (protein: bain natriuretic peptide). This hypertrophic phenotype in the heart and cultured cells is well reviewed by Dorn and others (Dorn et al., 2003). Enduring pressure overload and thus biomechanical stress switches the initial adaptive response to a maladaptive process, where the mechanical capacity of the heart decreases typically by remodeling of the heart tissue followed by myocardial infarction, chronic hypertension or valvular heart disease, among others (Ertl and Frantz, 2005; Frantz et al., 2009; Pfeffer and Braunwald, 1990; Zwadlo and Borlak, 2005). The aim was to identify new signaling pathways and therefore proteins involved in pathologic hypertrophy to possibly lay the foundation for the assessment of future therapy options. One of the best-studied signaling pathways leading to the development of hypertrophy after biomechanical stress is the calcineurin-NFAT signaling axis (van Berlo et al., 2013). Calcineurin is a calcium-calmodulin dependent serine-threonine protein phosphatase, that has previously been found to be a pro-hypertrophic signaling modulator (Molkentin et al., 1998). Extensive knowledge has been accumulated over the last 17 years about the role that calcineurin plays in the heart. Yet, besides the upstream calcium-calmodulin-axis, to date there are still few direct calcineurin activators known. Therefore, in the present study I aimed to identify alternative modulators of calcineurin-NFAT signaling and their influence on the development of cardiomyocyte hypertrophy. With SUMO2 a strong and direct activator of the calcineurin-NFAT axis was identified. This activation could be observed in two different cell types, C2C12 cells, a mouse skeletal myoblast cell line and in NRVCM, primary cultured cells from neonatal rat ventricles. The effects were first measured via NFAT-driven luciferase reporter and were very similar among the two different cell types. Moreover, it was discovered that SUMO2 induces

cardiomyocyte hypertrophy in NRVCM and does so in a sumoylation independent manner via a direct interaction with CnA.

The research efforts taken to identify endogenous modulators of calcineurin activity have been large, their majority yielding the identification of inhibitory molecules (reviewed in (Frey et al., 2004; Wilkins and Molkentin, 2004). Calcineurin is mainly activated by a rise of intracellular Ca^{2+} levels. Ca^{2+} ions bind to calmodulin that in turn induces a conformational change of calcineurin associated with displacement of its autoinhibitory domain, rendering the phosphatase active. It has been previously reported that a protein termed Dyxin, may act as a strong activator of calcineurin-mediated cardiac hypertrophy (Frank et al., 2010). On the other hand, a variety of CnA inhibitors have been published. For example the protein Cain, being a non-competitive inhibitor for Cn in neurons, whereas AKAP79 directly interacts with and blocks calcineurin activity in cardiomyocytes. A family of calcineurin-interacting proteins, calsarcins is also crucial for the hypertrophic calcineurin-NFAT pathway, negatively regulating CnA activity and thus NFAT activation (Frey et al., 2000). Consistently, calsarcin-1 knockout mice show exaggerated hypertrophy following pressure overload in mice (Frey et al., 2008). The two pharmacologic agents, ciclosporin and FK506/tacrolimus have been widely used in immunosuppressant therapy following organ transplant action and were only later found to inhibit calcineurin by binding to endogenous immunophilin proteins, termed cyclophilin A and FKBP12, respectively (Liu et al., 1991). This underscores the broad relevance of calcineurin mediated signal transduction apart from muscle tissue. Rcan1-4 is another essential calcineurin-NFAT modulator and also serves as an endogenous indicator of the activation of calcineurin-NFAT signaling (Yang et al., 2000). Rcan1-4 is one of the target genes of NFAT, but its precise function is still under debate due to both inhibitory and activator roles which have been observed under different experimental conditions (Fox and Heitman, 2005; Sanna et al., 2006; Vega et al., 2003a; Vega et al., 2003b). More recently however, employing a systems biology approach and using single-cell experimentation in combination with *in silico* simulations, Shin et al have suggested a dose dependent effect of Rcan1-4 as an inhibitor at lower levels but as a facilitator at higher expression levels, adding another layer of complexity to the regulation of calcineurin (Shin et al., 2011).

A luciferase mediated screening approach for modulators of specific proteins or signaling pathways has led to the identification of protein interactions in the past (Chang et al., 2005). Chang and colleagues performed a screening experiment for the identification of Histone-

deacetylase (HDAC) class II modulators (Chang et al., 2005). They designed a eukaryotic expression screen with two different fusion proteins and a Gal4-responsive luciferase to detect HDAC-modulating proteins. Therefor the transcription-factor Gal4 DNA binding domain was fused to the N-terminus of HDAC5, a class II HDAC as well as the fusion of the two transcription activating proteins V16 and 14-3-3. Transfection of these fusion proteins alongside an HDAC5-kinase modulating cDNA from a eukaryotic cDNA-library would result in an activation of luciferase expression by reconstituting a functional Gal4 transcriptional complex when HDAC5-Gal4 fusion protein could recruit the VP16-14-3-3 fusion protein. Similarly, a screening strategy based on an NFAT-reporter mediated firefly luciferase assay to search for yet unknown modulators of the calcineurin-NFAT signaling axis was designed. A C2C12 cell line subtype was generated, C2C12-NFAT which is a cell line of mouse myotube origin that stably expressed an NFAT-responsive element driven luciferase, making NFAT-activation in these cells visible through the enhanced expression of a firefly luciferase. This cell line enabled the screening approach of the human heart cDNA library, in a way where serial dilutions of this library were transfected into C2C12-NFAT cells and expressed in the presence of NFAT-reporter luciferase and calcineurin.

Several putative candidates were discovered that activated calcineurin-NFAT signaling, yet their activation of this pathway was lower than the positive control, that was set as a threshold for individual screening sets. Since the study initially aimed for the identification of activating molecules that modulate NFAT-signaling beyond the capabilities of the positive control, those low-activating candidates were excluded. After applying this rigorous cutoff filter, only two plausible calcineurin-NFAT signaling activators were identified, SUMO2 and PRP31. After repetition of the original screening experiment in a larger scale and with single clones, PRP31 failed to activate the NFAT-signaling in a sufficient manner, leading the focus on the investigation of SUMO2 and its calcineurin activation capabilities.

Here, I discovered SUMO2 to be an activator of the calcineurin-NFAT signaling pathway in mouse skeletal muscle cells. C2C12-NFAT cells were utilized for screening and verification processes, yet are not cells of cardiac origin as well as they are immortalized cells, reducing their ability to gain information about SUMO2's involvement in cardiac signaling. For this purpose the cell-system was changed to neonatal rat ventricular cardiomyocytes (NRVCM), a rat-ventricle derived primary cell culture that diminishes the bias from immortalized and non-cardiac cell lines. The calcineurin-NFAT activating properties of SUMO2 were well verified in

NRVCM, furthering the relevance in cardiac signaling in general and particularly for possible hypertrophy modulating properties in the heart. Along the same lines, a depletion of the available SUMO2 by micro-RNA mediated knockdown resulted in a significant decrease of NFAT activation at baseline levels as well as in challenged cells. This is shown when even in the presence of strong NFAT-signaling activators like phenylephrine or Ionomycin and PMA, the reduction of SUMO2-protein levels decreased the NFAT-signaling activation significantly. Consistent with the hypothesis of a direct calcineurin-modulation, Rcan1-4 was also downregulated upon SUMO2 knockdown under conditions of constitutive CnA activation, which further supports an involvement of endogenous SUMO2 in the calcineurin-NFAT signaling pathway.

SUMO proteins are a family of four in human (SUMO1-4 (Guo et al., 2004; Melchior, 2000)) that were discovered in the context of their ability to covalently and reversibly modify their target proteins, thereby influencing protein activity, localization and stability. SUMO proteins share Ubiquitin's three-dimensional structure yet only 20% of the amino-acid sequence (Bernier-Villamor et al., 2002; Huang et al., 2004; Mossessova et al., 2003). In cardiologic research SUMO2 and the other SUMO family members have been found to be involved in cellular signaling and disease. For that reason, studying the effect of SUMO2 in the context of cardiomyocytes is particularly interesting. An example of an association of SUMOs with cardiac diseases in humans was suggested by Kho *et al*, where they find a link between SUMO1 and the regulation of SERCA2a in the context of heart failure, stabilizing the protein and its ATPase activity (Kho et al., 2011). In failing hearts though, sumoylation of SERCA2a and general SUMO1 levels were greatly reduced (Kho et al., 2011). SUMO1 was the first member of the protein family identified and has been extensively characterized (Citro and Chiocca, 2013; Matunis et al., 1996; Pichler and Melchior, 2002). Very recently, Gupta and colleagues could show that the SUMO-conjugating enzyme UBC9, which is the only know SUMO2-E3 ligase yet discovered, is of great importance for protein quality control in cardiomyocytes (Gupta et al., 2014). Of note, SUMO2 has also been implicated in human cardiomyopathy where diminished sumoylation of Lamin A resulted in accelerated cell death. Lamin A is a direct SUMO2 target and shows two naturally occurring mutants associated with familial cardiomyopathy, localized to a sumoylation consensus-motif around Lysine^{201} (Zhang and Sarge, 2008). I here show that SUMO2 expression and SUMO2-dependent sumoylation is enhanced in two important mouse models of cardiac hypertrophy and pressure overload. Calcineurin transgenic as well as

transverse aortic constricted mice both show elevated levels of SUMO2 and an overall increase in sumoylated proteins compared to their wildtype littermates or sham operated animals. In line with the proposed mechanism of SUMO2 acting as a facilitator of Calcineurin-NFAT signaling, especially in calcineurin transgenic mice, elevated levels of SUMO2 could add to NFAT activation even though SUMO2 itself does not seem to regulate calcineurin expression levels.

The two proteins, atrial natriuretic peptide and brain natriuretic peptide are diuretic and natriuretic hormones that are produced by the fetal, but also adult heart (Sergeeva et al., 2014). Simultaneously, cardiac stress induces a ventricular expression of the encoding genes, *nppa (*atrial natriuretic peptide) and *nppb* (brain natriuretic peptide). For this reason, *Nppa* and *Nppb* are generally accepted markers for the hypertrophic response in cell culture (Pikkarainen et al., 2003) or for the development of hypertrophy and heart failure in animal models (Sergeeva and Christoffels, 2013; Sergeeva et al., 2014). Additionally, *rcan1-4* expression (Vega et al., 2003a) as well as the increase in cell surface area are used as markers for the emergence of hypertrophy in cell culture. To additionally support the facilitator effect for SUMO2 on calcineurin-NFAT signaling not only elevated expression levels of the hypertrophy associated genes *nppa and nppb* were observed but also of the direct NFAT target *rcan1-4*. Furthermore, these molecular changes were accompanied by an increase in cell surface area when overexpressing SUMO2, fulfilling all of the above mentioned characteristics for the incurrence of cellular hypertrophy. These effects could be augmented by co-overexpression of constitutively active CnA, implying a direct functional interaction between CnA and SUMO2 that is also supported by the elevated expression levels of *rcan1-4*. In further support of this notion, a direct interaction between CnA and SUMO2 in both skeletal muscle cells and mouse heart tissue as visualized by the co-immunoprecipitation experiments was observed. Recently, another direct interaction partner for CnA has been identified, also leading to the activation of the NFAT-signaling pathway. The plasma membrane Na^+/H^+-exchanger 1 was found to stimulate hypertrophic gene expression in NRVCM via calcineurin (Hisamitsu et al., 2012).

The majority of SUMO-dependent modulations and modifications published so far are based on the sumoylation of target proteins. SUMO is expressed as a precursor protein that has to be cleaved in order to be activated through accessibility of two C-terminal glycines (SUMO diglycine motif). Apart from the well-studied sumoylation modifications, there has been a recent discovery of non-covalent sumo-interaction or –binding motifs (SIM/SBM) (Hecker et al., 2006;

Song et al., 2004) which influence their targets, all of which are themselves sumoylated proteins (Lin et al., 2006; Minty et al., 2000; Shen et al., 2006; Song et al., 2004). Initially intended as a control for functional SUMO2, a construct (SUMO2ΔGG) was designed that is missing the diglycine motif and is thus deficient for sumoylation. Surprisingly, this sumoylation-deficient construct resembled the observed effect of SUMO2 in almost every investigated parameter. Expression levels of *nppa, nppb* and *rcan1-4* and the cell surface area was elevated and interestingly also the exaggeration of ΔCnA mediated effects on the cell surface area was resembled. From these observations, I draw the conclusion that the presented mechanism of calcineurin activation is independent of sumoylation of calcineurin. Such sumoylation-independent mechanisms of protein activity modulation have been published before. These so-called SUMO interacting/binding motifs (SIM/SBM) are subject of research and have led to a proposed consensus sequence for non-covalent SUMO-interactions (Seu and Chen, 2009; Song et al., 2004). There are several examples of sumoylation independent non-covalent functional SUMO1 interactions. For example, SUMO1 inhibits RAD51-mediated homologous recombination by interaction with RAD51 (Li et al., 2000). Similarly, SUMO1 protects against cell death by non-covalent interactions with Fas and tumor necrosis factor receptor 1 (TNFR1) (Okura et al., 1996). SUMO1 can also inhibit dynamin-dependent endocytosis without a covalent modification of dynamin (Mishra et al., 2004). Lee and colleagues have shown that SUMO1 represses apoptosis signal-regulating kinase 1 (ASK-1)-activation through physical interaction and not through sumoylation (Lee et al., 2005). Similarly, SUMO3 can co-activate EBNA2 (Epstein-Barr virus nuclear antigen 2) in the absence of direct conjugation to EBNA2 (Rosendorff et al., 2004). Finally, SUMO3 has been found to enhance Androgen Receptor (AR) transcription independent of SUMO3's sumoylation ability and AR sumoylation sites in prostate cancer cells (Zheng et al., 2006). Of note, Alontaga and others have recently published a method for the utilization of a high-throughput screening assay to identify small molecule inhibitors for SUMO1-interaction motifs (Alontaga et al., 2015). Applying this method to the identification of SUMO2-interaction disturbing molecules is particularly interesting to advance the knowledge about the proposed mechanism as well as the investigation of possible therapeutic approaches in the future. However, to the best of my knowledge, SUMO2 has not been implicated in any non-covalent, sumoylation-independent functional interactions so far. Here, a direct endogenous functional interaction between SUMO2 and CnA was demonstrated that could be well correlated with SUMO2-mediated

activation of calcineurin-NFAT signaling. As a possible mechanism of action for the SUMO2 induced activation of calcineurin, I hypothesize a tethering of CnA to the nucleus.

Nuclear translocation of activated calcineurin has already been reported in failing human hearts and this nuclear pool of calcineurin is important in the development of cardiac hypertrophy (Burkard et al., 2005). Although the exact role of calcineurin in the nucleus is still unknown, it has been hypothesized that it is a transcriptional co-activator through direct interaction with DNA-bound NFAT (Heineke and Ritter, 2012). The inhibition of nuclear calcineurin import with an artificial import blocking peptide prevents myocardial hypertrophy (Hallhuber et al., 2006). With SUMO2, a protein was identified that is directly involved in the cytosolic to nuclear translocation and/or a nuclear retention of a pool of calcineurin A, suggesting this may represent the mechanism by which SUMO2 induces cardiomyocyte hypertrophy and general activation of calcineurin-NFAT signaling. This nuclear-retention of calcineurin seems to be independent of SUMO2's sumoylation capabilities since nuclear CnA can be found in cells overexpressing SUMO2 or SUMO2ΔGG but not in the control cells. Supporting this hypothesis, bioinformatics prediction of SIM/SBM for CnA reveals a possible 5 amino acid motif "LFLLR" in close proximity to the proposed nuclear localization site and the phosphatase-domain (Ren et al., 2009; Zhao et al., 2014). SUMO2-induced conformational change could expose the NLS and possibly explain a shift towards nuclear localization of CnA upon SUMO2 overexpression. The understanding of posttranslational modifications like sumoylation or the protein-protein interactions through SIM/SBM seems to be of great importance for the understanding the molecular mechanism leading to heart failure and cardiac hypertrophy. Modulation of these pathways could prove an effective means for altering disease development and progression in the future. SUMO2 was found as an interesting candidate for the modulation of the calcineurin-NFAT driven cardiac hypertrophy via SUMO-interaction with CnA.

In conclusion, based on an unbiased screening experiment, SUMO2 was linked to increased NFAT-activation, the induction of hypertrophy-associated genes, and an increase in cardiomyocyte surface area+. Moreover, a direct interaction between SUMO2 and CnA was found as well as an involvement of endogenous SUMO2 in the activation of NFAT signaling. Surprisingly, similar results for SUMO2 and sumoylation-deficient SUMO2ΔGG were obtained in every parameter investigated, which ruled out a sole sumoylation-dependent effect. I thus

propose a mechanism where SUMO2 activates cardiac hypertrophy independent of sumoylation by direct interaction with CnA, facilitating its translocation to the nucleus.

Given the relevance of the calcineurin-NFAT axis in a multitude of cells and organ systems, the further investigation of this mechanism might be valuable for other fields of research such as immunology, where calcineurin plays an indispensable role in the activation of the immune response via NFAT and where the pharmacologic inhibition of calcineurin results in immunosuppression. This thesis presents a mechanism for the involvement of SUMO2 on a major signaling pathway in the heart and implies a multitude of regulatory roles on cellular signaling in other organ systems. To clarify a possible role for SUMO2 in the modulation of the immune response could be of great value.

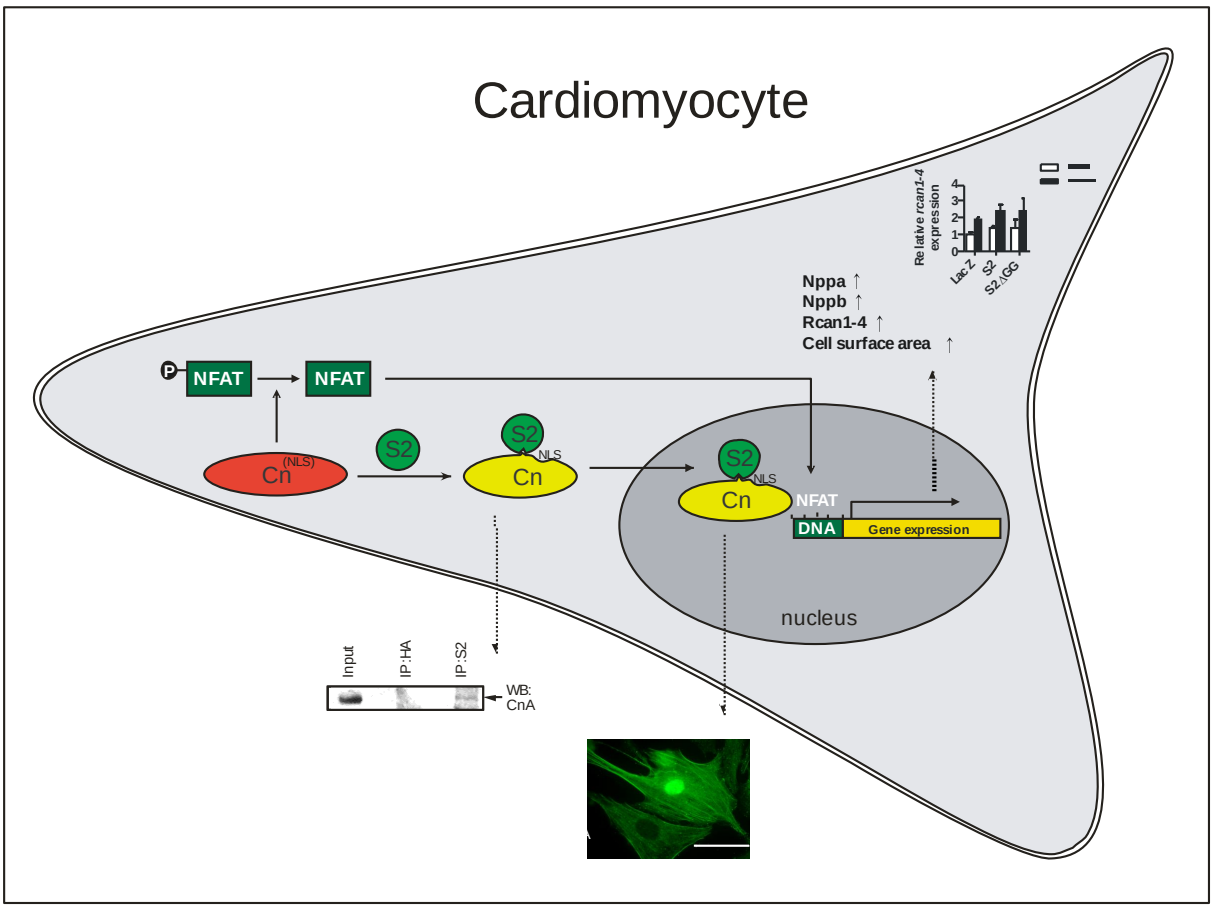

Figure 16: Schematic drawing of a possible mechanism by which SUMO2 induces cardiomyocyte hypertrophy.

7.1 Outlook

The proposed mechanism for a sumoylation-independent activation of calcineurin-NFAT signaling by tethering calcineurin to the nucleus is a first step towards the characterization of the role of small ubiquitin-related modifier 2 in general and in the context of cardiology in particular. To further elaborate this mechanism, the interaction between SUMO2 and calcineurin has to be mapped and analyzed. Figure 17 shows a schematic overview of the calcineurin protein, indicating two putative SUMO-interaction motifs, one based on the consensus sequence for SUMO2 protein-protein interaction sites, the other based on a bioinformatics approach. Therefore, mutation-studies have to be carried out to pinpoint the location of SUMO2-calcineurin interaction and thus providing evidence for the verification of our proposed mechanism.

Secondly, the role for SUMO2 in the development of pathologic cardiac hypertrophy has to be investigated *in vivo*. One possible approach that does not involve the generation of heart-specific knockdown or overexpression mouse-models could be achieved by generating specific adeno-associated viruses (AAV). AAV subtypes can be specifically modified and injected into mouse tail-veins for the tissue-specific expression of a nucleic acid of interest (Pleger et al., 2011; Ying et al., 2010). AAV9 specifically targets the heart (and also the liver) and can be used to overexpress SUMO2 in the heart of wild-type mice to investigate the possible development of a cardiac hypertrophy that would prove SUMO2 to be a sufficient inducer of hypertrophy. Similarly, a knockdown of SUMO2 in mice challenged with pressure-overload and consequent development of hypertrophy could be a useful tool to assess the necessity of SUMO2 for the hypertrophic signaling and to investigate possible benefits by the modulation of SUMO2 expression levels.

All these lines of experiments are fundamental for future studies in humans and will need to be supplemented by collecting information about the SUMO2 expression levels in samples from patients that suffer from cardiac disease. After the verification of a pathophysiologic relevance of SUMO2 in the development of disease, the design of specific pharmacologic inhibitors for disturbing the calcineurin-SUMO2 interaction could be a useful tool for future therapy approaches.

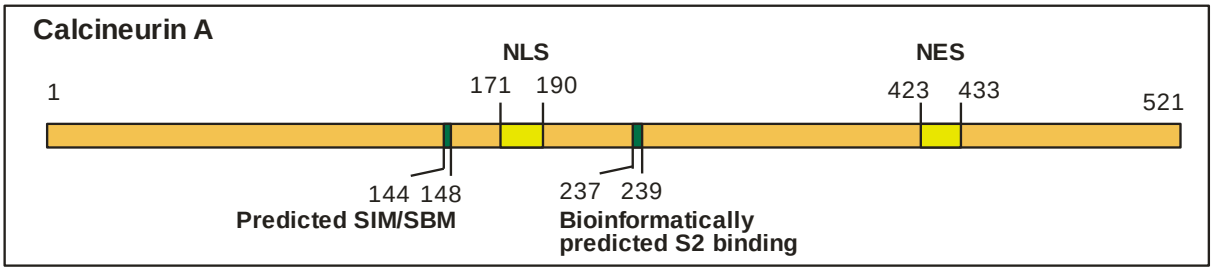

Figure 17: Schematic drawing of CnA with nuclear localization site (NLS), nuclear export site (NES) and predicted putative sumoylation interaction/binding motifs (SIM/SBM) from both, consensus-motif search as well as independent bioinformatically predicted motif.

8 Literature

Alkuraya, F.S., I. Saadi, J.J. Lund, A. Turbe-Doan, C.C. Morton, and R.L. Maas. 2006. SUMO1 haploinsufficiency leads to cleft lip and palate. *Science*. 313:1751.

Alontaga, A.Y., Y. Li, C.H. Chen, C.T. Ma, S. Malany, D.E. Key, E. Sergienko, Q. Sun, D.A. Whipple, D.S. Matharu, B. Li, R. Vega, Y.J. Li, F.J. Schoenen, B.S. Blagg, T.D. Chung, and Y. Chen. 2015. Design of High Throughput Screening Assays and Identification of a SUMO1-Specific Small Molecule Chemotype Targeting the SUMO-Interacting Motif-Binding Surface. *ACS combinatorial science*.

Antos, C.L., T.A. McKinsey, N. Frey, W. Kutschke, J. McAnally, J.M. Shelton, J.A. Richardson, J.A. Hill, and E.N. Olson. 2002. Activated glycogen synthase-3 beta suppresses cardiac hypertrophy in vivo. *Proc Natl Acad Sci U S A*. 99:907-912.

Baba, D., N. Maita, J.G. Jee, Y. Uchimura, H. Saitoh, K. Sugasawa, F. Hanaoka, H. Tochio, H. Hiroaki, and M. Shirakawa. 2005. Crystal structure of thymine DNA glycosylase conjugated to SUMO-1. *Nature*. 435:979-982.

Barford, D., A.K. Das, and M.P. Egloff. 1998. The structure and mechanism of protein phosphatases: insights into catalysis and regulation. *Annual review of biophysics and biomolecular structure*. 27:133-164.

Bernier-Villamor, V., D.A. Sampson, M.J. Matunis, and C.D. Lima. 2002. Structural basis for E2-mediated SUMO conjugation revealed by a complex between ubiquitin-conjugating enzyme Ubc9 and RanGAP1. *Cell*. 108:345-356.

Beullens, M., A. Van Eynde, W. Stalmans, and M. Bollen. 1992. The isolation of novel inhibitory polypeptides of protein phosphatase 1 from bovine thymus nuclei. *J Biol Chem*. 267:16538-16544.

Brattstrom, A., A. Schapowal, I. Maillet, B. Schnyder, B. Ryffel, and R. Moser. 2010. Petasites extract Ze 339 (PET) inhibits allergen-induced Th2 responses, airway inflammation and airway hyperreactivity in mice. *Phytotherapy research : PTR*. 24:680-685.

Bueno, O.F., E. van Rooij, J.D. Molkentin, P.A. Doevendans, and L.J. De Windt. 2002a. Calcineurin and hypertrophic heart disease: novel insights and remaining questions. *Cardiovascular research*. 53:806-821.

Bueno, O.F., B.J. Wilkins, K.M. Tymitz, B.J. Glascock, T.F. Kimball, J.N. Lorenz, and J.D. Molkentin. 2002b. Impaired cardiac hypertrophic response in Calcineurin Abeta -deficient mice. *Proc Natl Acad Sci U S A*. 99:4586-4591.

Burkard, N., J. Becher, C. Heindl, L. Neyses, K. Schuh, and O. Ritter. 2005. Targeted proteolysis sustains calcineurin activation. *Circulation*. 111:1045-1053.

Cappadocia, L., X.H. Mascle, V. Bourdeau, S. Tremblay-Belzile, M. Chaker-Margot, M. Lussier-Price, J. Wada, K. Sakaguchi, M. Aubry, G. Ferbeyre, and J.G. Omichinski. 2015. Structural and functional characterization of the phosphorylation-dependent interaction between PML and SUMO1. *Structure*. 23:126-138.

Chang, S., S. Bezprozvannaya, S. Li, and E.N. Olson. 2005. An expression screen reveals modulators of class II histone deacetylase phosphorylation. *Proc Natl Acad Sci U S A*. 102:8120-8125.

Chen, A., H. Mannen, and S.S. Li. 1998. Characterization of mouse ubiquitin-like SMT3A and SMT3B cDNAs and gene/pseudogenes. *Biochemistry and molecular biology international*. 46:1161-1174.

Chow, C.W., M. Rincon, J. Cavanagh, M. Dickens, and R.J. Davis. 1997. Nuclear accumulation of NFAT4 opposed by the JNK signal transduction pathway. *Science*. 278:1638-1641.

Citro, S., and S. Chiocca. 2013. Sumo paralogs: redundancy and divergencies. *Front Biosci (Schol Ed)*. 5:544-553.

Cohen, P. 1989. The structure and regulation of protein phosphatases. *Annual review of biochemistry*. 58:453-508.

Colella, M., F. Grisan, V. Robert, J.D. Turner, A.P. Thomas, and T. Pozzan. 2008. Ca2+ oscillation frequency decoding in cardiac cell hypertrophy: role of calcineurin/NFAT as Ca2+ signal integrators. *Proc Natl Acad Sci U S A*. 105:2859-2864.

Cook, W.J., L.C. Jeffrey, M. Carson, Z. Chen, and C.M. Pickart. 1992. Structure of a diubiquitin conjugate and a model for interaction with ubiquitin conjugating enzyme (E2). *J Biol Chem*. 267:16467-16471.

Di Bacco, A., and G. Gill. 2006. SUMO-specific proteases and the cell cycle. An essential role for SENP5 in cell proliferation. *Cell Cycle*. 5:2310-2313.

Di Bacco, A., J. Ouyang, H.Y. Lee, A. Catic, H. Ploegh, and G. Gill. 2006. The SUMO-specific protease SENP5 is required for cell division. *Molecular and cellular biology*. 26:4489-4498.

Ding, H., Y. Xu, Q. Chen, H. Dai, Y. Tang, J. Wu, and Y. Shi. 2005. Solution structure of human SUMO-3 C47S and its binding surface for Ubc9. *Biochemistry*. 44:2790-2799.

Dorn, G.W., 2nd, J. Robbins, and P.H. Sugden. 2003. Phenotyping hypertrophy: eschew obfuscation. *Circ Res*. 92:1171-1175.

Ertl, G., and S. Frantz. 2005. Wound model of myocardial infarction. *Am J Physiol Heart Circ Physiol*. 288:H981-983.

Fox, D.S., and J. Heitman. 2005. Calcineurin-binding protein Cbp1 directs the specificity of calcineurin-dependent hyphal elongation during mating in Cryptococcus neoformans. *Eukaryot Cell*. 4:1526-1538.

Frank, D., R. Frauen, C. Hanselmann, C. Kuhn, R. Will, J. Gantenberg, L. Fuzesi, H.A. Katus, and N. Frey. 2010. Lmcd1/Dyxin, a novel Z-disc associated LIM protein, mediates cardiac hypertrophy in vitro and in vivo. *J Mol Cell Cardiol*. 49:673-682.

Frantz, S., J. Bauersachs, and G. Ertl. 2009. Post-infarct remodelling: contribution of wound healing and inflammation. *Cardiovascular research*. 81:474-481.

Frey, N., D. Frank, S. Lippl, C. Kuhn, H. Kogler, T. Barrientos, C. Rohr, R. Will, O.J. Muller, H. Weiler, R. Bassel-Duby, H.A. Katus, and E.N. Olson. 2008. Calsarcin-2 deficiency increases exercise capacity in mice through calcineurin/NFAT activation. *J Clin Invest*. 118:3598-3608.

Frey, N., H.A. Katus, E.N. Olson, and J.A. Hill. 2004. Hypertrophy of the heart: a new therapeutic target? *Circulation*. 109:1580-1589.

Frey, N., J.A. Richardson, and E.N. Olson. 2000. Calsarcins, a novel family of sarcomeric calcineurin-binding proteins. *Proc Natl Acad Sci U S A*. 97:14632-14637.

Geiss-Friedlander, R., and F. Melchior. 2007. Concepts in sumoylation: a decade on. *Nat Rev Mol Cell Biol*. 8:947-956.

Gong, L., and E.T. Yeh. 2006. Characterization of a family of nucleolar SUMO-specific proteases with preference for SUMO-2 or SUMO-3. *J Biol Chem*. 281:15869-15877.

Goodson, M.L., Y. Hong, R. Rogers, M.J. Matunis, O.K. Park-Sarge, and K.D. Sarge. 2001. Sumo-1 modification regulates the DNA binding activity of heat shock transcription factor 2, a promyelocytic leukemia nuclear body associated transcription factor. *J Biol Chem*. 276:18513-18518.

Gorlich, D., M.J. Seewald, and K. Ribbeck. 2003. Characterization of Ran-driven cargo transport and the RanGTPase system by kinetic measurements and computer simulation. *The EMBO journal*. 22:1088-1100.

Guerini, D., C. Montell, and C.B. Klee. 1992. Molecular cloning and characterization of the genes encoding the two subunits of Drosophila melanogaster calcineurin. *J Biol Chem*. 267:22542-22549.

Guo, D., M. Li, Y. Zhang, P. Yang, S. Eckenrode, D. Hopkins, W. Zheng, S. Purohit, R.H. Podolsky, A. Muir, J. Wang, Z. Dong, T. Brusko, M. Atkinson, P. Pozzilli, A. Zeidler, L.J. Raffel, C.O. Jacob, Y. Park, M. Serrano-Rios, M.T. Larrad, Z. Zhang, H.J. Garchon, J.F. Bach, J.I. Rotter, J.X. She, and C.Y. Wang. 2004. A functional variant of SUMO4, a new I kappa B alpha modifier, is associated with type 1 diabetes. *Nat Genet*. 36:837-841.

Gupta, M.K., J. Gulick, R. Liu, X. Wang, J.D. Molkentin, and J. Robbins. 2014. Sumo E2 enzyme UBC9 is required for efficient protein quality control in cardiomyocytes. *Circ Res*. 115:721-729.

Hallhuber, M., N. Burkard, R. Wu, M.H. Buch, S. Engelhardt, L. Hein, L. Neyses, K. Schuh, and O. Ritter. 2006. Inhibition of nuclear import of calcineurin prevents myocardial hypertrophy. *Circ Res*. 99:626-635.

Haq, S., G. Choukroun, H. Lim, K.M. Tymitz, F. del Monte, J. Gwathmey, L. Grazette, A. Michael, R. Hajjar, T. Force, and J.D. Molkentin. 2001. Differential activation of signal transduction pathways in human hearts with hypertrophy versus advanced heart failure. *Circulation*. 103:670-677.

Hecker, C.M., M. Rabiller, K. Haglund, P. Bayer, and I. Dikic. 2006. Specification of SUMO1- and SUMO2-interacting motifs. *J Biol Chem*. 281:16117-16127.

Heineke, J., M. Auger-Messier, R.N. Correll, J. Xu, M.J. Benard, W. Yuan, H. Drexler, L.V. Parise, and J.D. Molkentin. 2010. CIB1 is a regulator of pathological cardiac hypertrophy. *Nat Med*. 16:872-879.

Heineke, J., and O. Ritter. 2012. Cardiomyocyte calcineurin signaling in subcellular domains: from the sarcolemma to the nucleus and beyond. *J Mol Cell Cardiol*. 52:62-73.

Hisamitsu, T., T.Y. Nakamura, and S. Wakabayashi. 2012. Na(+)/H(+) exchanger 1 directly binds to calcineurin A and activates downstream NFAT signaling, leading to cardiomyocyte hypertrophy. *Molecular and cellular biology*. 32:3265-3280.

Hochstrasser, M. 2001. SP-RING for SUMO: new functions bloom for a ubiquitin-like protein. *Cell*. 107:5-8.

Hogan, P.G., L. Chen, J. Nardone, and A. Rao. 2003. Transcriptional regulation by calcium, calcineurin, and NFAT. *Genes & development*. 17:2205-2232.

Hogan, P.G., and A. Rao. 1999. Transcriptional regulation. Modification by nuclear export? *Nature*. 398:200-201.

Huang, W.C., T.P. Ko, S.S. Li, and A.H. Wang. 2004. Crystal structures of the human SUMO-2 protein at 1.6 A and 1.2 A resolution: implication on the functional differences of SUMO proteins. *Eur J Biochem*. 271:4114-4122.

Hwang, K.W., T.J. Won, H. Kim, H.J. Chun, T. Chun, and Y. Park. 2011. Characterization of the regulatory roles of the SUMO. *Diabetes/metabolism research and reviews*. 27:854-861.

Iwaki, K., V.P. Sukhatme, H.E. Shubeita, and K.R. Chien. 1990. Alpha- and beta-adrenergic stimulation induces distinct patterns of immediate early gene expression in neonatal rat myocardial cells. fos/jun expression is associated with sarcomere assembly; Egr-1 induction is primarily an alpha 1-mediated response. *J Biol Chem*. 265:13809-13817.

Jans, D.A., C.Y. Xiao, and M.H. Lam. 2000. Nuclear targeting signal recognition: a key control point in nuclear transport? *BioEssays : news and reviews in molecular, cellular and developmental biology*. 22:532-544.

Kerscher, O. 2007. SUMO junction-what's your function? New insights through SUMO-interacting motifs. *EMBO reports*. 8:550-555.

Kho, C., A. Lee, D. Jeong, J.G. Oh, A.H. Chaanine, E. Kizana, W.J. Park, and R.J. Hajjar. 2011. SUMO1-dependent modulation of SERCA2a in heart failure. *Nature*. 477:601-605.

Kim, E.Y., Y. Zhang, I. Beketaev, A.M. Segura, W. Yu, Y. Xi, J. Chang, and J. Wang. 2015. SENP5, a SUMO isopeptidase, induces apoptosis and cardiomyopathy. *J Mol Cell Cardiol*. 78:154-164.

Kim, K.I., and S.H. Baek. 2009. Small ubiquitin-like modifiers in cellular malignancy and metastasis. *International review of cell and molecular biology*. 273:265-311.

Komatsu, T., H. Mizusaki, T. Mukai, H. Ogawa, D. Baba, M. Shirakawa, S. Hatakeyama, K.I. Nakayama, H. Yamamoto, A. Kikuchi, and K. Morohashi. 2004. Small ubiquitin-like modifier 1 (SUMO-1) modification of the synergy control motif of Ad4 binding protein/steroidogenic factor 1 (Ad4BP/SF-1) regulates synergistic transcription between Ad4BP/SF-1 and Sox9. *Mol Endocrinol*. 18:2451-2462.

Kuhn, C., D. Frank, R. Will, C. Jaschinski, R. Frauen, H.A. Katus, and N. Frey. 2009. DYRK1A is a novel negative regulator of cardiomyocyte hypertrophy. *J Biol Chem*. 284:17320-17327.

Lee, Y.S., M.S. Jang, J.S. Lee, E.J. Choi, and E. Kim. 2005. SUMO-1 represses apoptosis signal-regulating kinase 1 activation through physical interaction and not through covalent modification. *EMBO reports*. 6:949-955.

Li, W., B. Hesabi, A. Babbo, C. Pacione, J. Liu, D.J. Chen, J.A. Nickoloff, and Z. Shen. 2000. Regulation of double-strand break-induced mammalian homologous recombination by UBL1, a RAD51-interacting protein. *Nucleic Acids Res*. 28:1145-1153.

Lim, H.W., and J.D. Molkentin. 1999. Calcineurin and human heart failure. *Nat Med*. 5:246-247.

Lin, D.Y., Y.S. Huang, J.C. Jeng, H.Y. Kuo, C.C. Chang, T.T. Chao, C.C. Ho, Y.C. Chen, T.P. Lin, H.I. Fang, C.C. Hung, C.S. Suen, M.J. Hwang, K.S. Chang, G.G. Maul, and H.M. Shih. 2006. Role of SUMO-interacting motif in Daxx SUMO modification, subnuclear localization, and repression of sumoylated transcription factors. *Molecular cell*. 24:341-354.

Lin, X., B. Sun, M. Liang, Y.Y. Liang, A. Gast, J. Hildebrand, F.C. Brunicardi, F. Melchior, and X.H. Feng. 2003. Opposed regulation of corepressor CtBP by SUMOylation and PDZ binding. *Molecular cell*. 11:1389-1396.

Liu, J., J.D. Farmer, Jr., W.S. Lane, J. Friedman, I. Weissman, and S.L. Schreiber. 1991. Calcineurin is a common target of cyclophilin-cyclosporin A and FKBP-FK506 complexes. *Cell*. 66:807-815.

Maejima, Y., and J. Sadoshima. 2014. SUMOylation: A Novel Protein Quality Control Modifier in the Heart. *Circ Res*. 115:686-689.

Maillet, M., J. Davis, M. Auger-Messier, A. York, H. Osinska, J. Piquereau, J.N. Lorenz, J. Robbins, R. Ventura-Clapier, and J.D. Molkentin. 2010. Heart-specific deletion of CnB1 reveals multiple mechanisms whereby calcineurin regulates cardiac growth and function. *J Biol Chem*. 285:6716-6724.

Matsuzaki, K., T. Minami, M. Tojo, Y. Honda, Y. Uchimura, H. Saitoh, H. Yasuda, S. Nagahiro, H. Saya, and M. Nakao. 2003. Serum response factor is modulated by the SUMO-1 conjugation system. *Biochemical and biophysical research communications*. 306:32-38.

Matunis, M.J., E. Coutavas, and G. Blobel. 1996. A novel ubiquitin-like modification modulates the partitioning of the Ran-GTPase-activating protein RanGAP1 between the cytosol and the nuclear pore complex. *The Journal of cell biology*. 135:1457-1470.

Mayer, R.J., M. Landon, and R. Layfield. 1998. Ubiquitin superfolds: intrinsic and attachable regulators of cellular activities? *Folding & design*. 3:R97-99.

Melchior, F. 2000. SUMO--nonclassical ubiquitin. *Annual review of cell and developmental biology*. 16:591-626.

Minty, A., X. Dumont, M. Kaghad, and D. Caput. 2000. Covalent modification of p73alpha by SUMO-1. Two-hybrid screening with p73 identifies novel SUMO-1-interacting proteins and a SUMO-1 interaction motif. *J Biol Chem*. 275:36316-36323.

Mishra, R.K., S.S. Jatiani, A. Kumar, V.R. Simhadri, R.V. Hosur, and R. Mittal. 2004. Dynamin interacts with members of the sumoylation machinery. *J Biol Chem*. 279:31445-31454.

Molkentin, J.D. 2006. Dichotomy of Ca2+ in the heart: contraction versus intracellular signaling. *J Clin Invest*. 116:623-626.

Molkentin, J.D., J.R. Lu, C.L. Antos, B. Markham, J. Richardson, J. Robbins, S.R. Grant, and E.N. Olson. 1998. A calcineurin-dependent transcriptional pathway for cardiac hypertrophy. *Cell*. 93:215-228.

Mossessova, E., R.A. Corpina, and J. Goldberg. 2003. Crystal structure of ARF1*Sec7 complexed with Brefeldin A and its implications for the guanine nucleotide exchange mechanism. *Molecular cell*. 12:1403-1411.

Mukhopadhyay, D., F. Ayaydin, N. Kolli, S.H. Tan, T. Anan, A. Kametaka, Y. Azuma, K.D. Wilkinson, and M. Dasso. 2006. SUSP1 antagonizes formation of highly SUMO2/3-conjugated species. *The Journal of cell biology*. 174:939-949.

Nacerddine, K., F. Lehembre, M. Bhaumik, J. Artus, M. Cohen-Tannoudji, C. Babinet, P.P. Pandolfi, and A. Dejean. 2005. The SUMO pathway is essential for nuclear integrity and chromosome segregation in mice. *Developmental cell*. 9:769-779.

Okura, T., L. Gong, T. Kamitani, T. Wada, I. Okura, C.F. Wei, H.M. Chang, and E.T. Yeh. 1996. Protection against Fas/APO-1- and tumor necrosis factor-mediated cell death by a novel protein, sentrin. *J Immunol*. 157:4277-4281.

Oshima, M., J. Mimura, H. Sekine, H. Okawa, and Y. Fujii-Kuriyama. 2009. SUMO modification regulates the transcriptional repressor function of aryl hydrocarbon receptor repressor. *J Biol Chem*. 284:11017-11026.

Pfeffer, M.A., and E. Braunwald. 1990. Ventricular remodeling after myocardial infarction. Experimental observations and clinical implications. *Circulation*. 81:1161-1172.

Pichler, A., P. Knipscheer, E. Oberhofer, W.J. van Dijk, R. Korner, J.V. Olsen, S. Jentsch, F. Melchior, and T.K. Sixma. 2005. SUMO modification of the ubiquitin-conjugating enzyme E2-25K. *Nature structural & molecular biology*. 12:264-269.

Pichler, A., and F. Melchior. 2002. Ubiquitin-related modifier SUMO1 and nucleocytoplasmic transport. *Traffic*. 3:381-387.

Pickart, C.M. 1997. Targeting of substrates to the 26S proteasome. *FASEB journal : official publication of the Federation of American Societies for Experimental Biology*. 11:1055-1066.

Pikkarainen, S., H. Tokola, T. Majalahti-Palviainen, R. Kerkela, N. Hautala, S.S. Bhalla, F. Charron, M. Nemer, O. Vuolteenaho, and H. Ruskoaho. 2003. GATA-4 is a nuclear mediator of mechanical stretch-activated hypertrophic program. *J Biol Chem*. 278:23807-23816.

Pleger, S.T., C. Shan, J. Ksienzyk, R. Bekeredjian, P. Boekstegers, R. Hinkel, S. Schinkel, B. Leuchs, J. Ludwig, G. Qiu, C. Weber, P. Raake, W.J. Koch, H.A. Katus, O.J. Muller, and P. Most. 2011. Cardiac AAV9-S100A1 gene therapy rescues post-ischemic heart failure in a preclinical large animal model. *Science translational medicine*. 3:92ra64.

Prudden, J., S. Pebernard, G. Raffa, D.A. Slavin, J.J. Perry, J.A. Tainer, C.H. McGowan, and M.N. Boddy. 2007. SUMO-targeted ubiquitin ligases in genome stability. *The EMBO journal*. 26:4089-4101.

Ren, J., X. Gao, C. Jin, M. Zhu, X. Wang, A. Shaw, L. Wen, X. Yao, and Y. Xue. 2009. Systematic study of protein sumoylation: Development of a site-specific predictor of SUMOsp 2.0. *Proteomics*. 9:3409-3412.

Ritter, O., S. Hack, K. Schuh, N. Rothlein, A. Perrot, K.J. Osterziel, H.D. Schulte, and L. Neyses. 2002. Calcineurin in human heart hypertrophy. *Circulation*. 105:2265-2269.

Rosendorff, A., D. Illanes, G. David, J. Lin, E. Kieff, and E. Johannsen. 2004. EBNA3C coactivation with EBNA2 requires a SUMO homology domain. *Journal of virology*. 78:367-377.

Rout, M.P., and J.D. Aitchison. 2001. The nuclear pore complex as a transport machine. *J Biol Chem*. 276:16593-16596.

Saitoh, H., and J. Hinchey. 2000. Functional heterogeneity of small ubiquitin-related protein modifiers SUMO-1 versus SUMO-2/3. *J Biol Chem*. 275:6252-6258.

Saitoh, H., D.B. Sparrow, T. Shiomi, R.T. Pu, T. Nishimoto, T.J. Mohun, and M. Dasso. 1998. Ubc9p and the conjugation of SUMO-1 to RanGAP1 and RanBP2. *Current biology : CB*. 8:121-124.

Sanna, B., E.B. Brandt, R.A. Kaiser, P. Pfluger, S.A. Witt, T.R. Kimball, E. van Rooij, L.J. De Windt, M.E. Rothenberg, M.H. Tschop, S.C. Benoit, and J.D. Molkentin. 2006. Modulatory calcineurin-interacting proteins 1 and 2 function as calcineurin facilitators in vivo. *Proc Natl Acad Sci U S A*. 103:7327-7332.

Sergeeva, I.A., and V.M. Christoffels. 2013. Regulation of expression of atrial and brain natriuretic peptide, biomarkers for heart development and disease. *Biochimica et biophysica acta*. 1832:2403-2413.

Sergeeva, I.A., I.B. Hooijkaas, I. Van Der Made, W.M. Jong, E.E. Creemers, and V.M. Christoffels. 2014. A transgenic mouse model for the simultaneous monitoring of ANF and BNP gene activity during heart development and disease. *Cardiovascular research*. 101:78-86.

Seu, C.S., and Y. Chen. 2009. Identification of SUMO-binding motifs by NMR. *Methods Mol Biol*. 497:121-138.

Shen, T.H., H.K. Lin, P.P. Scaglioni, T.M. Yung, and P.P. Pandolfi. 2006. The mechanisms of PML-nuclear body formation. *Molecular cell*. 24:331-339.

Shen, Z., P.E. Pardington-Purtymun, J.C. Comeaux, R.K. Moyzis, and D.J. Chen. 1996. UBL1, a human ubiquitin-like protein associating with human RAD51/RAD52 proteins. *Genomics*. 36:271-279.

Shenolikar, S., and A.C. Nairn. 1991. Protein phosphatases: recent progress. *Advances in second messenger and phosphoprotein research*. 23:1-121.

Shin, S.Y., H.W. Yang, J.R. Kim, W.D. Heo, and K.H. Cho. 2011. A hidden incoherent switch regulates RCAN1 in the calcineurin-NFAT signaling network. *J Cell Sci*. 124:82-90.

Song, J., L.K. Durrin, T.A. Wilkinson, T.G. Krontiris, and Y. Chen. 2004. Identification of a SUMO-binding motif that recognizes SUMO-modified proteins. *Proc Natl Acad Sci U S A*. 101:14373-14378.

Song, J., Z. Zhang, W. Hu, and Y. Chen. 2005. Small ubiquitin-like modifier (SUMO) recognition of a SUMO binding motif: a reversal of the bound orientation. *J Biol Chem*. 280:40122-40129.

Stemmer, P.M., and C.B. Klee. 1994. Dual calcium ion regulation of calcineurin by calmodulin and calcineurin B. *Biochemistry*. 33:6859-6866.

Taigen, T., L.J. De Windt, H.W. Lim, and J.D. Molkentin. 2000. Targeted inhibition of calcineurin prevents agonist-induced cardiomyocyte hypertrophy. *Proc Natl Acad Sci U S A*. 97:1196-1201.

Tatham, M.H., E. Jaffray, O.A. Vaughan, J.M. Desterro, C.H. Botting, J.H. Naismith, and R.T. Hay. 2001. Polymeric chains of SUMO-2 and SUMO-3 are conjugated to protein substrates by SAE1/SAE2 and Ubc9. *J Biol Chem*. 276:35368-35374.

Thakar, K., R. Niedenthal, E. Okaz, S. Franken, A. Jakobs, S. Gupta, S. Kelm, and F. Dietz. 2008. SUMOylation of the hepatoma-derived growth factor negatively influences its binding to chromatin. *The FEBS journal*. 275:1411-1426.

Ueki, K., T. Muramatsu, and R.L. Kincaid. 1992. Structure and expression of two isoforms of the murine calmodulin-dependent protein phosphatase regulatory subunit (calcineurin B). *Biochemical and biophysical research communications*. 187:537-543.

van Berlo, J.H., M. Maillet, and J.D. Molkentin. 2013. Signaling effectors underlying pathologic growth and remodeling of the heart. *J Clin Invest*. 123:37-45.

Vega, R.B., R. Bassel-Duby, and E.N. Olson. 2003a. Control of cardiac growth and function by calcineurin signaling. *The Journal of biological chemistry*. 278:36981-36984.

Vega, R.B., B.A. Rothermel, C.J. Weinheimer, A. Kovacs, R.H. Naseem, R. Bassel-Duby, R.S. Williams, and E.N. Olson. 2003b. Dual roles of modulatory calcineurin-interacting protein 1 in cardiac hypertrophy. *Proc Natl Acad Sci U S A*. 100:669-674.

Wang, J. 2011. Cardiac function and disease: emerging role of small ubiquitin-related modifier. *Wiley interdisciplinary reviews. Systems biology and medicine*. 3:446-457.

Wang, J., X.H. Feng, and R.J. Schwartz. 2004. SUMO-1 modification activated GATA4-dependent cardiogenic gene activity. *J Biol Chem*. 279:49091-49098.

Wang, J., A. Li, Z. Wang, X. Feng, E.N. Olson, and R.J. Schwartz. 2007. Myocardin sumoylation transactivates cardiogenic genes in pluripotent 10T1/2 fibroblasts. *Molecular and cellular biology*. 27:622-632.

Wang, J., and R.J. Schwartz. 2010. Sumoylation and regulation of cardiac gene expression. *Circ Res*. 107:19-29.

Wang, J., H. Zhang, D. Iyer, X.H. Feng, and R.J. Schwartz. 2008. Regulation of cardiac specific nkx2.5 gene activity by small ubiquitin-like modifier. *J Biol Chem*. 283:23235-23243.

Wang, J.H., and R. Desai. 1976. A brain protein and its effect on the Ca2+-and protein modulator-activated cyclic nucleotide phosphodiesterase. *Biochemical and biophysical research communications*. 72:926-932.

Wang, L., C. Wansleeben, S. Zhao, P. Miao, W. Paschen, and W. Yang. 2014. SUMO2 is essential while SUMO3 is dispensable for mouse embryonic development. *EMBO reports*. 15:878-885.

Wera, S., and B.A. Hemmings. 1995. Serine/threonine protein phosphatases. *The Biochemical journal*. 311 (Pt 1):17-29.

Wilkins, B.J., Y.S. Dai, O.F. Bueno, S.A. Parsons, J. Xu, D.M. Plank, F. Jones, T.R. Kimball, and J.D. Molkentin. 2004. Calcineurin/NFAT coupling participates in pathological, but not physiological, cardiac hypertrophy. *Circ Res*. 94:110-118.

Wilkins, B.J., L.J. De Windt, O.F. Bueno, J.C. Braz, B.J. Glascock, T.F. Kimball, and J.D. Molkentin. 2002. Targeted disruption of NFATc3, but not NFATc4, reveals an intrinsic defect in calcineurin-mediated cardiac hypertrophic growth. *Molecular and cellular biology*. 22:7603-7613.

Wilkins, B.J., and J.D. Molkentin. 2004. Calcium-calcineurin signaling in the regulation of cardiac hypertrophy. *Biochemical and biophysical research communications*. 322:1178-1191.

Xu, Z., and S.W. Au. 2005. Mapping residues of SUMO precursors essential in differential maturation by SUMO-specific protease, SENP1. *The Biochemical journal*. 386:325-330.

Yang, J., B. Rothermel, R.B. Vega, N. Frey, T.A. McKinsey, E.N. Olson, R. Bassel-Duby, and R.S. Williams. 2000. Independent signals control expression of the calcineurin inhibitory proteins MCIP1 and MCIP2 in striated muscles. *Circ Res*. 87:E61-68.

Yang, S.A., and C.B. Klee. 2000. Low affinity Ca2+-binding sites of calcineurin B mediate conformational changes in calcineurin A. *Biochemistry*. 39:16147-16154.

Ying, Y., O.J. Muller, C. Goehringer, B. Leuchs, M. Trepel, H.A. Katus, and J.A. Kleinschmidt. 2010. Heart-targeted adeno-associated viral vectors selected by in vivo biopanning of a random viral display peptide library. *Gene therapy*. 17:980-990.

Yuan, H., J. Zhou, M. Deng, X. Liu, M. Le Bras, H. de The, S.J. Chen, Z. Chen, T.X. Liu, and J. Zhu. 2010. Small ubiquitin-related modifier paralogs are indispensable but functionally redundant during early development of zebrafish. *Cell research*. 20:185-196.

Zhang, F.P., L. Mikkonen, J. Toppari, J.J. Palvimo, I. Thesleff, and O.A. Janne. 2008. Sumo-1 function is dispensable in normal mouse development. *Molecular and cellular biology*. 28:5381-5390.

Zhang, Y.Q., and K.D. Sarge. 2008. Sumoylation regulates lamin A function and is lost in lamin A mutants associated with familial cardiomyopathies. *The Journal of cell biology*. 182:35-39.

Zhao, Q., Y. Xie, Y. Zheng, S. Jiang, W. Liu, W. Mu, Z. Liu, Y. Zhao, Y. Xue, and J. Ren. 2014. GPS-SUMO: a tool for the prediction of sumoylation sites and SUMO-interaction motifs. *Nucleic acids research*. 42:W325-330.

Zheng, Z., C. Cai, J. Omwancha, S.Y. Chen, T. Baslan, and L. Shemshedini. 2006. SUMO-3 enhances androgen receptor transcriptional activity through a sumoylation-independent mechanism in prostate cancer cells. *The Journal of biological chemistry*. 281:4002-4012.

Zhu, J., and F. McKeon. 1999. NF-AT activation requires suppression of Crm1-dependent export by calcineurin. *Nature*. 398:256-260.

Zwadlo, C., and J. Borlak. 2005. Disease-associated changes in the expression of ion channels, ion receptors, ion exchangers and Ca(2+)-handling proteins in heart hypertrophy. *Toxicology and applied pharmacology*. 207:244-256.

9 Abbreviations

AAV	Adeno-associated virus
ADS	Buffer for isolation of neonatal rat ventricular cardiomyocytes
Ad	Adenovirus
AF	AlexaFluor® - fluorescent dye
AID	Autoinhibitory domain
AMP	Adenosine monophosphate
ANF	Atrial-Natriuretic Factor
ATP	Adenosine triphosphate
BNP	Brain-Natriuretic Protein
bp	Basepairs
BSA	Bovine Serum-Albumin
°C	Degree Celsius
Ca^{2+}	Calcium
CDC	Cyclin-dependent kinase
cDNA	copy-DNA
CMV	Cytomegalovirus
Co-IP	Co-Immunoprecipitation
Ctrl	Control
Da	Dalton
ddH_2O	Double distilled water
DEPC	Diethyl pyrocarbonate
DMEM	Dulbecco's Modified Eagle Medium

DMSO	Dimethyl sulfoxide
DNA	Deoxyribonucleic acid
dNTP	Desoxyribonucleotide triphosphate
DTT	Dithiothreithol
ECL	Enhanced Chemiluminescence
E. *coli*	Escherichia coli
EDTA	Ethylendiamine-N,N,N',N'-tetraacetate
FBS	Fetal bovine serum
FCS	Fetal calf serum
Fig	Figure
FITC	Fluorescein Isothiocyanate – fluorescent dye
g	Gram
GAPDH	Glyceraldehyde-3-phosphate-Dehydrogenase
GFP	Green fluorescent protein
h	Hour
HDAC	Histone-deacetylase
HRP	Horseradish Peroxidase
ifu	infectious units
IκB	Inhibitor of kabba-B
IONO	Ionomycin
kb	Kilobasepairs
KCl	Potassium chloride
kDa	Kilodalton
kV	Kilovolt

L	Liter
λ	Lambda
LacZ	Gene, coding for the enzyme ß-Galactosidase
LB	Luria-broth
M	Molar
$MgCl_2$	Magnesium chloride
min	Minute
miRNA	Micro-RNA
MW	Molecular weight
n	Nano
NaCl	Sodium chloride
NCS	Newborn calf serum
NES	Nuclear export sequence
NFAT	Nuclear factor of activated T-Cells
NFκB	Nuclear factor kappa-B
NLS	Nuclear localization sequence
NMR	Nuclear magnetic resonance
NRVCM	Neonatal rat ventricular cardiomyocytes
OD	Optical density
PBS	Phosphate buffered salines
PCR	Polymerase chain reaction
PDB	Protein database
PE	Phenylephrine
PFA	Paraformaldehyde

pH	Negative decadic logarithm of the hydronium ion concentration
PMA	Phorbol-12-myristate-13-acetate
Rcan1-4	Regulator of Calcineurin 1-4
RE	Responsive element
RNA	Ribonucleic acid
rpm	Rounds per minute
RT	Room temperature
SBM	SUMO binding motif (=SIM)
SDS	Sodium dodecyl sulfate
SEM	Standard error of the mean
SENP	Sentrin-specific protease
SIM	SUMO interaction motif (=SBM)
siRNA	Small interfering RNA
SUMO	Small ubiquitin-related modifier
TAC	Transverse aortic constriction
TBS	Tris Buffered Saline
TEMED	N,N,N',N'-Tetramethylendiamin
Tg	Transgene
TRIS	Tris(hydroxymethyl)-aminomethan
UV	Ultraviolet
v/v	volume/volume
wt	Wildtype
w/v	weight/volume

10 Curriculum vitae

Personal information

Alexander Bernt, M.Sc.

Born on February the 7th 1986 in Kiel

Studies

01.05.2012 - 30.04.2015	PhD student in the Clinic for Internal Medicine III – Cardiology and Angiology, UK-SH, Campus Kiel.
19.02.2011 - 31.10.2011	Master thesis at the Institute for experimental tumor research, UK-SH, Campus Kiel.
06.12.2011 - 18.02.2011	Practical course at the Institute for experimental tumor research, UK-SH, Campus Kiel.
23.08.2011 - 05.11.2011	Practice course at the Institute for Toxicology, UK-SH Campus Kiel.
07.10.2011 - 31.03.2012	Study of the *Molecular Life Science* (Master) at the University of Lübeck. Degree: Master of Science, Grade 1.5.
01.03.2009 - 06.10.2009	Bachelor thesis at the Institute for Neurosurgery, UK-SH, Campus Lübeck.
15.10.2006 - 06.10.2009	Study of the *Molecular Life Science* (Bachelor) at the University of Lübeck. Degree: Bachelor of Science.

Occupation

Feb. 2011 – Dec. 2014	Lecturer for biology at the Ergotherapeutic-Institute, Schleswig.

List of publications

Frank, D., A.Y. Rangrez, R. Poyanmehr, T.S. Seeger, C. Kuhn, M. Eden, K. Stiebeling, **A. Bernt**, C. Grund, W.W. Franke, and N. Frey. 2014. Mice with cardiac-restricted overexpression of Myozap are sensitized to biomechanical stress and develop a protein-aggregate-associated cardiomyopathy. **J Mol Cell Cardiol**. 72:196-207.

Haselmann, V., A. Kurz, U. Bertsch, S. Hubner, M. Olempska-Muller, J. Fritsch, R. Hasler, A. Pickl, H. Fritsche, F. Annewanter, C. Engler, B. Fleig, **A. Bernt**, C. Roder, H. Schmidt, C. Gelhaus, C. Hauser, J.H. Egberts, C. Heneweer, A.M. Rohde, C. Boger, U. Knippschild, C. Rocken, D. Adam, H. Walczak, S. Schutze, O. Janssen, F.G. Wulczyn, H. Wajant, H. Kalthoff, and A. Trauzold. 2014. Nuclear death receptor TRAIL-R2 inhibits maturation of let-7 and promotes proliferation of pancreatic and other tumor cells. **Gastroenterology**. 146:278-290.

Rangrez, A.Y., **A. Bernt**, R. Poyanmehr, V. Harazin, I. Boomgaarden, C. Kuhn, A. Rohrbeck, D. Frank, and N. Frey. 2013. Dysbindin is a potent inducer of RhoA-SRF-mediated cardiomyocyte hypertrophy. **The Journal of cell biology**. 203:643-656.

Willkomm, S.*, **A. Bernt***, C. Ueck, I. Choschzick, V. Tronnier, and C. Zechel. 2010. Proliferative capacity of stem-like human glioma cells. **JSRM**. 6:141.

11 Acknowledgements

A thesis like this is a long and tough journey that would not have been possible without the intellectual and foremost enthusiastic help of many people.

First of all I thank Professor Dr. Norbert Frey for giving me the chance to work on my thesis in his laboratories and for the help he has provided me over the years. Secondly I thank Prof. Dr. Eric Beitz for taking the time to review my thesis.

I would like to point out my dear colleagues who have always been helpful on the science-side, many of whom have evolved to become more than colleagues during my time in the lab. Thank you friends, it has been - is - and always will be a pleasure to work with such fine scientists, technicians, PhD students and MD students. Cheers to Kathi, Vanessa, Christin, Gabi, Susi, Franzi, Vio and all of you other countless magnificent people. Especially I would like to point out the guidance that Dr. Ashraf Rangrez has given me as a PhD student. He always took the time to discuss problems and experiments with me and has made me a better scientist in many a way. Your help is greatly appreciated, thank you.

I thank my dearest friends on earth from the bottom of my heart for their enduring support. You, my ‘second family’ have given me all the strength and stamina that was necessary to keep up the good work and finish this thesis. Thank you Maike, Till and Trine. Another friend that I would not dare to exclude in this list is Sascha Kretschmann a friend that has accompanied me on the science-track since day one. Even though you are far away, we walk this path together. I thank all of you for the good times and memories that we shared over the years and may there be many more to come.

Another driving force behind this thesis was my family. I very much appreciate the help and support from my mother, Barbara Bernt and my brother, Stephan Bernt as well as my father Joachim Bernt. You raised the bar and with this last leap I will now follow in your footsteps. I hope you are proud dad, wherever you are now.

Lastly I would like to give a heartfelt thank you to my advisor Dr. Derk Frank for his constant commitment to my work. While working endless hours in the clinic, he always managed to take the time to discuss my work and provide valuable ideas. Without his help, completing a work like this within three years would have been unimaginable. Derk, it was and is a pleasure working with you, thank you for everything you have enabled me to do. Over the last years I took giant steps towards my goals, many of them greatly supported by you. I could not think of a better advisor to have for this thesis.